CMB spectral distortions workshop. KICP, Chicago

May 18-20, 2015

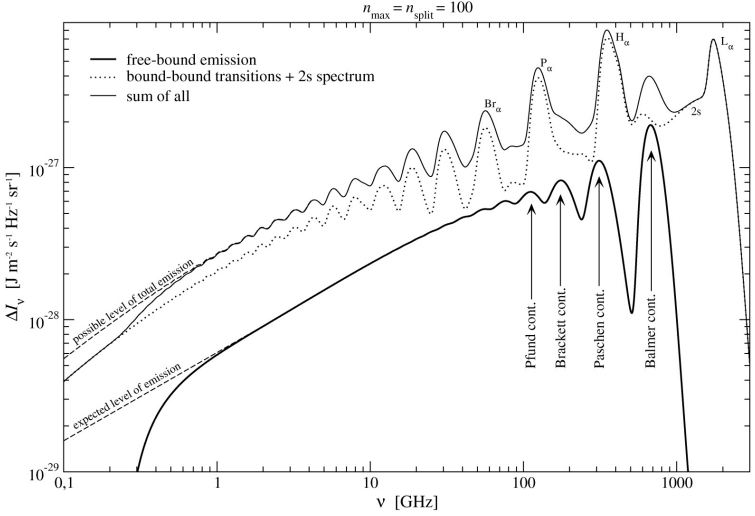

Two milestones in the life of the Universe:

Last Scattering Surface and Black Body Photosphere

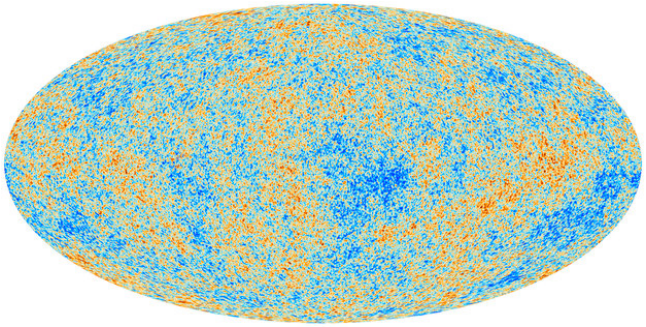

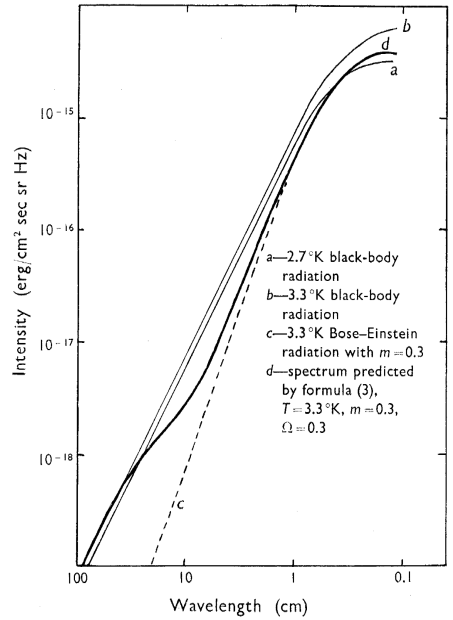

Rashid Sunyaev

Max-Planck Institut fuer Astrophysik, Garching

Space Research Institute, RAS, Moscow

Institute for Advanced Study, Princeton

with Rishi Khatri (MPA)

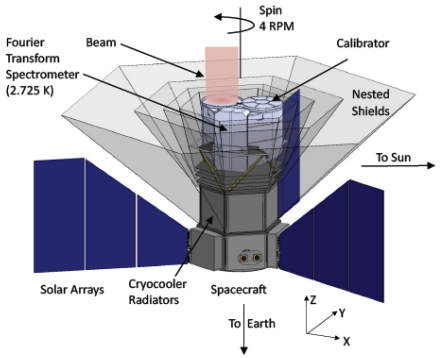

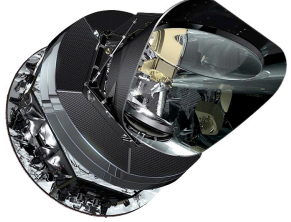

black body spectrum

Tr = 2.725 (1+z)K

practically isotropic

COBE-Firas:

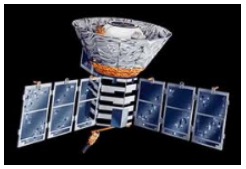

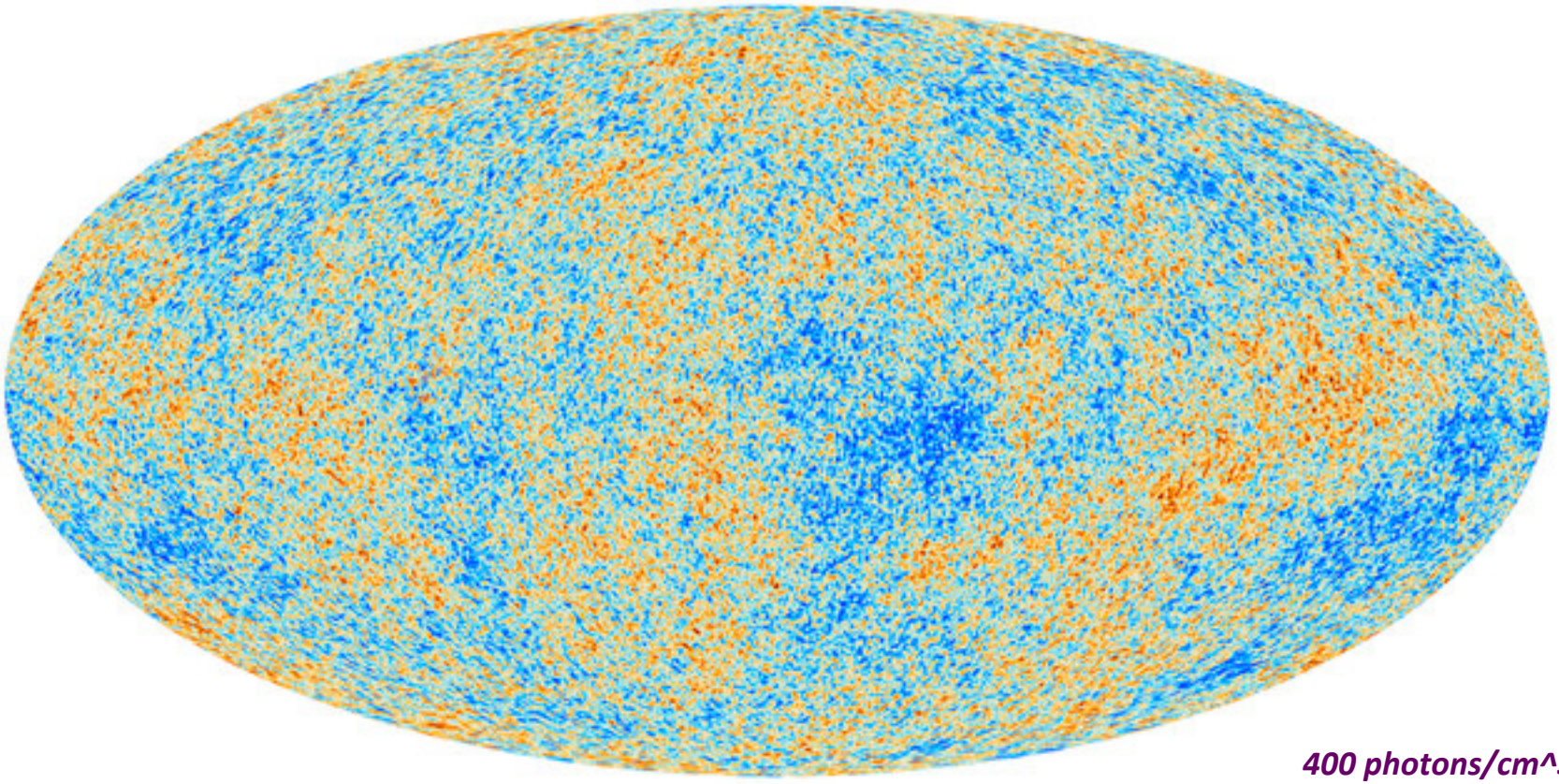

400 photons/cm^3

dark blue - 200 microK

red +200 microK

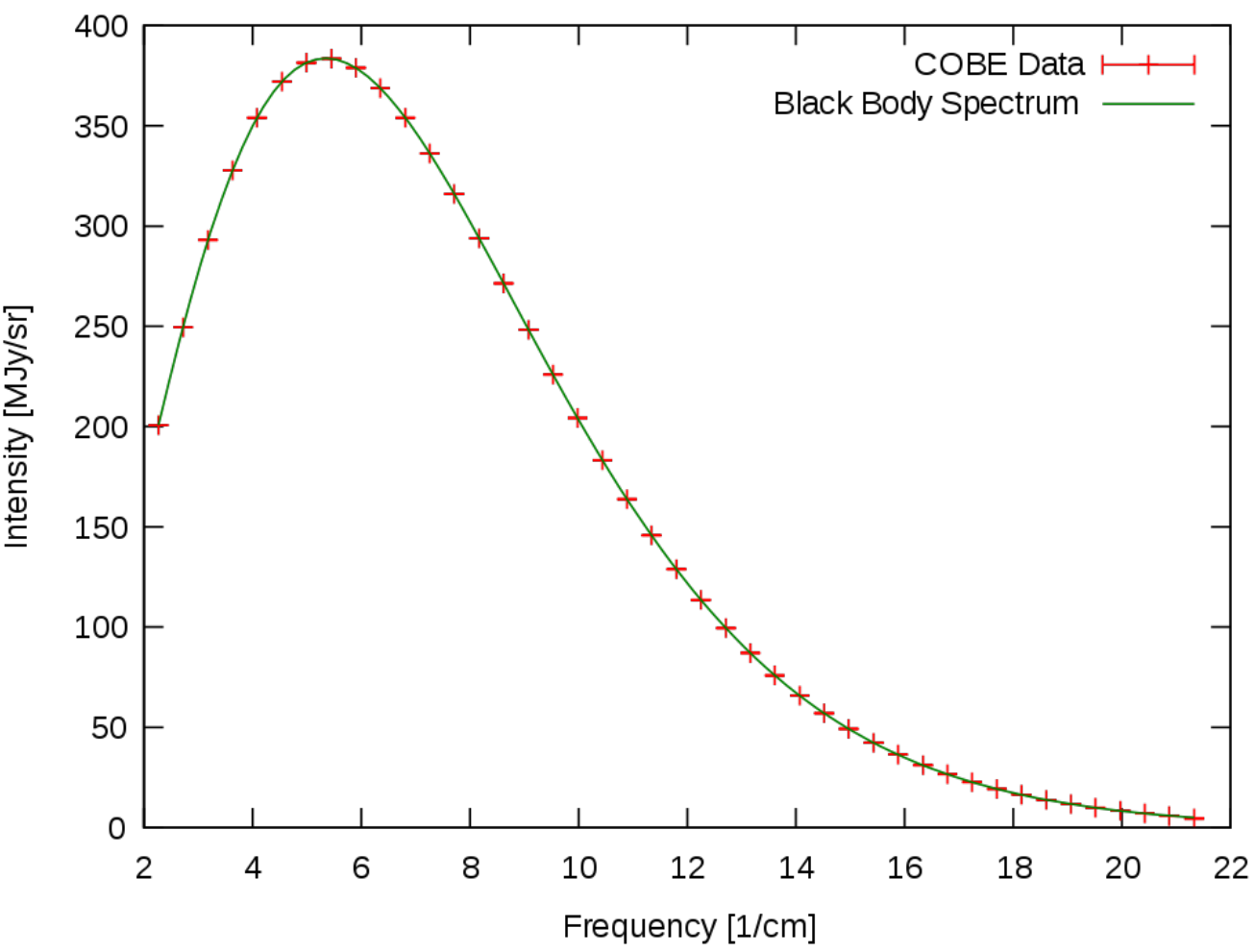

COBE/ FIRAS

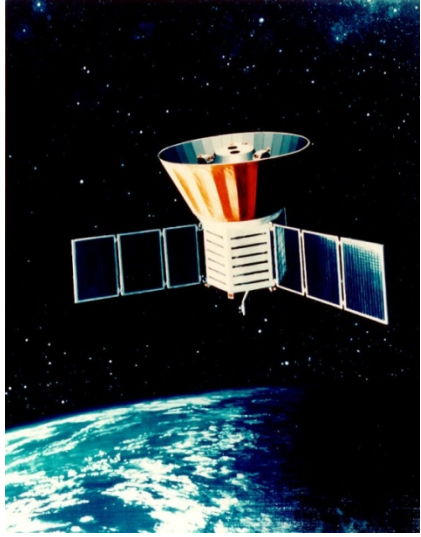

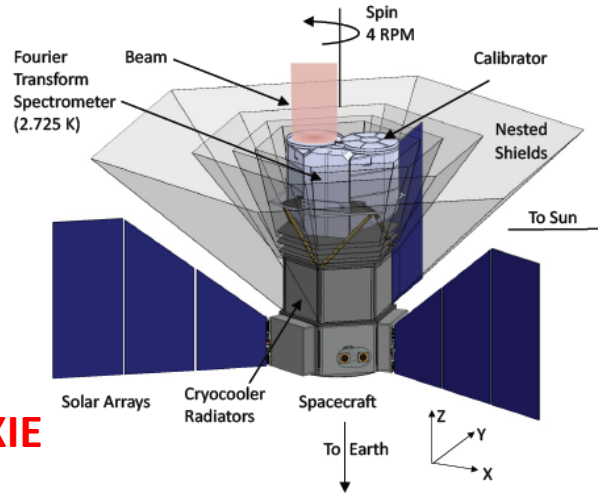

PIXIE

Cosmic Microwave Background (CMB): The most precise black body known: $T = 2.725K \pm 1mK$

No spectral deviations are detected by COBE !

Energy density of Planck spectrum

$$E_\nu = \frac{8\pi h\nu^3}{c^3}\frac{1}{e^{\frac{h\nu}{kT}} - 1}$$

$$E = a_R T^4$$

PIXIE: up to thousand times more sensitive !

Adiabatic expansion of the Universe preserves the blackbody spectrum established at early times (for example during electron-positron annihilation)

(In general $x = \nu/T$ is invariant w.r.t. expansion of the Universe.)

Great progress in the technology of experiments and especially of detectors

Improvement – 7 orders of magnitude after 1970

THERE ARE MANY THEORETICAL MODELS PREDICTING SIGNIFICANT ENERGY RELEASE IN THE EARLY UNIVERSE

I WILL SPEAK TODAY ONLY ABOUT UNAVOIDABLE SPECTRAL FEATURES,
WHICH ARE PREDICTED WITHIN STANDARD COSMOLOGICAL MODEL

SEVERAL EXAMPLES:

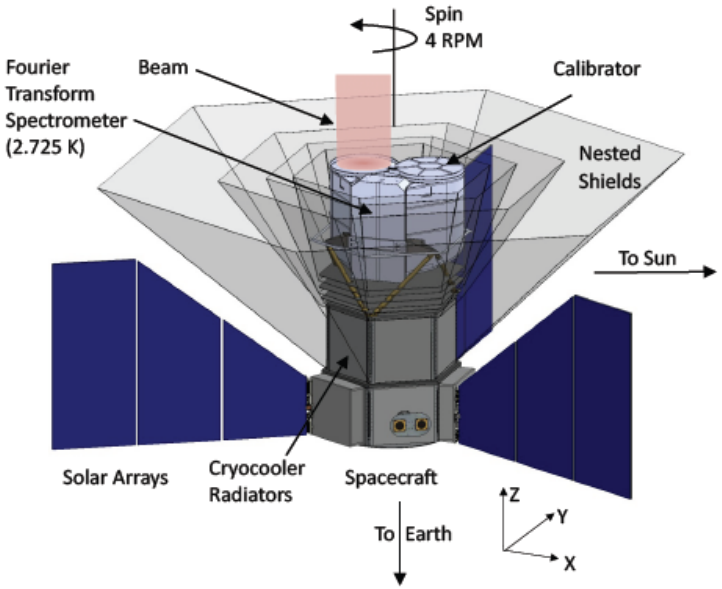

The instrument is maintained at 2.725 K

1000 times more
sensitive than COBE/FIRAS
for CMB spectral distortions

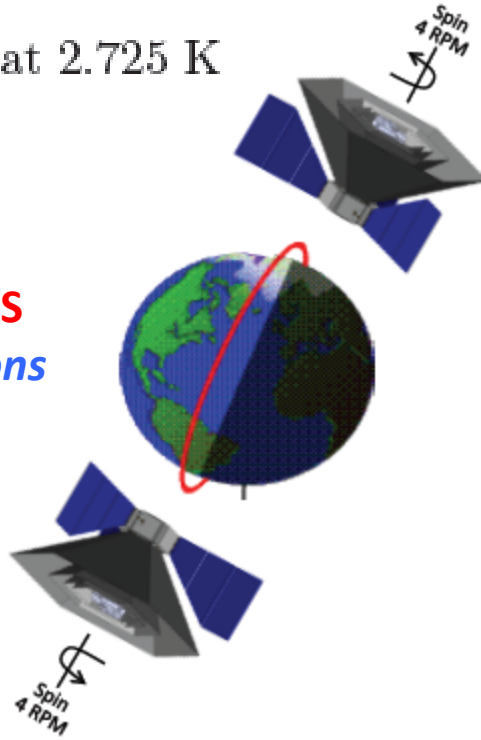

The Primordial Inflation Explorer (PIXIE): A Nulling Polarimeter for Cosmic Microwave Background Observations

A. Kogut[1] D.J. Fixsen[1,2] D.T. Chuss[1] J. Dotson[3] E. Dwek[1] M. Halpern[4] G.F. Hinshaw[4] S.M. Meyer[5] S.H. Moseley[1] M.D. Seiffert[6] D.N. Spergel[7] and E.J. Wollack[1]

[1]Code 665, Goddard Space Flight Center, Greenbelt, MD 20771 USA

Two milestones in the life of the Universe:

Last Scattering Surface and Black Body Photosphere

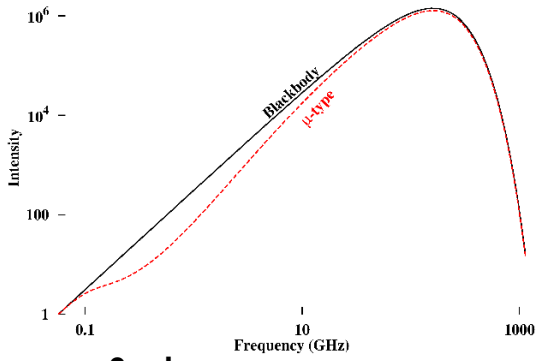

Time →

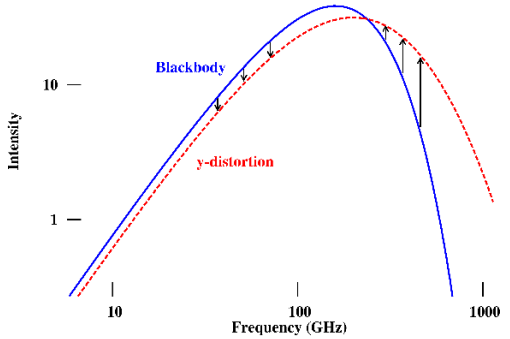

3 mins

Nucleosynthesis

$z \sim 3 \times 10^8$

e^+/e^- **annihilation**

$10^9 > z > 10^8$

18 yrs

380000 yrs

Recombination

Last scattering surface

13.82 billion years

CMB Spectral Distortions

Blackbody photosphere

y–type

Reionization

μ–type **i–type**

2×10^6 2×10^5 1.5×10^4 1100 30 6 0

← Redshift

with Rishi Khatri and Jens Chluba

Black body photosphere of the Universe

In 1966 Yakov Zeldovich asked me to review on the group seminar the papers of Layzer and Burbidges stating that CMB spectrum is just the stellar light thermalized by the dust.
I decided to check in addition the usual mechanism responsible for black body spectrum production inside hot stars: **the Rosseland free-free optical depth of the Universe for CMB – it was negligibly small up to the time of positron-electron annihilation.**

$$\tau_{\rm free-free} \sim \int_0^{t(z)} {\rm d}t\, {n_{\rm e}}^2 \sigma_{\rm T} c \frac{\alpha_{\rm fs}}{(24\pi^3)^{1/2}} \left(\frac{k_{\rm B}T_{\rm e}}{m_{\rm e}c^2}\right)^{-7/2} \left(\frac{h}{m_{\rm e}c x_{\rm e}}\right)^3 (1-e^{-x_{\rm e}})$$

$$\sim 4\times 10^{-5} \left(\frac{1+z}{10^8}\right)^{1/2},$$

but Thomson optical depth was huge.

$$\tau_{\rm Thomson} = \int_0^{t(z)} n_{\rm e}\sigma_{\rm T} c {\rm d}t \overset{z\gg z_{\rm eq}}{\approx} 0.21(1+z)$$ ~ 2 10^7 (z/10^8)

Optical depth – probability for the photon to be absorbed or scattered

Comptonization

$$\gamma + e^- \rightarrow \gamma + e^-$$

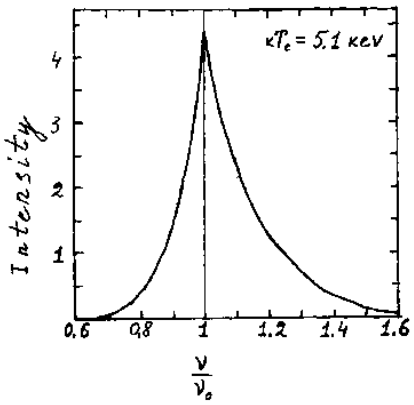

$$\text{Doppler}: \frac{\delta\nu}{\nu} \sim \frac{v_e}{c} \sim \left(\frac{kT_e}{m_e c^2}\right)^{1/}$$

$$\text{2ndorderDoppler}: \left(\frac{\delta\nu}{\nu}\right)_{rms} \sim 4\left(\frac{kT_e}{m_e c^2}\right)$$

$$\text{Recoil}: \frac{\delta\nu}{\nu} = -\frac{h\nu}{m_e c^2}(1 - \cos\theta)$$

==========

y: Amplitude of distortion

$$y = \int dt\, c\sigma_T n_e \frac{k_B\left(T_e - T_\gamma\right)}{m_e c^2}$$

(Zeldovich and Sunyaev 1969)

COBE-FIRAS limit (95%): $y \lesssim 1.5 \times 10^{-5}$ *(Fixsen et al. 1996)*

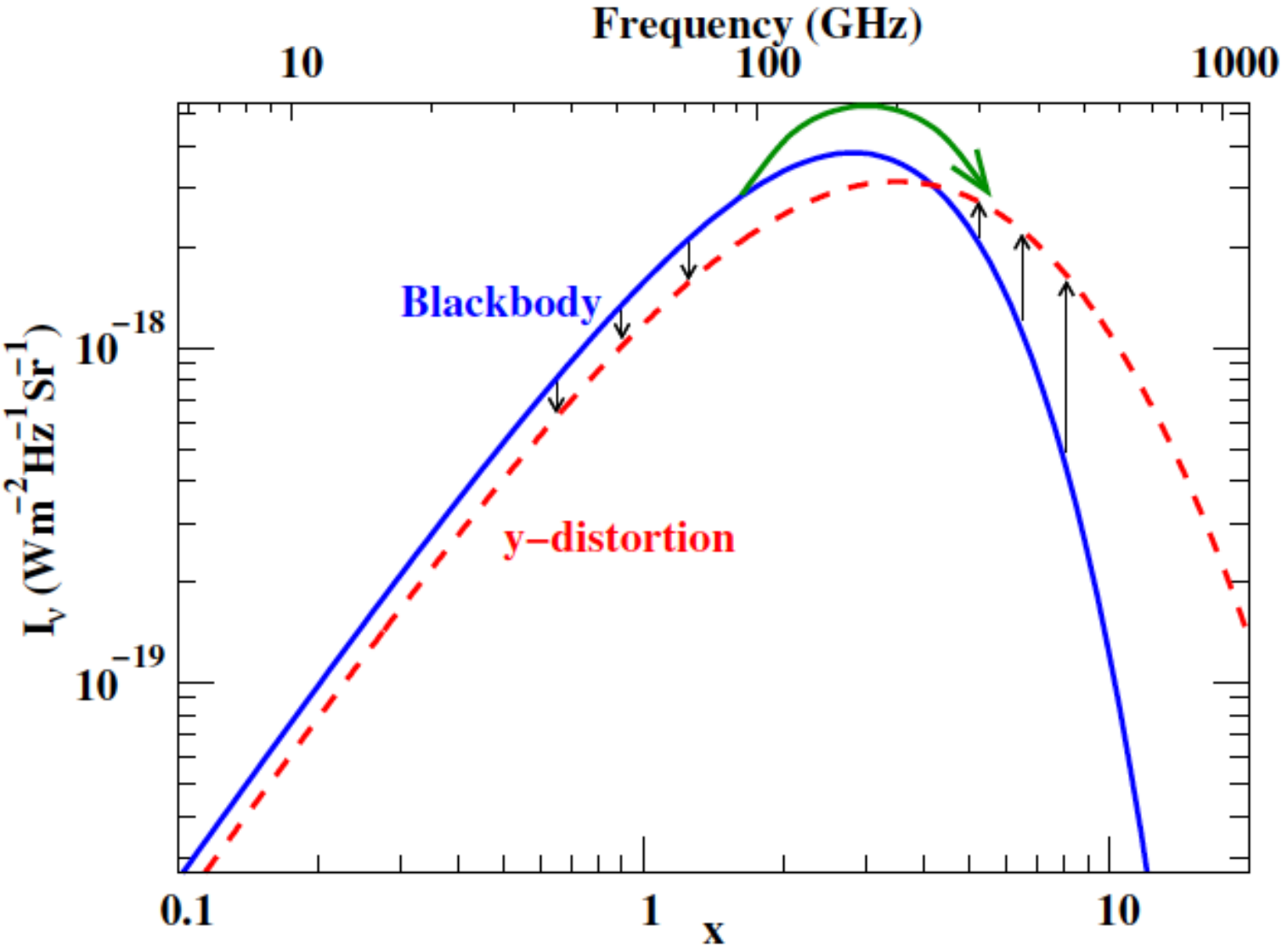

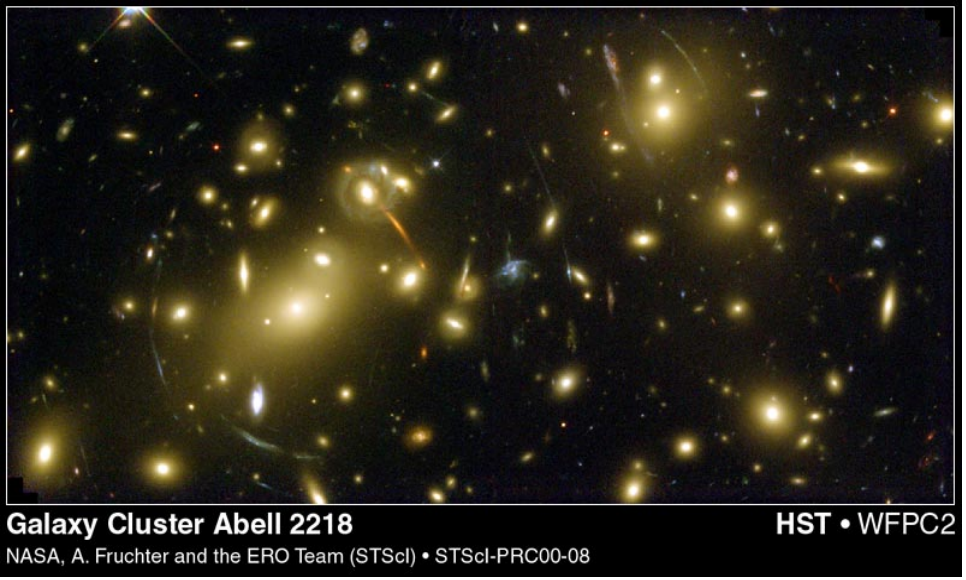

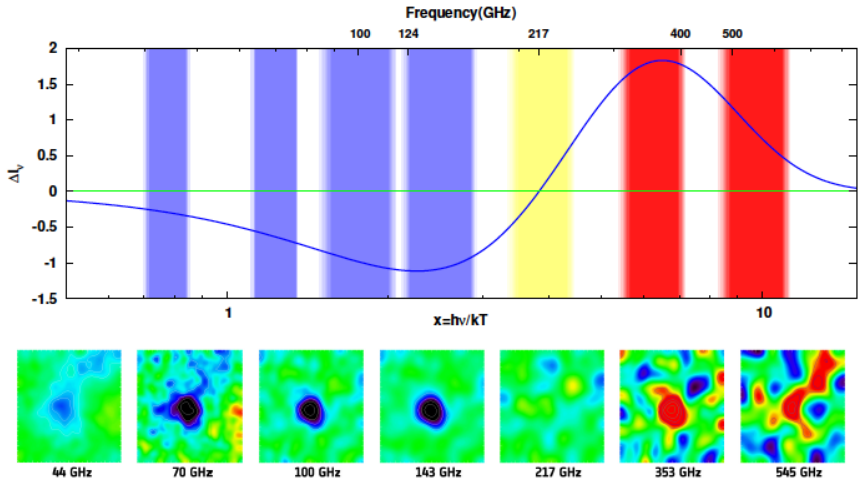

Image credit: ESA / HFI & LFI Consortia

$$n_{SZ} = y\ T^4 \frac{\partial}{\partial T}\frac{1}{T^2}\frac{\partial n_{\rm Pl}}{\partial T}$$

$$= \mathbf{y}\ \frac{\mathbf{x e^x}}{(\mathbf{e^x}-\mathbf{1})^{\mathbf{2}}}\left(\mathbf{x}\frac{\mathbf{e^x}+\mathbf{1}}{\mathbf{e^x}-\mathbf{1}}-\mathbf{4}\right)$$

$$\Delta I_{sz} = I_{sz} - I_{planck} = \frac{2h\nu^3}{c^2} n_{sz}$$

(Zeldovich and Sunyaev 1969)

COBE-FIRAS limit (95%): $y \lesssim 1.5\times10^{-5}$ *(Fixsen et al. 1996)*

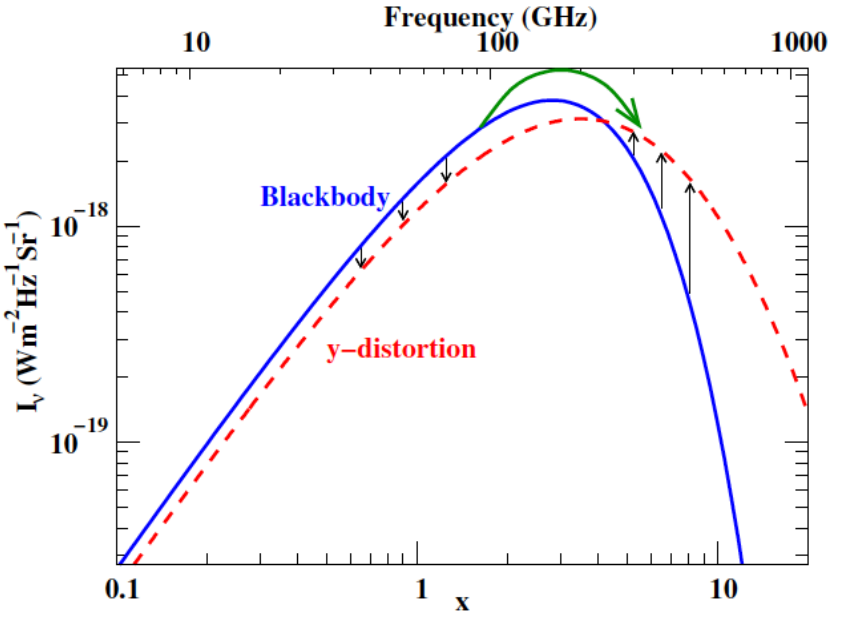

cluster Abell 2319 seen by Planck

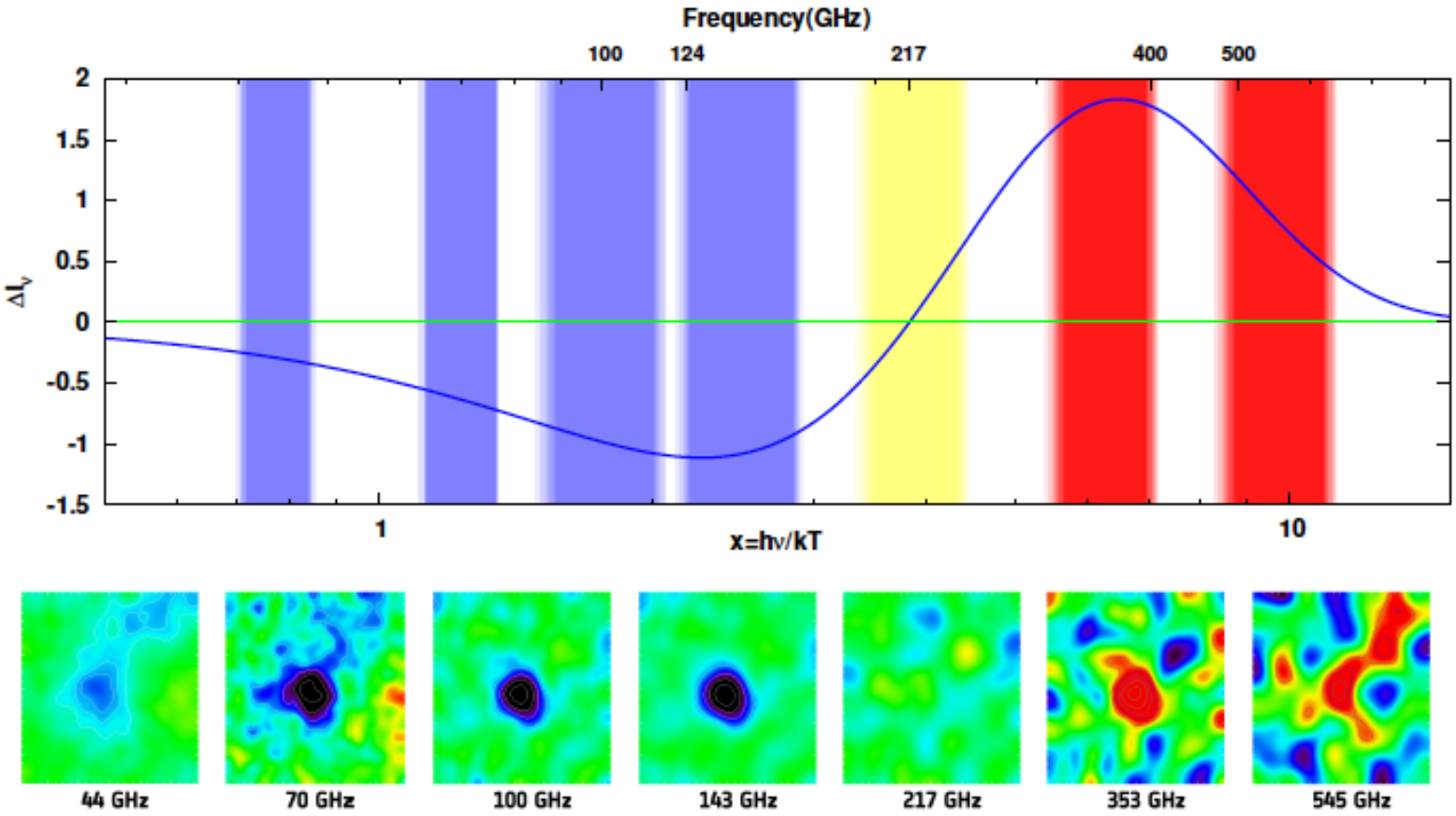

Image credit: ESA / HFI & LFI Consortia

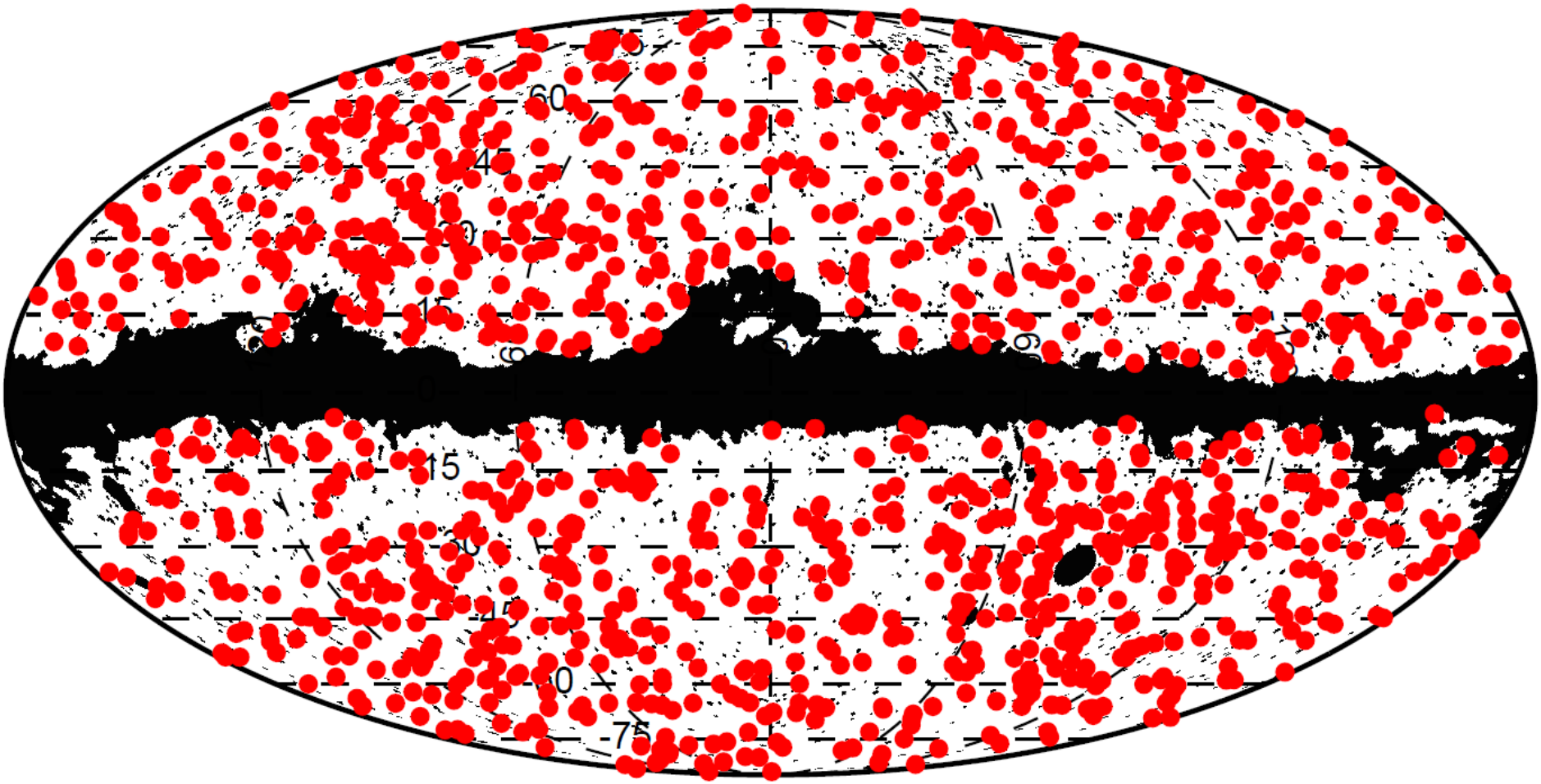

Fig. 2: The distribution, shown in Mollweide projection with the Galactic plane horizontal and the Milky Way centre in the middle, of the 1227 *Planck* clusters and candidates across the sky (red thick dots). The masked point-sources (black thin dots), the Magellanic clouds (large black areas) and the Galactic mask, covering a total of 16.3% of the sky and used by the SZ-finder algorithms to detect SZ sources, are also shown.

SOUTH POLE TELESCOPE

PI: J.Carlstrom

10m dish; 95, 150, 220 GHz
1’

Photograph by: Glenn Grant
National Science Foundation

Kavli Institute for Cosmological Physics AT THE UNIVERSITY OF CHICAGO
Berkeley University of California
Case CASE WESTERN RESERVE UNIVERSITY
THE UNIVERSITY OF CHICAGO
UCDAVIS UNIVERSITY OF CALIFORNIA
ASTRONOMY UNIVERSITY OF ILLINOIS AT URBANA-CHAMPAIGN
McGill
Harvard-Smithsonian Center for Astrophysics
CARDIFF UNIVERSITY
PRIFYSGOL CAERDYDD
Colorado University of Colorado at Boulder
BERKELEY LAB

Lower limit on $\langle y \rangle$ from Planck and SPT detected clusters

Sum the $\langle y \rangle$ from Planck clusters at $z < 0.3$ and SPT clusters at $z > 0.3$

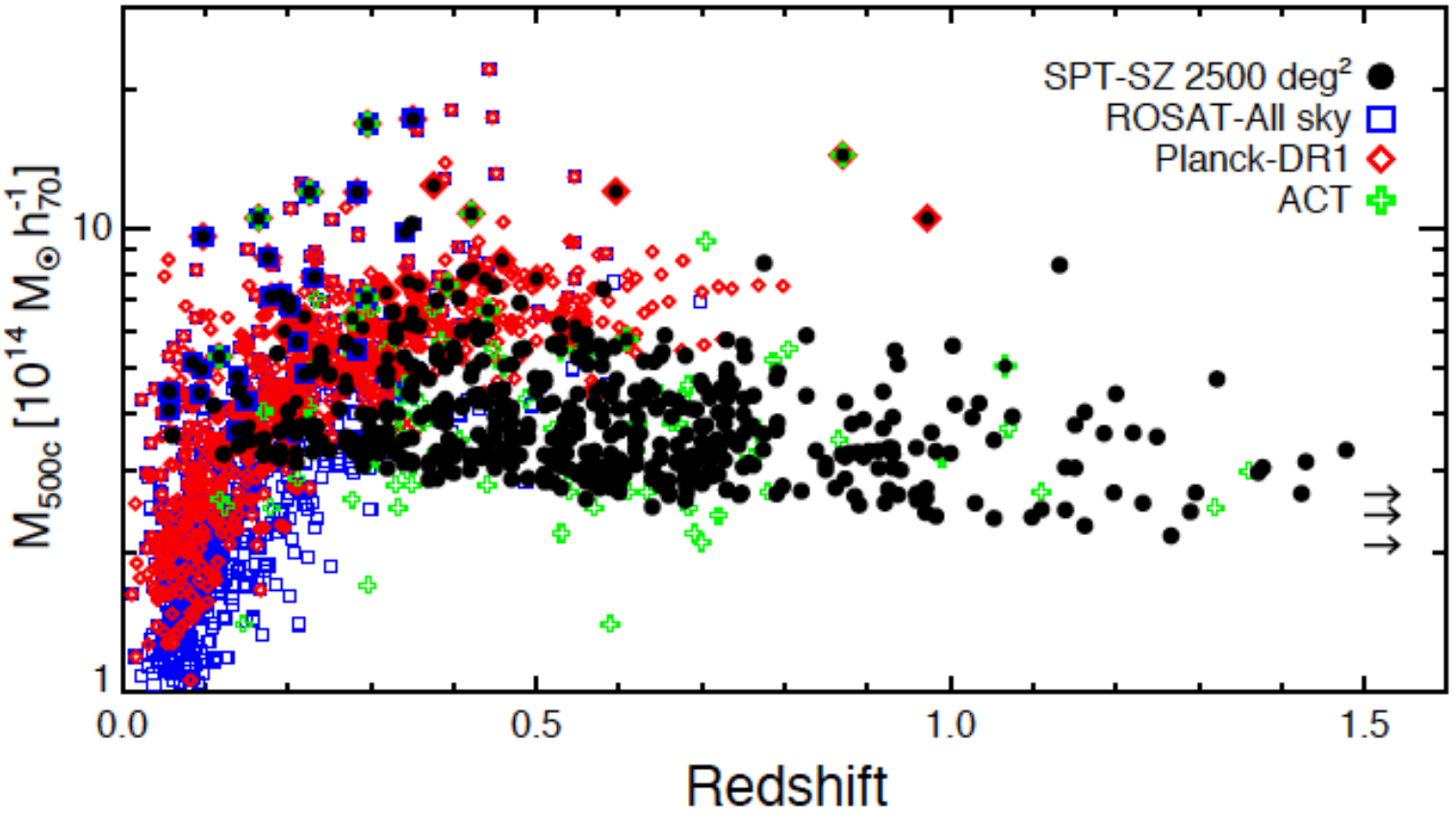

Fig. from Bleem et al. 2015 (SPT) arXiv:1409.0850

Lower limit on $\langle y \rangle$ from Planck and SPT detected clusters

Observed clusters $\Rightarrow$ Minimum average y-distortion in the CMB

$\langle y \rangle > 5.4 \times 10^{-8}$ (*Khatri & Sunyaev 2015*)

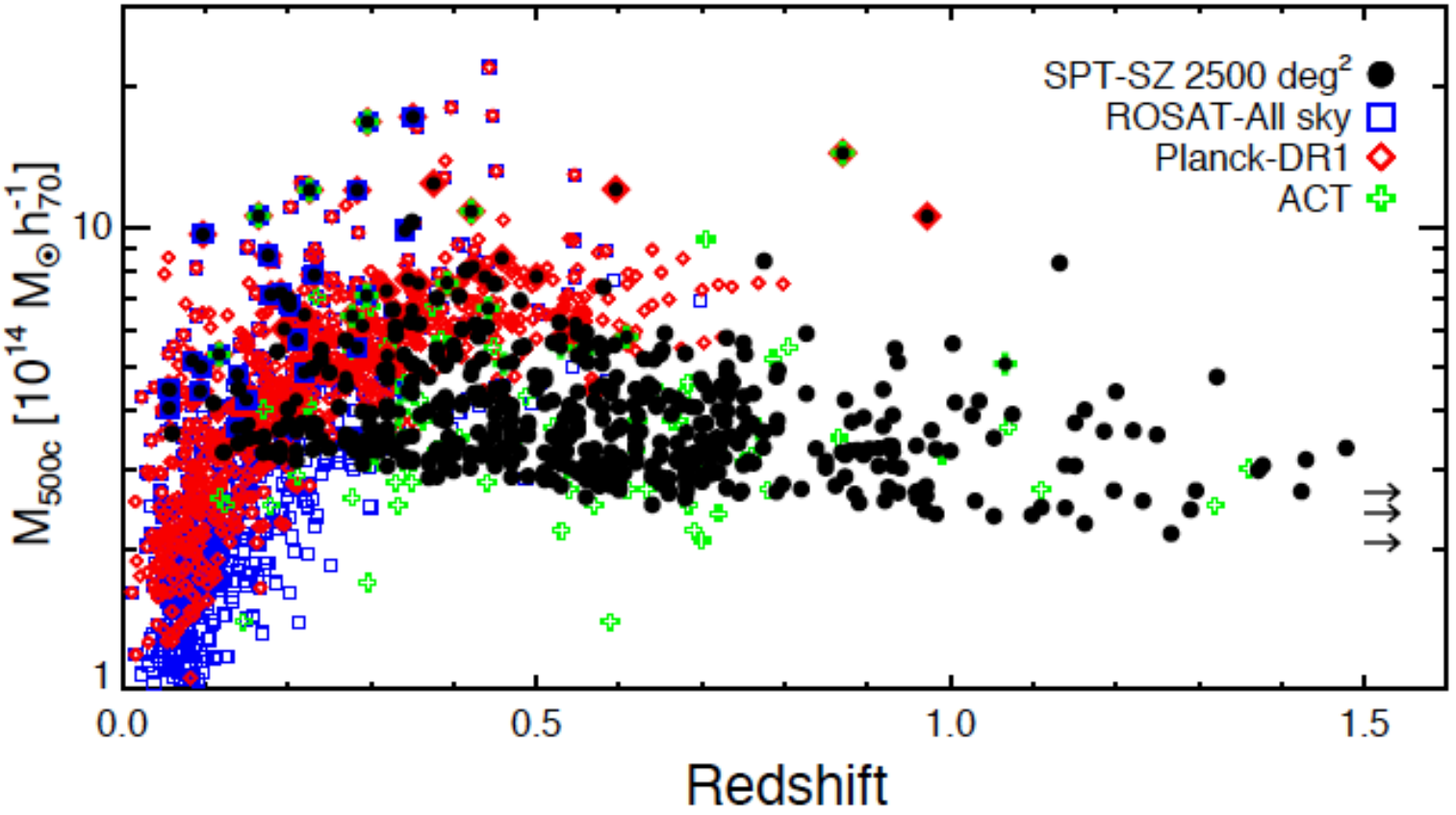

Fig. from Bleem et al. 2015 (SPT) arXiv:1409.0850

Dolag *et al, 2014*

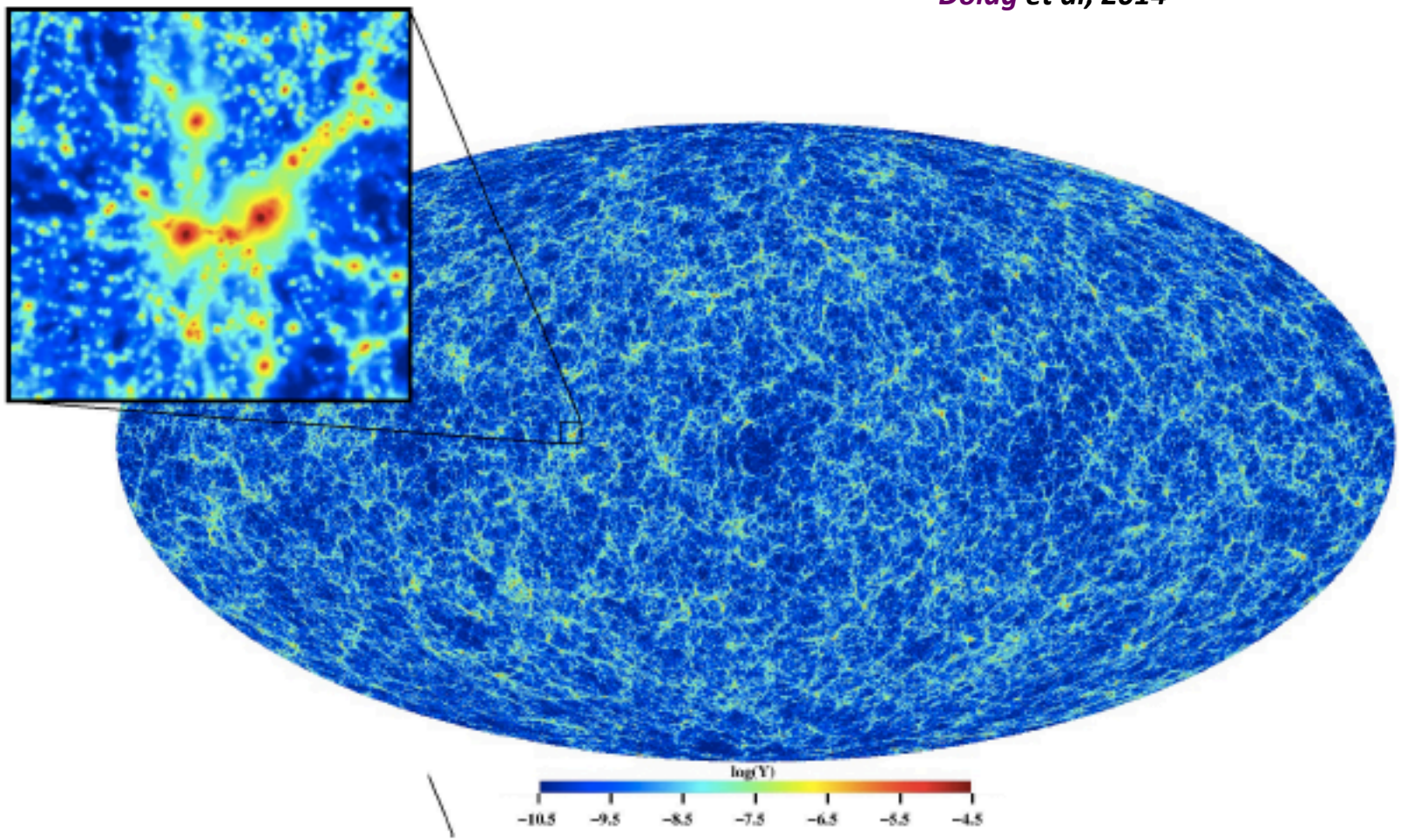

Figure 34. Map of simulated y-distortion taken from [207]. The y-type signal from the post-reionization epoch is dominated by the collapsed objects and filaments in the large scale structure.

New upper limit on $\langle y \rangle$ from y-map created by combining Planck HFI channels

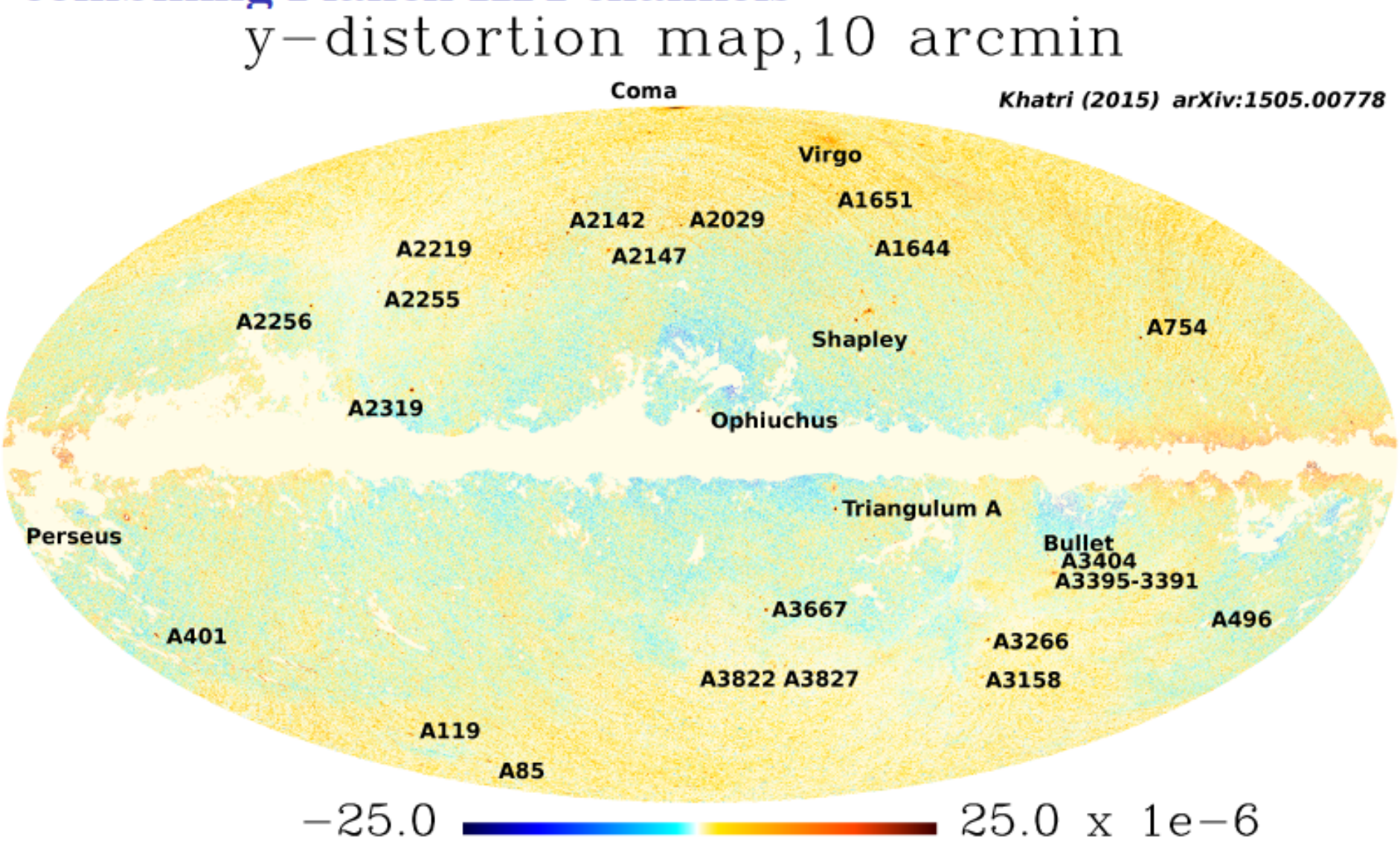

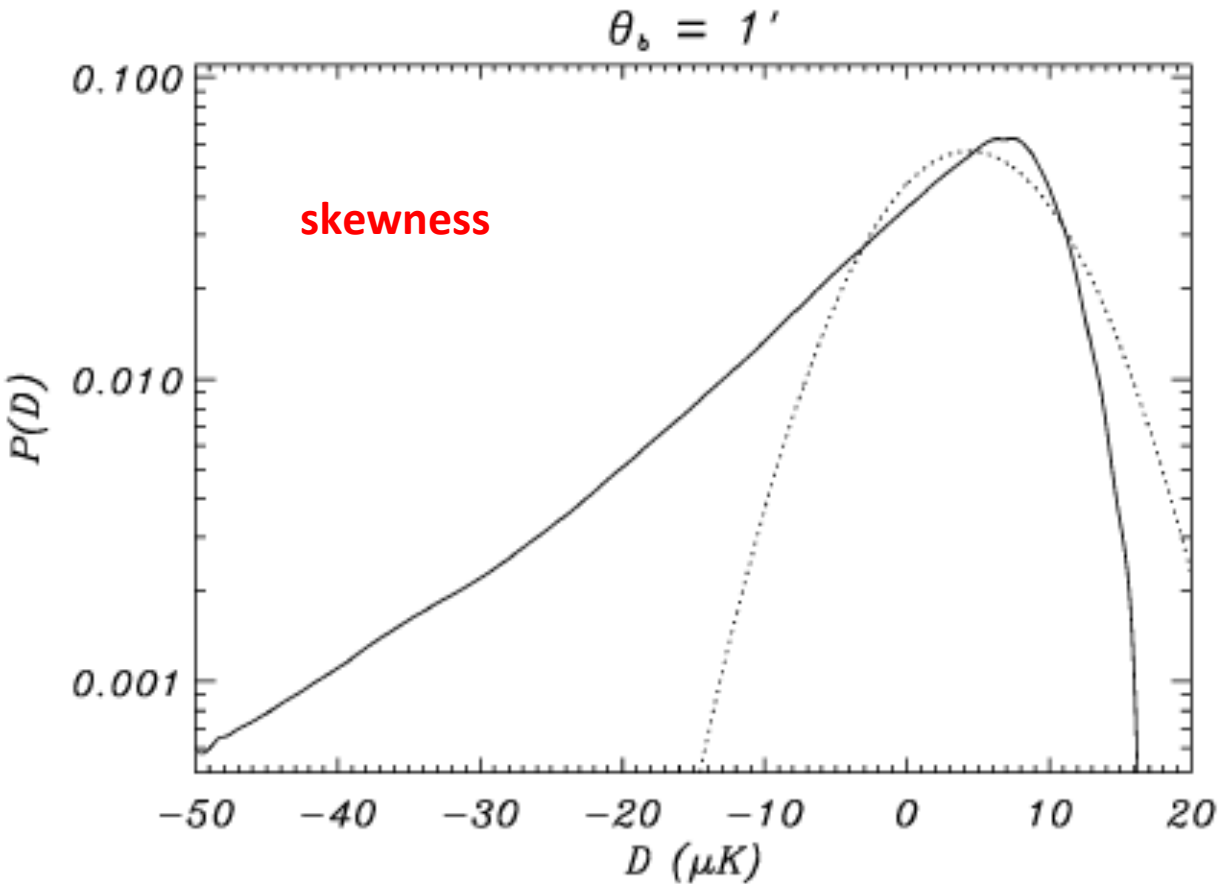

Figure 2. Example of the strong non-Gaussianity of the $P(D)$ function for SZ clusters. We present the $P(D)$ function for a SZ map in the Rayleigh–Jeans region of the spectrum, where clusters are 'negative' sources. For comparison, we also show the best Gaussian fit to this $P(D)$ curve (σ = 6.1 μK). This curve will be explained in detail in Section 7.

J. A. Rubiño-Martín and R. A. Sunyaev , 2003

D - deviation

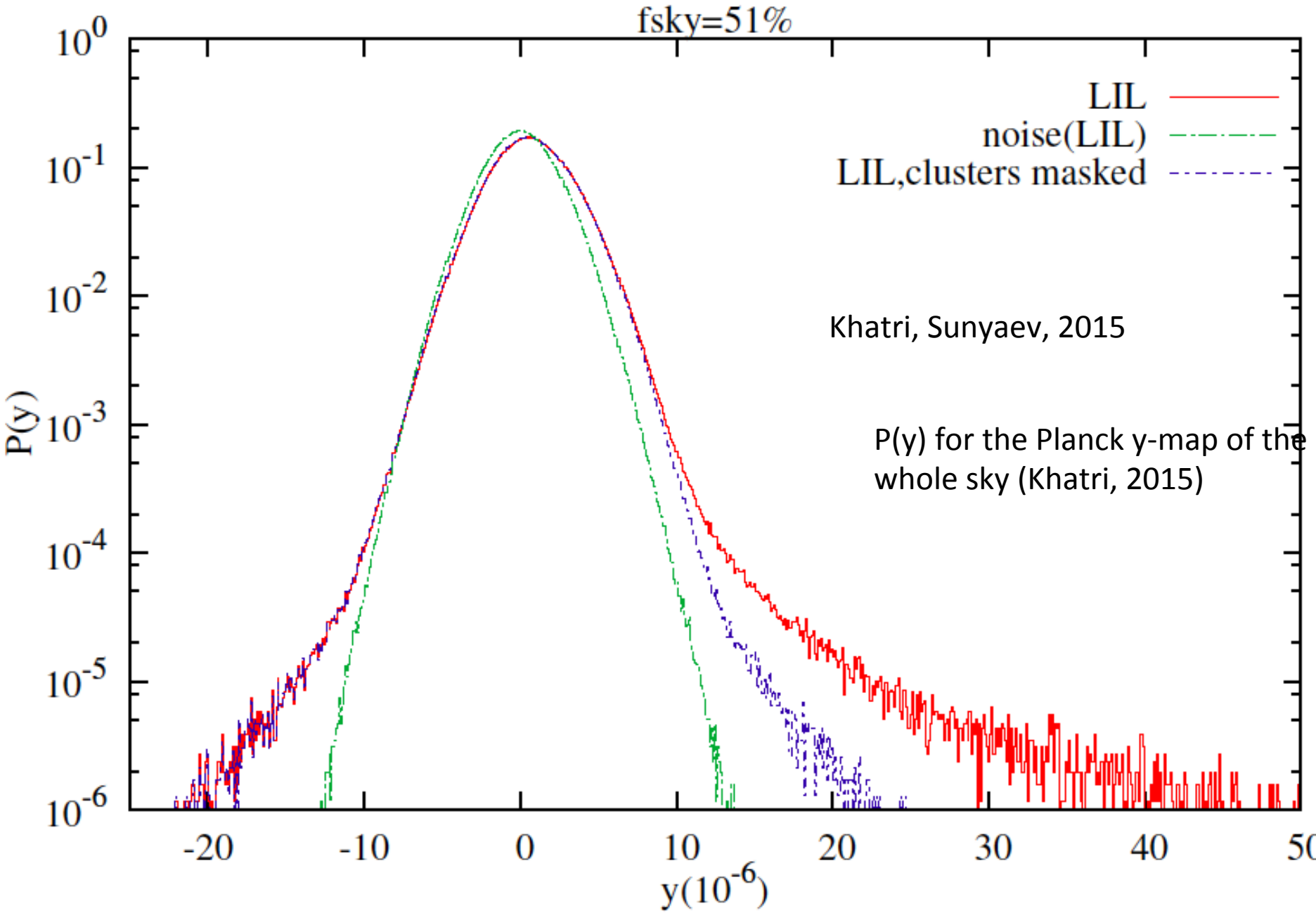

Khatri, Sunyaev, 2015

P(y) for the Planck y-map of the whole sky (Khatri, 2015)

New upper limit on $\langle y \rangle$ from y-map created by combining Planck HFI channels

A simple conservative approach:

- Take all the positive pixels in the map (excluding contaminated regions)
- Average the y-distortion in the pixels (All pixels have equal area)

Result: $\langle y \rangle < 2.2 \times 10^{-6}$ *(Khatri & Sunyaev 2015)*

6.8 times stronger compared to the COBE-FIRAS upper limit:
$\langle y \rangle < 15 \times 10^{-6}$ *(Fixsen et al. 1996)*

New upper limit on $\langle y \rangle$ from y-map created by combining Planck HFI channels

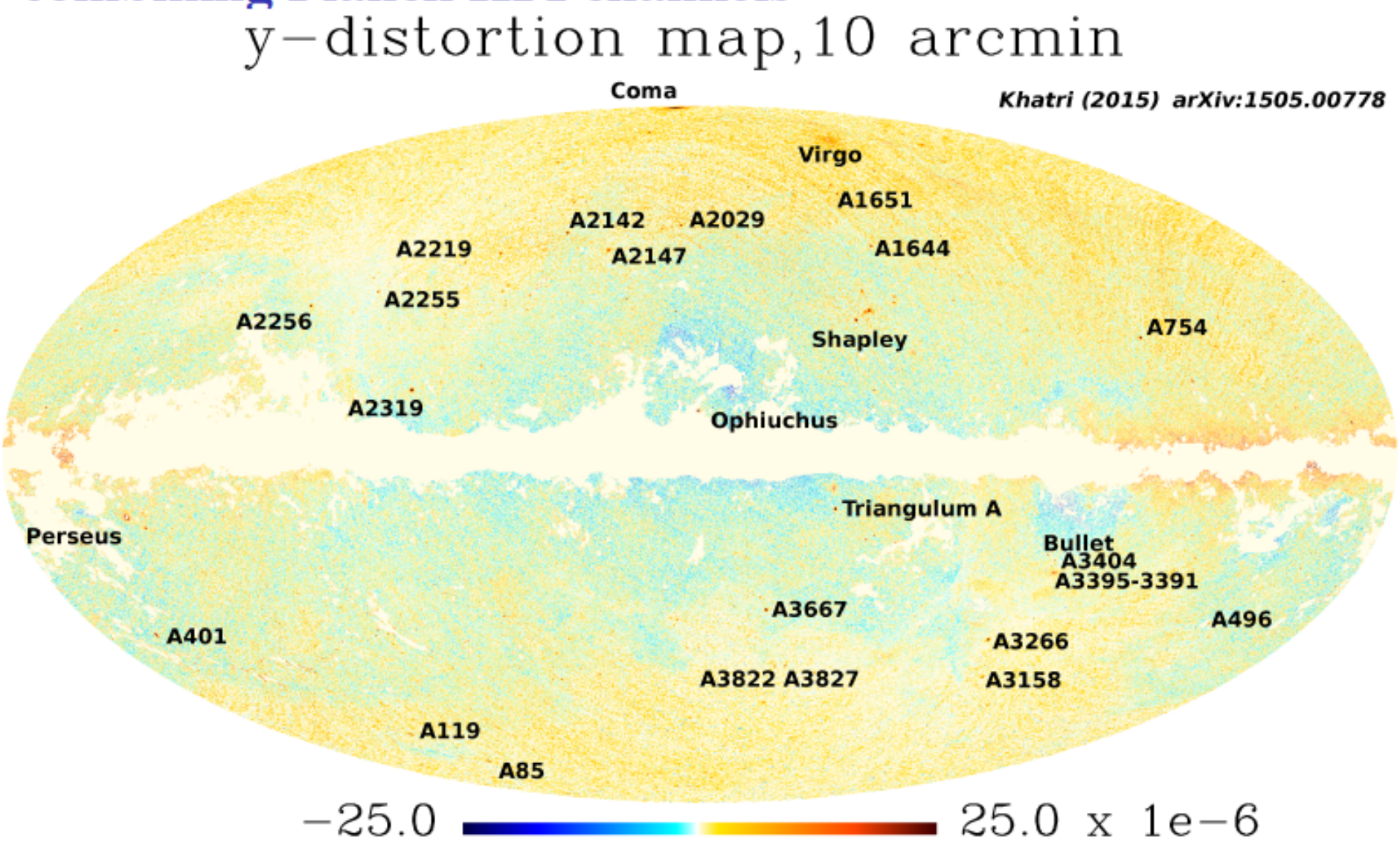

Brief history

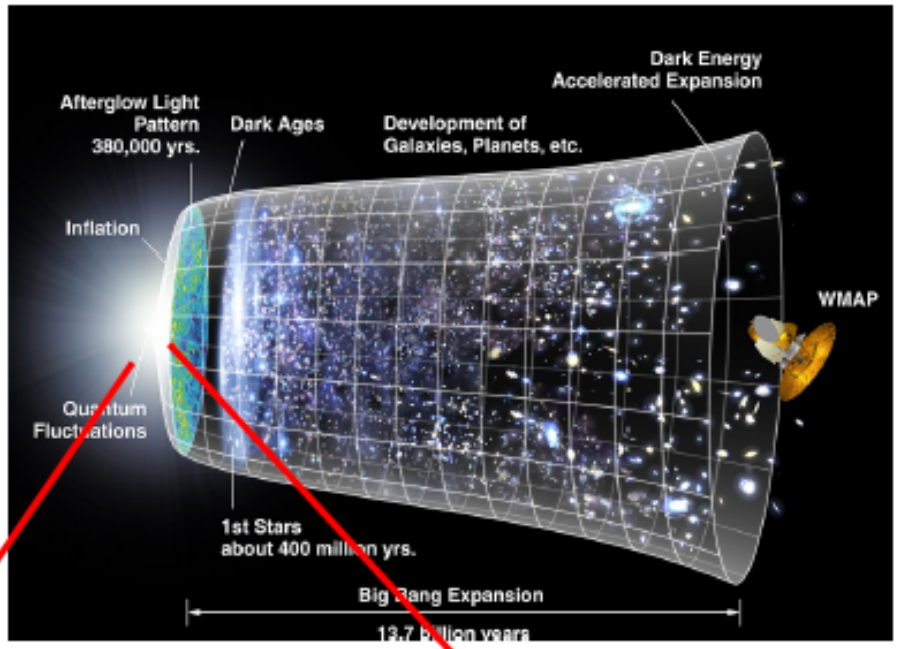

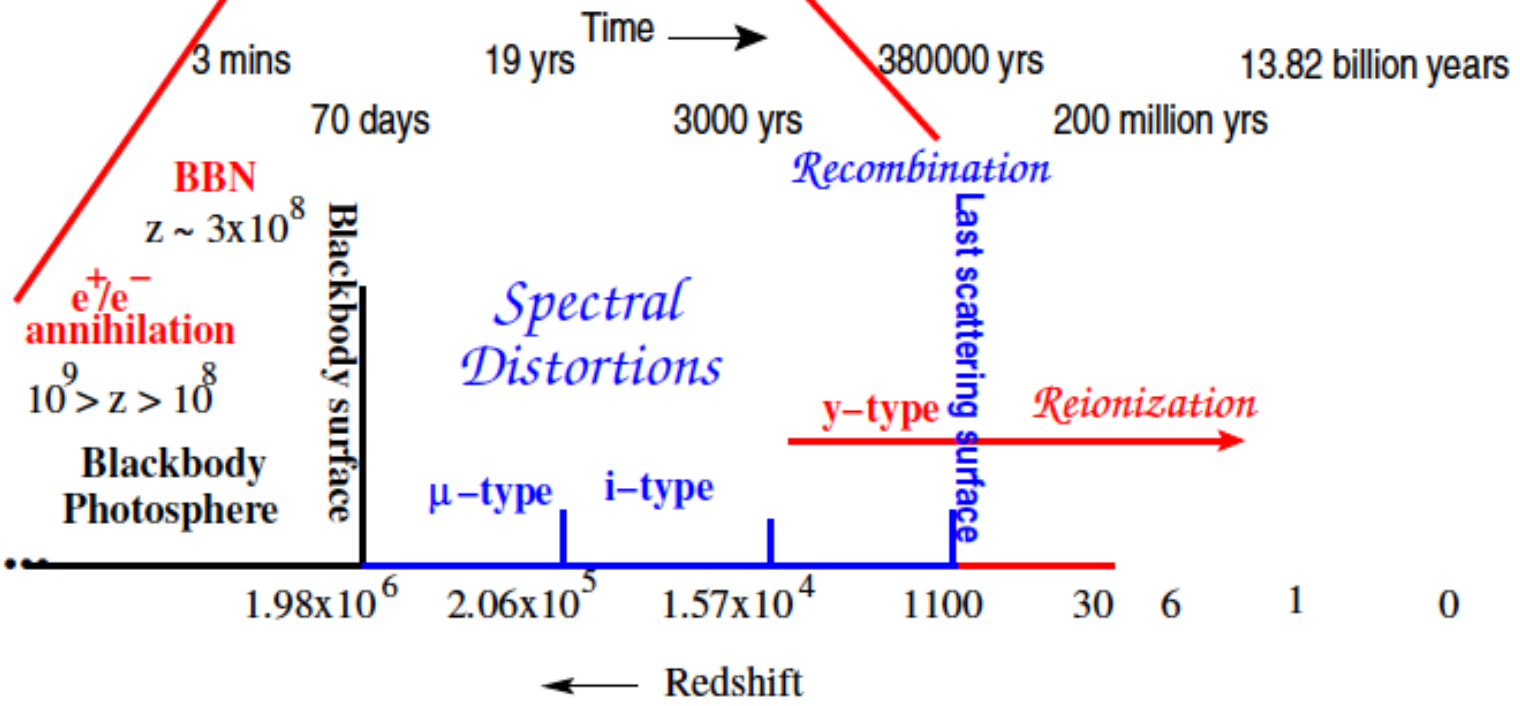

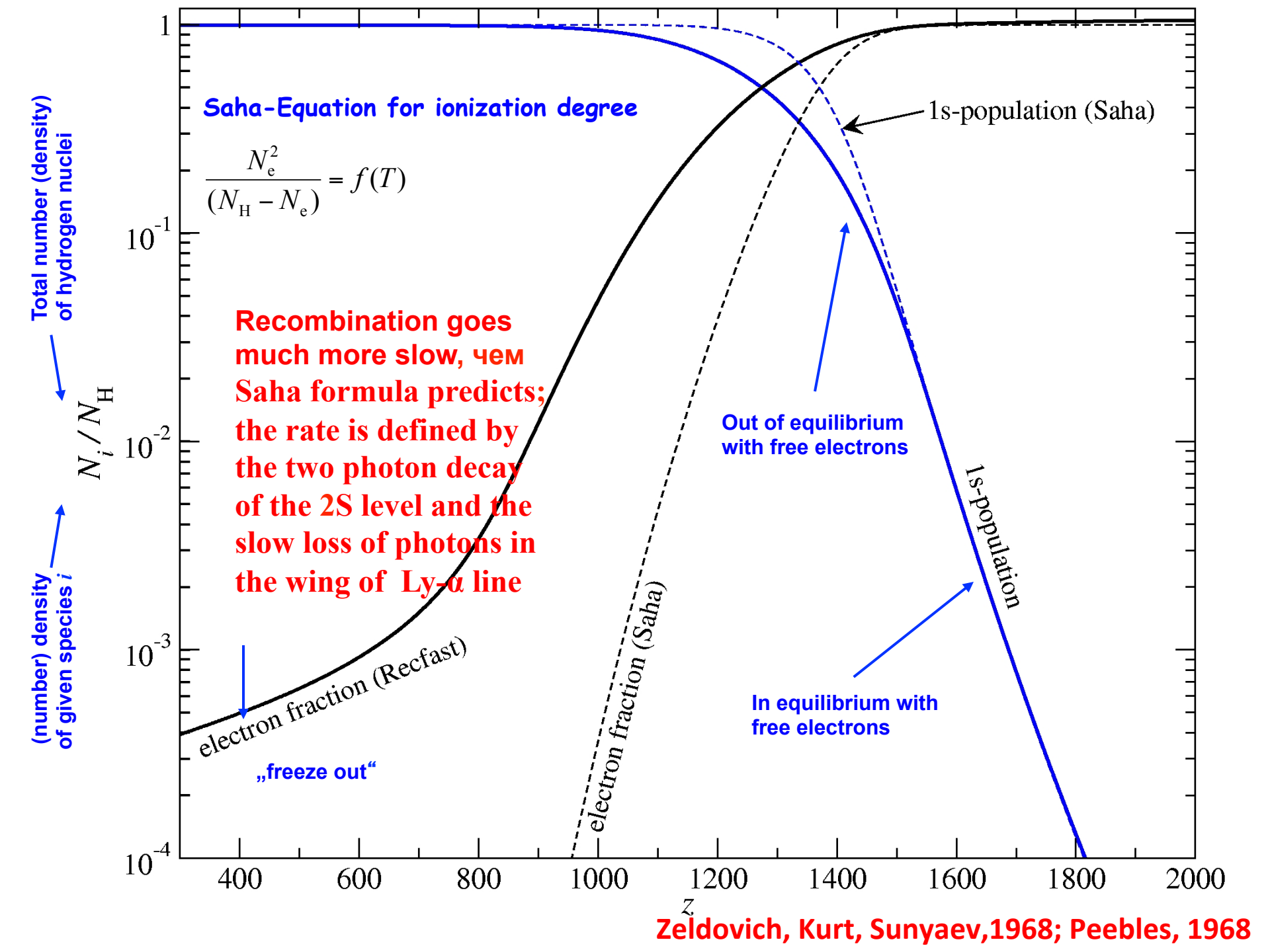
Saha-Equation for ionization degree
$\frac{N_e^2}{(N_H - N_e)} = f(T)$
Total number (density) of hydrogen nuclei
(number) density of given species i
N_i / N_H
1
10^{-1}
10^{-2}
10^{-3}
10^{-4}
400
600
800
1000
1200
1400
1600
1800
2000
z
1s-population (Saha)
Recombination goes much more slow, чем Saha formula predicts; the rate is defined by the two photon decay of the 2S level and the slow loss of photons in the wing of Ly-α line
Out of equilibrium with free electrons
1s-population
In equilibrium with free electrons
electron fraction (Recfast)
„freeze out“
electron fraction (Saha)
Zeldovich, Kurt, Sunyaev,1968; Peebles, 1968

Visibility function

Last scattering surface

SMALL-SCALE FLUCTUATIONS OF RELIC RADIATION*

R. A. SUNYAEV and YA. B. ZELDOVICH
(Received 11 September, 1969)
Astrophysics and Space Science 7 (1970) 3

Below we will need the function

$$e^{-\tau}\frac{d\tau}{dz} = \sigma_T n_c c H_0^{-1} A z^{-1/2} \exp\left\{-az^{3/2}e^{-B/z} - \frac{B}{z} - \tau_0\right\}, \qquad (6)$$

which in agreement with (3) has a sharp maximum for $z_{max} = 1055$ ($e^{-\tau}(d\tau/dz)_{z=z[max]} = 3.32 \times 10^{-3}$) and exponentially decreases in both directions, the value of the function decreasing to half its maximum value for $z_3 = 960$ and $z_4 = 1135$. It will be convenient in what follows to approximate this function by a Gaussian function with dispersion $\sigma_z = 75$ whose integral equals 1.

The redshift and the width of this function were very well confirmed by WMAP
And recently PLANCK (few percent precision)

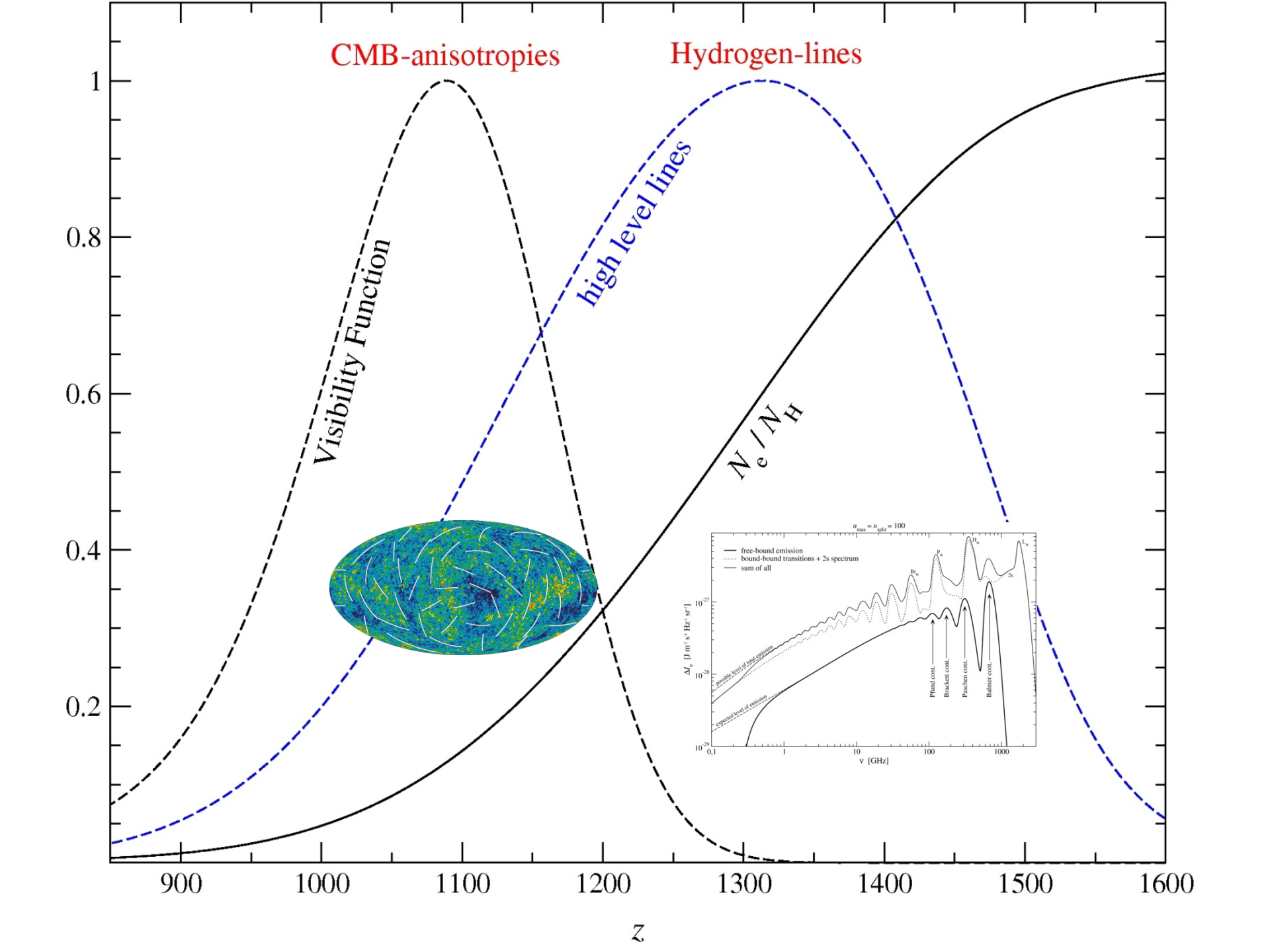
CMB-anisotropies
Hydrogen-lines
Visibility Function
high level lines
N_e / N_H
1
0.8
0.6
0.4
0.2
900
1000
1100
1200
1300
1400
1500
1600
z
$n_{max} = n_{split} = 100$
free-bound emission
bound-bound transitions + 2s spectrum
sum of all
P_α
H_α
L_α
Br_α
2s
possible level of total emission
expected level of emission
Pfund cont.
Brackett cont.
Paschen cont.
Balmer cont.
ΔI_ν [J m^2 s^{-1} Hz^{-1} sr^{-1}]
10^{-22}
10^{-28}
10^{-29}
0,1
1
10
100
1000
ν [GHz]

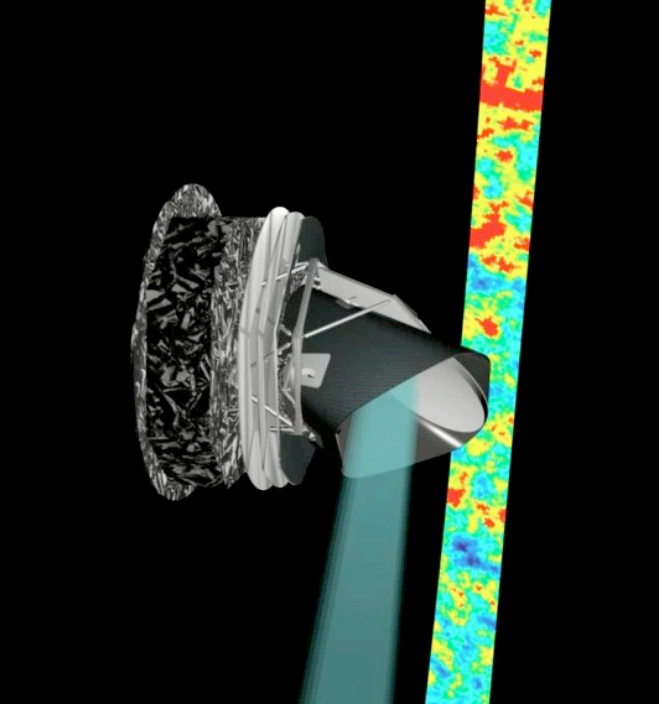

PLANCK spacecraft scans the sky

From paper Sunyaev, Zeldovich 1970

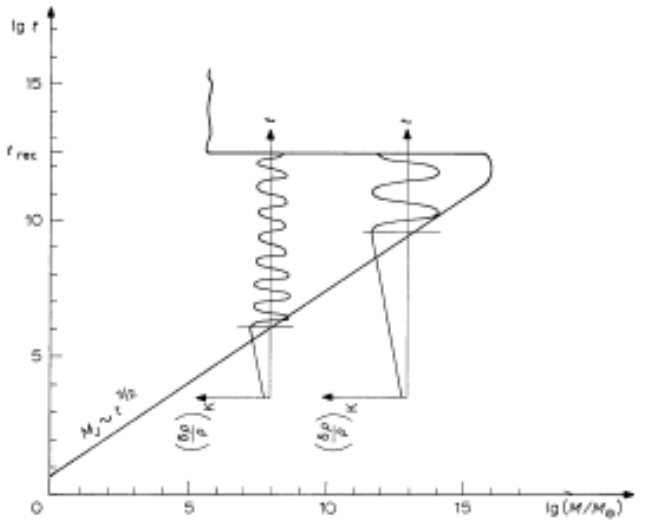

Fig. 1a. Diagram of gravitational instability in the 'big-bang' model. The region of instability is located to the right of the line $M_J(t)$; the region of stability to the left. The two additional lines of the graph demonstrate the temporal evolution of density perturbations of matter: growth until the moment when the considered mass is smaller than the Jeans mass and oscillations thereafter. It is apparent that at the moment of recombination perturbations corresponding to different masses correspond to different phases.

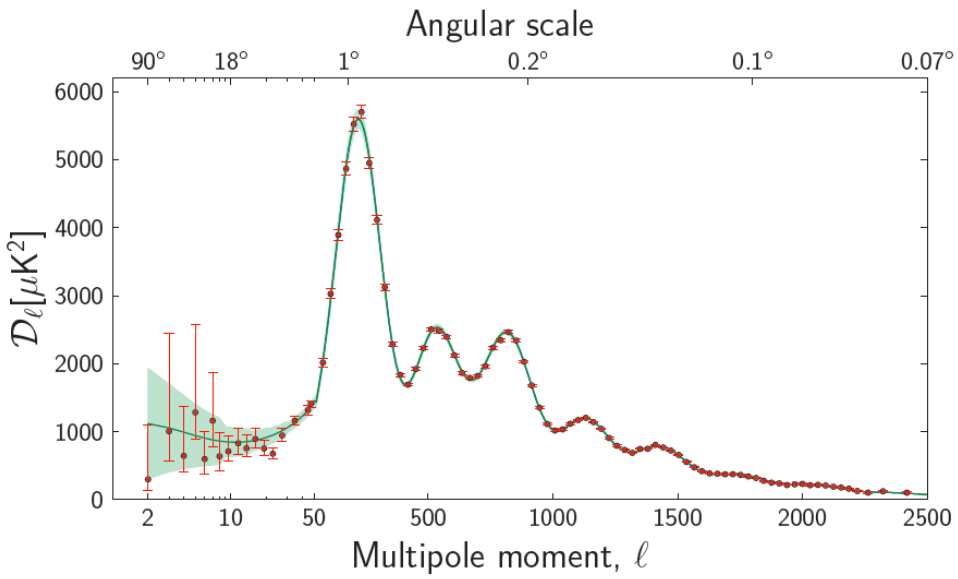

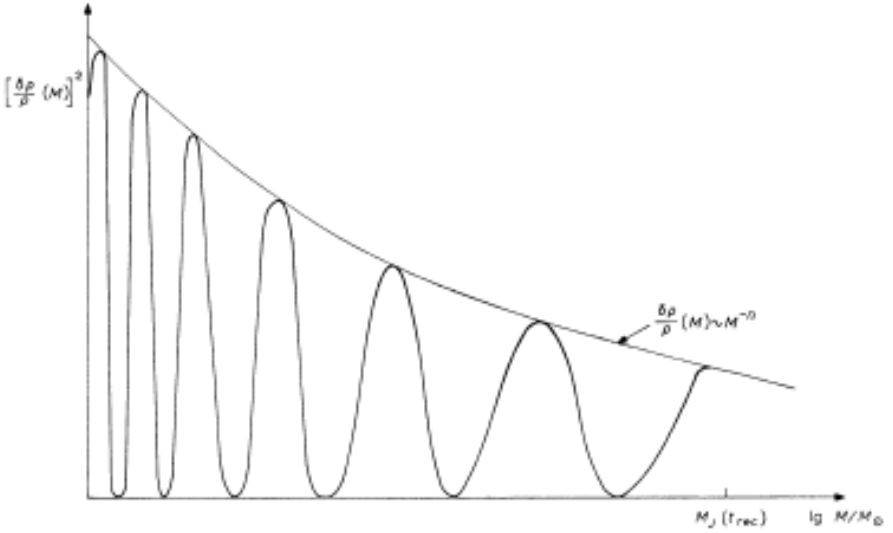

Fig. 1b. The dependence of the square of the amplitude of density perturbations of matter on scale. The fine line designates the usually assumed dependence $(\delta\rho/\rho)_M \sim M^{-n}$. It is apparent that fluctuations of relic radiation should depend on scale in a similar manner.

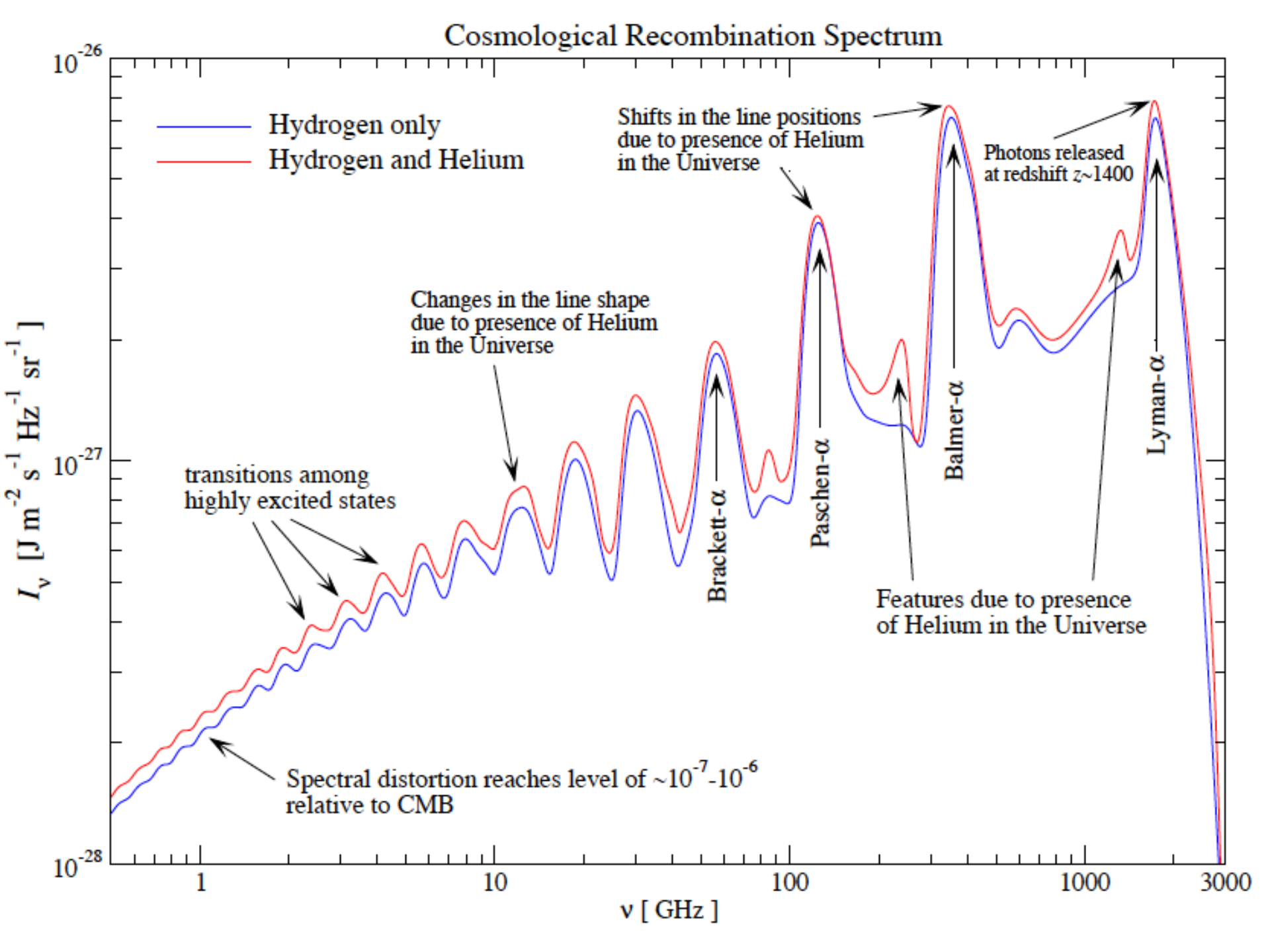
Cosmological Recombination Spectrum
Hydrogen only
Hydrogen and Helium
Shifts in the line positions due to presence of Helium in the Universe
Photons released at redshift z~1400
Changes in the line shape due to presence of Helium in the Universe
transitions among highly excited states
Brackett-α
Paschen-α
Balmer-α
Lyman-α
Features due to presence of Helium in the Universe
Spectral distortion reaches level of ~10^-7-10^-6 relative to CMB
10^-26
10^-27
10^-28
I_ν [J m^-2 s^-1 Hz^-1 sr^-1]
1
10
100
1000
3000
ν [GHz]

Planck spectrum

$$I_\nu = \frac{2h\nu^3}{c^2}\frac{1}{e^{h\nu/(k_{\rm B}T)}-1}$$

Relativistic invariant occupation number/phase space density

$$n(\nu) \equiv \frac{c^2}{2h\nu^3} I_\nu$$

$$n(x) = \frac{1}{e^x - 1} \quad , \quad x = \frac{h\nu}{k_{\rm B}T}$$

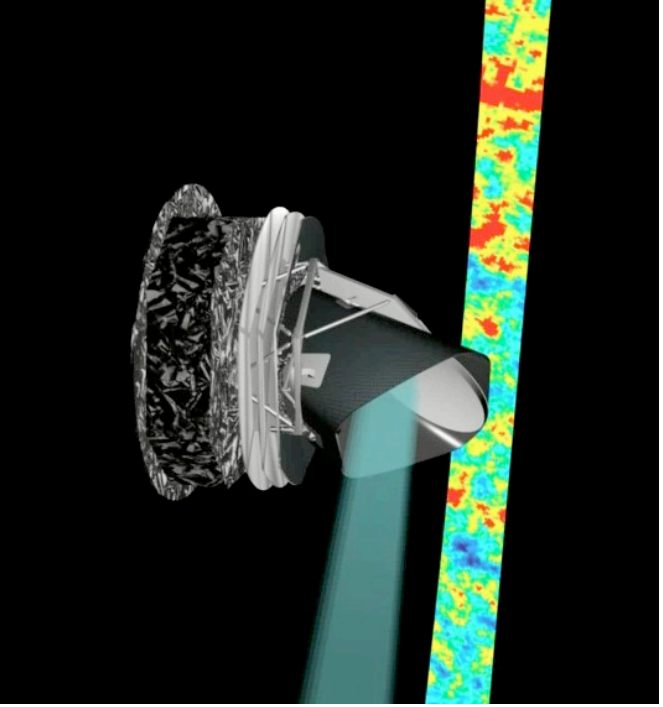

PLANCK spacecraft scans the sky

standing sound waves (Lifshits, 1946)

From paper Sunyaev, Zeldovich 1970

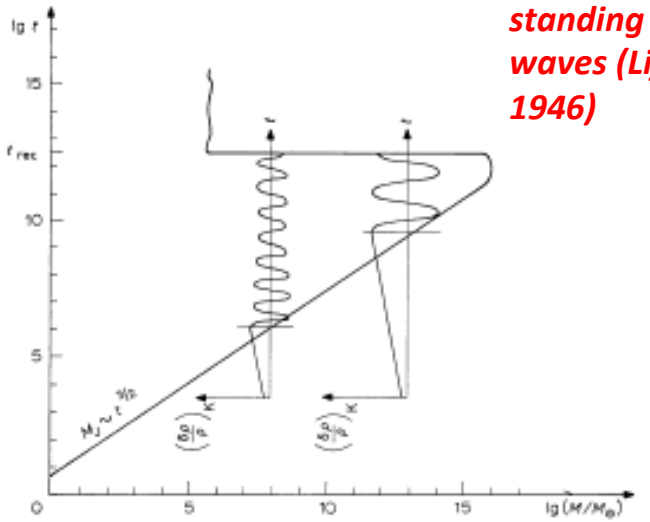

Fig. 1a. Diagram of gravitational instability in the 'big-bang' model. The region of instability is located to the right of the line $M_J(t)$; the region of stability to the left. The two additional lines of the graph demonstrate the temporal evolution of density perturbations of matter: growth until the moment when the considered mass is smaller than the Jeans mass and oscillations thereafter. It is apparent that at the moment of recombination perturbations corresponding to different masses correspond to different phases.

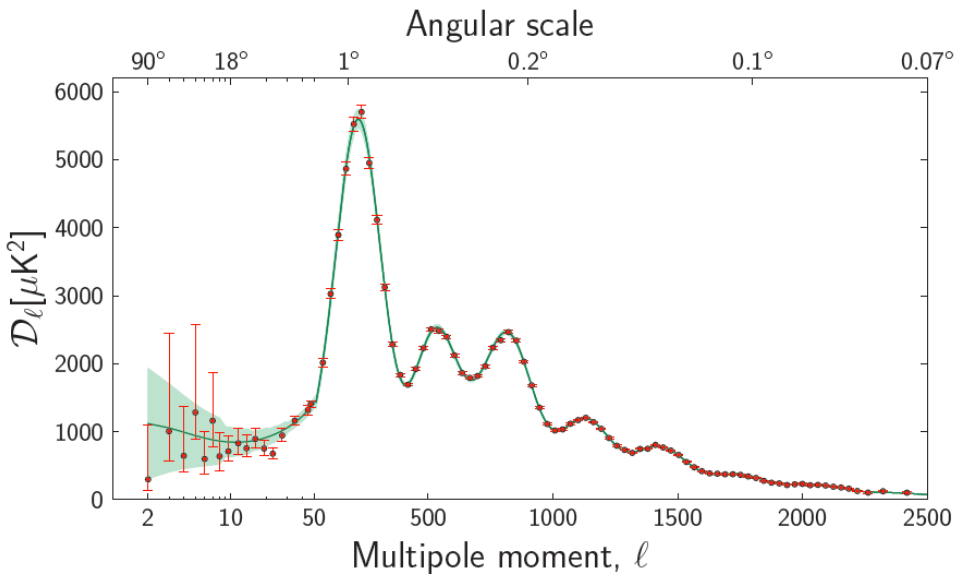

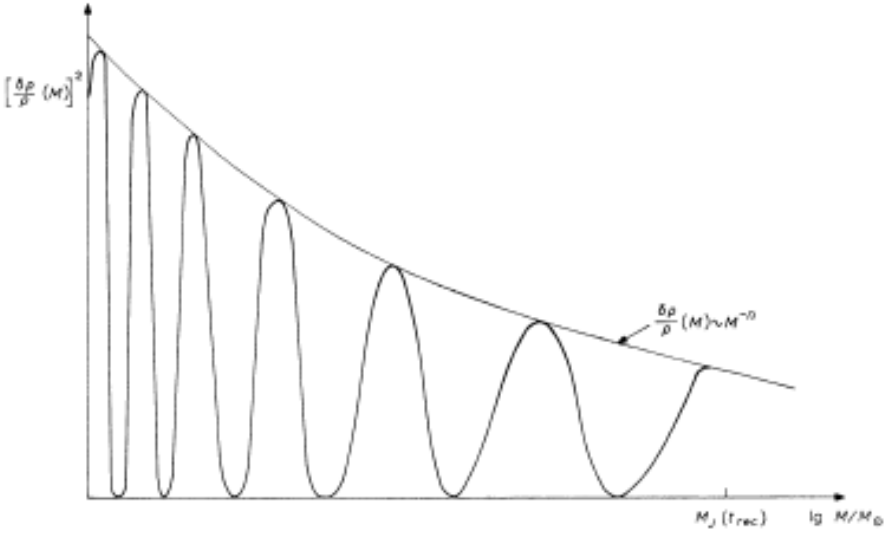

Fig. 1b. The dependence of the square of the amplitude of density perturbations of matter on scale. The fine line designates the usually assumed dependence $(\delta\rho/\rho)_M \sim M^{-n}$. It is apparent that fluctuations of relic radiation should depend on scale in a similar manner.

We have reached the resolution limit for CMB anisotropies

Silk damping of standing sound waves due to radiative viscosity and thermal conductivity

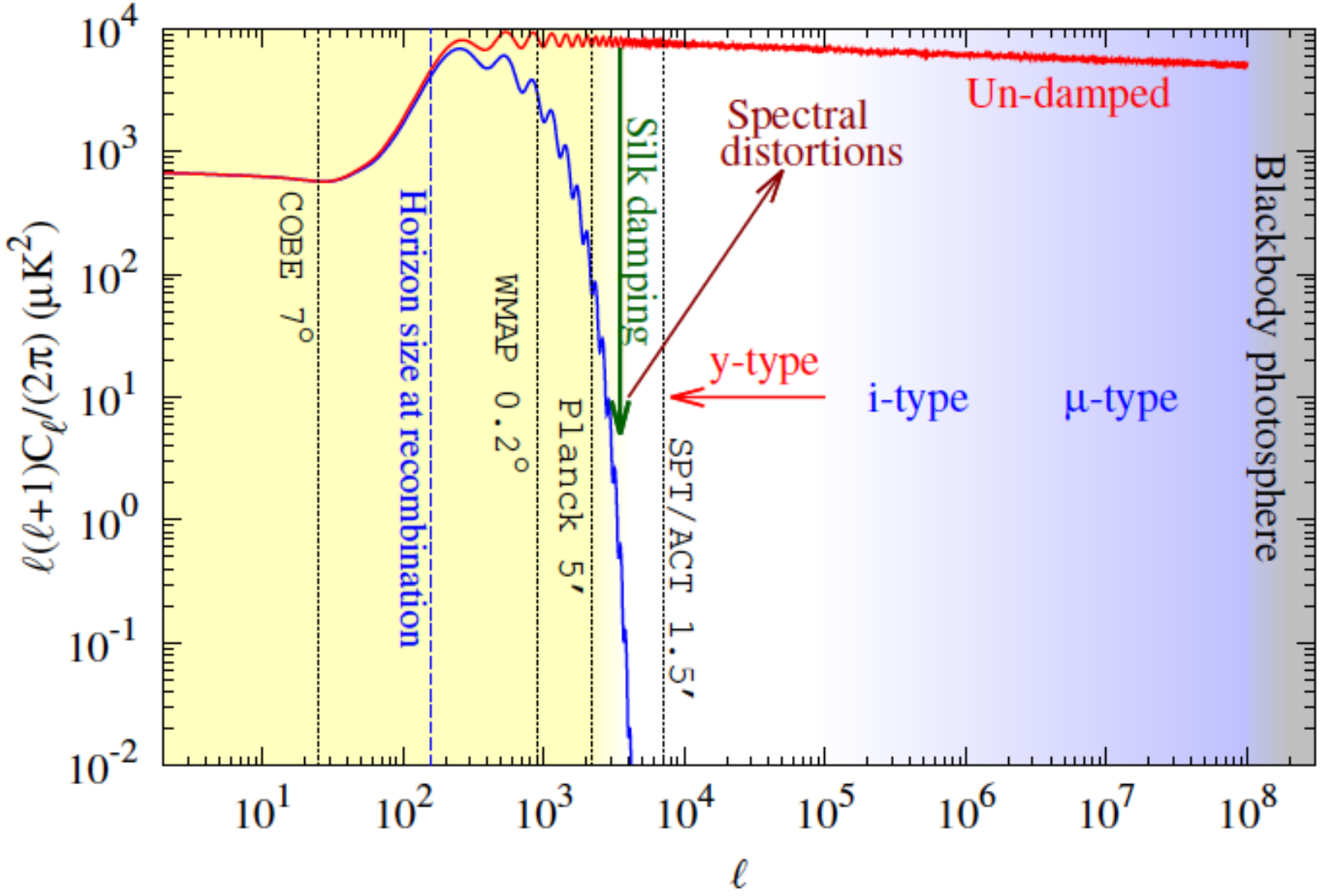

Going from 7 to 17 e-folds of inflation

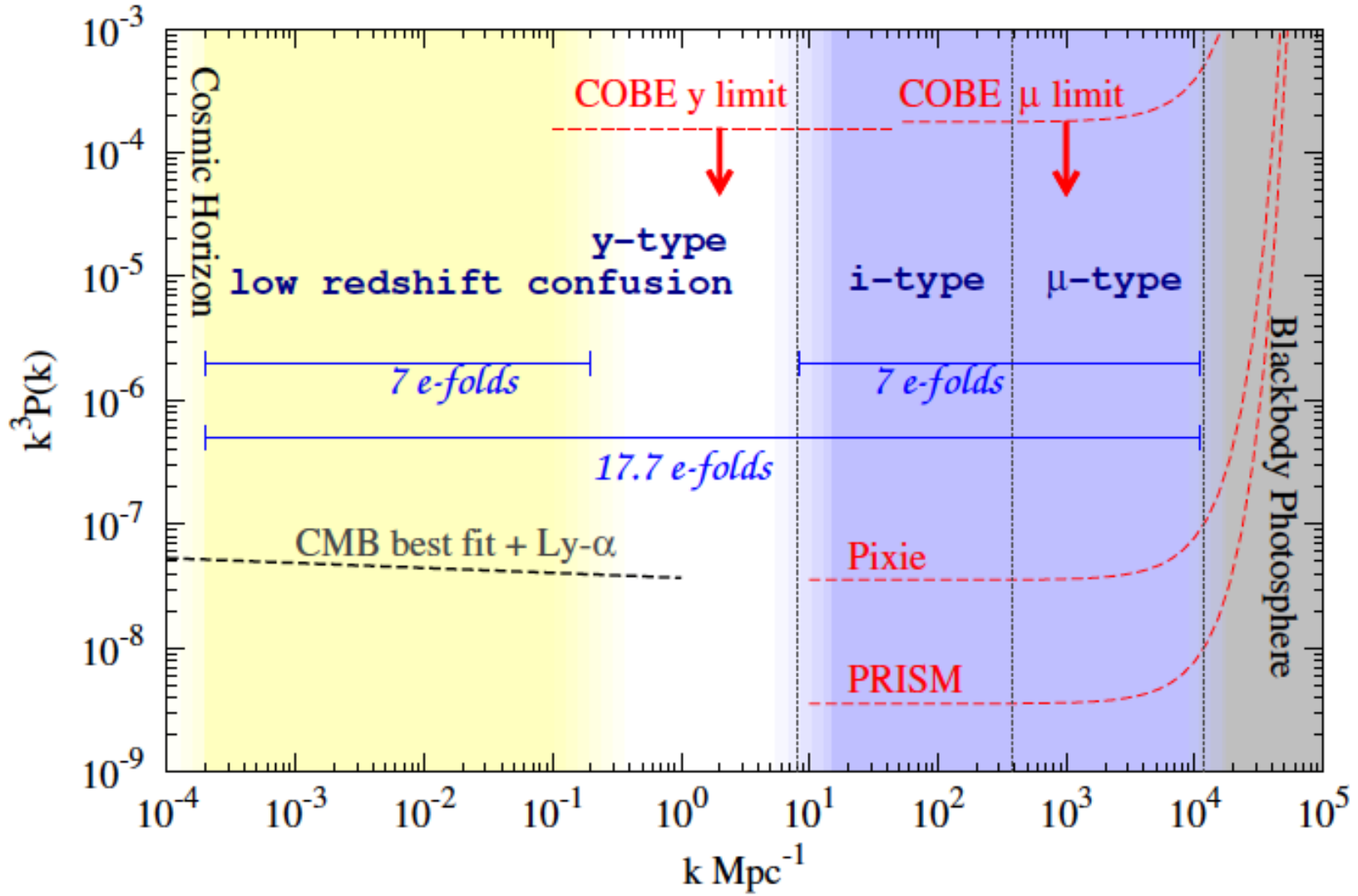

Pivot point $k_0 = 42\ \mathrm{Mpc}^{-1}$

Power spectrum of initial density perturbations

$$P_\zeta = (A_\zeta 2\pi^2/k^3)(k/k_0)^{n_s-1+\frac{1}{2}\mathrm{d}n_s/\mathrm{d}\ln k(\ln k/k_0)}$$

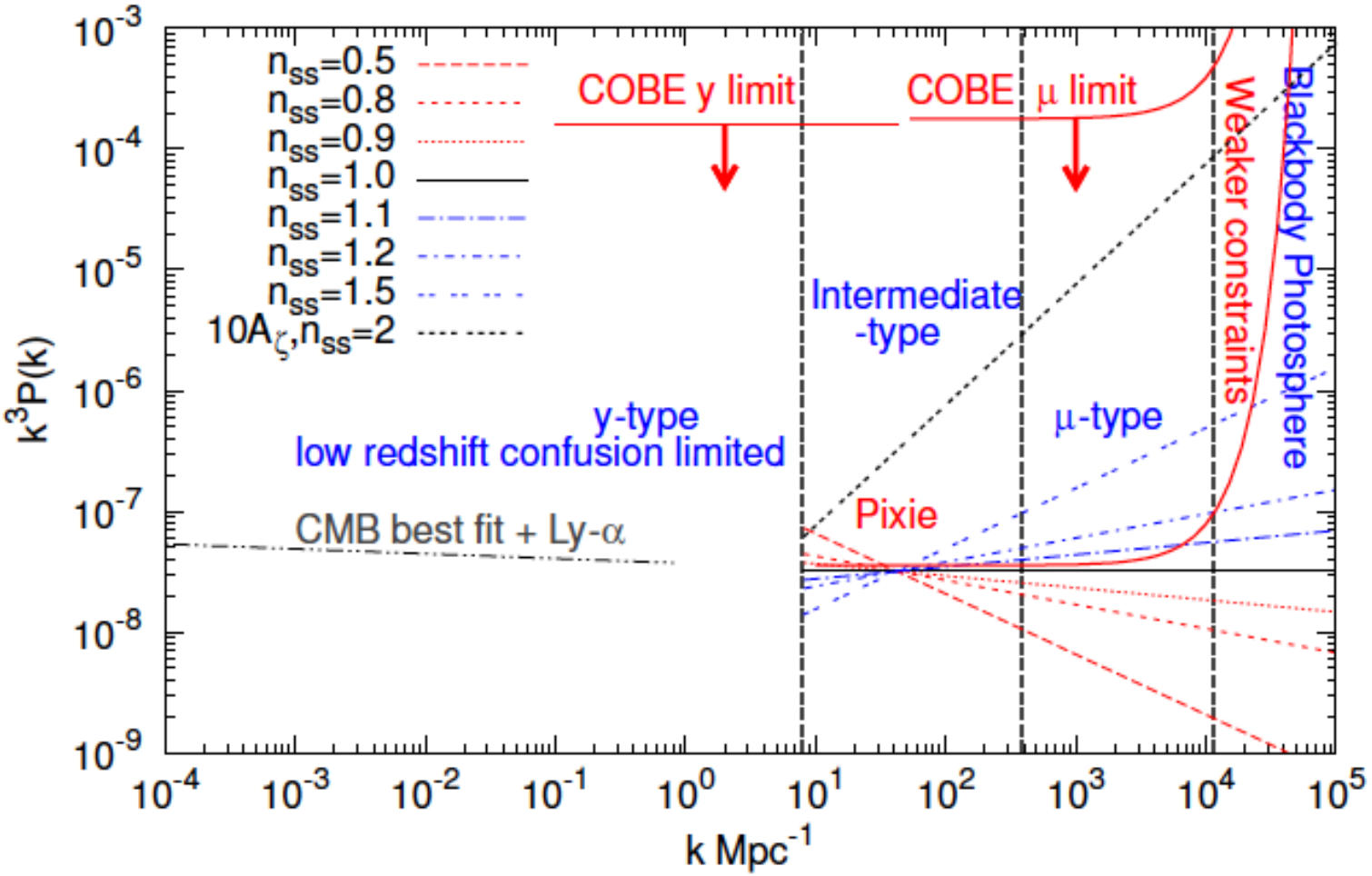

Planck spectrum

$$I_\nu = \frac{2h\nu^3}{c^2}\frac{1}{e^{h\nu/(k_B T)} - 1}$$

Relativistic invariant occupation number/phase space density

$$n(\nu) \equiv \frac{c^2}{2h\nu^3} I_\nu$$

$$n(x) = \frac{1}{e^x - 1} \quad , \quad x = \frac{h\nu}{k_B T}$$

Efficiency of energy exchange between electrons and photons

Recoil:

$$y_\gamma = \int \mathrm{d}t\, c\sigma_\mathrm{T} n_\mathrm{e} \frac{k_\mathrm{B} T_\gamma}{m_\mathrm{e} c^2}, \qquad T_\gamma = 2.725(1+z)$$

Doppler effect:

$$y_e = \int \mathrm{d}t\, c\sigma_\mathrm{T} n_\mathrm{e} \frac{k_\mathrm{B} T_\mathrm{e}}{m_\mathrm{e} c^2}$$

In early Universe $y_\gamma \approx y_\mathrm{e}$

y: Amplitude of distortion

$$y = \int \mathrm{d}t\, c\sigma_\mathrm{T} n_\mathrm{e} \frac{k_\mathrm{B} \left(T_\mathrm{e} - T_\gamma\right)}{m_\mathrm{e} c^2}$$

Efficiency of energy exchange between electrons and photons

Recoil:

$$y_\gamma = \int \mathrm{d}t\, c\sigma_\mathrm{T} n_e \frac{k_\mathrm{B} T_\gamma}{m_\mathrm{e} c^2}, \qquad T_\gamma = 2.725(1+z)$$

No. of scatterings

Doppler effect:

$$y_e = \int \mathrm{d}t\, c\sigma_\mathrm{T} n_\mathrm{e} \frac{k_\mathrm{B} T_\mathrm{e}}{m_\mathrm{e} c^2}$$

In early Universe $y_\gamma \approx y_\mathrm{e}$

y: Amplitude of distortion

$$y = \int \mathrm{d}t\, c\sigma_\mathrm{T} n_\mathrm{e} \frac{k_\mathrm{B} \left(T_\mathrm{e} - T_\gamma\right)}{m_\mathrm{e} c^2}$$

Efficiency of energy exchange between electrons and photons

Recoil:

$$y_\gamma = \int \mathrm{d}t\, c\sigma_\mathrm{T} n_e \frac{k_\mathrm{B} T_\gamma}{m_\mathrm{e} c^2}, \qquad T_\gamma = 2.725(1+z)$$

No. of scatterings Energy transfer per scattering

Doppler effect:

$$y_e = \int \mathrm{d}t\, c\sigma_\mathrm{T} n_\mathrm{e} \frac{k_\mathrm{B} T_\mathrm{e}}{m_\mathrm{e} c^2}$$

In early Universe $y_\gamma \approx y_\mathrm{e}$

y: Amplitude of distortion

$$y = \int \mathrm{d}t\, c\sigma_\mathrm{T} n_\mathrm{e} \frac{k_\mathrm{B}\left(T_\mathrm{e} - T_\gamma\right)}{m_\mathrm{e} c^2}$$

y-type (Sunyaev-Zeldovich effect) from clusters/reionization

$$y_\gamma \ll 1 \ , \ T_e \sim 10^4$$

$$y = (\tau_{\rm reionization}) \frac{k_B T_e}{m_e c^2} \sim (0.1)(1.6 \times 10^{-6}) \sim 10^{-7}$$

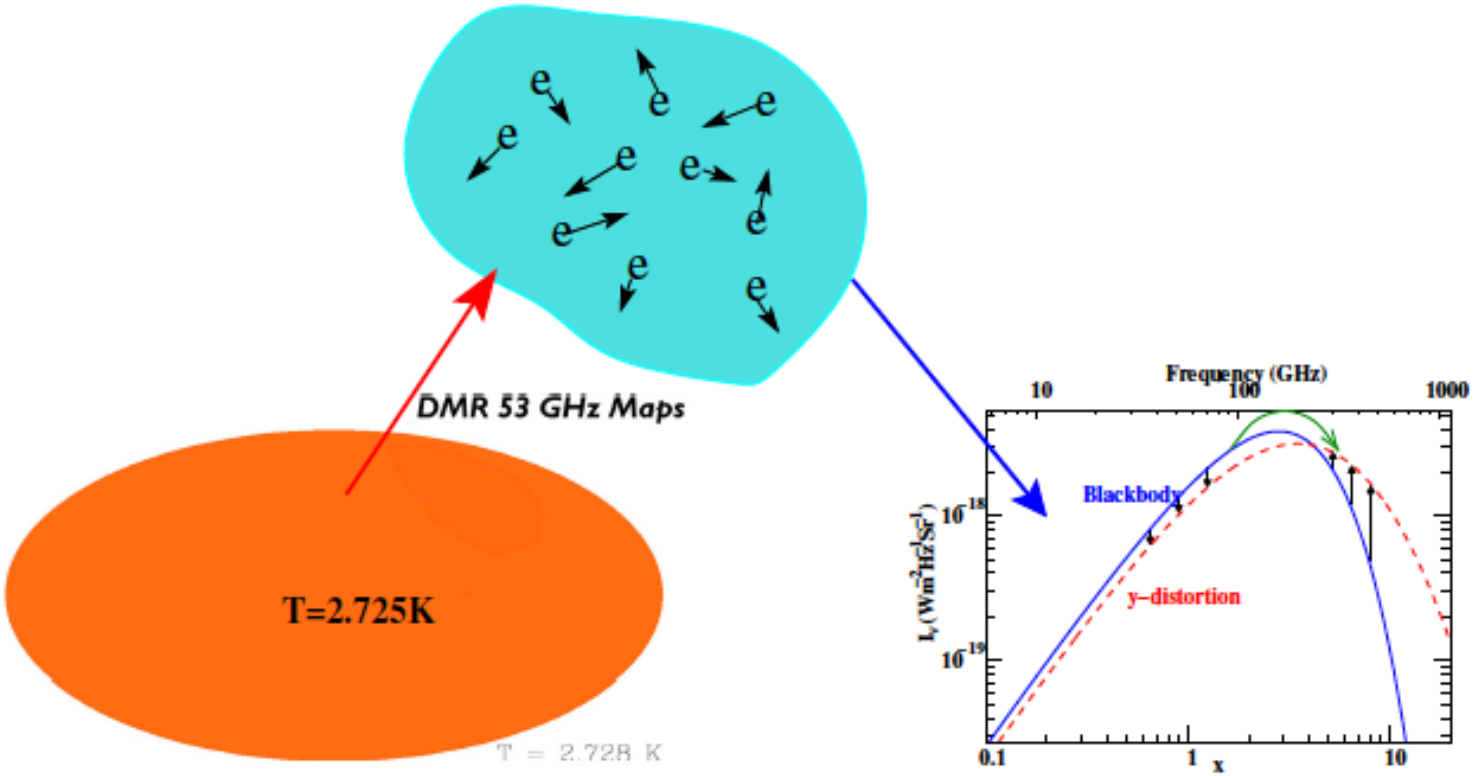

y-type (Sunyaev-Zeldovich effect) from clusters/reionization

$$n_{SZ} = y \; T^4 \frac{\partial}{\partial T} \frac{1}{T^2} \frac{\partial n_{\rm Pl}}{\partial T}$$

$$= \mathbf{y} \; \frac{\mathbf{x e^x}}{\mathbf{(e^x - 1)^2}} \left(\mathbf{x} \frac{\mathbf{e^x + 1}}{\mathbf{e^x - 1}} - \mathbf{4} \right)$$

$$\Delta I_{sz} = I_{sz} - I_{planck} = \frac{2h\nu^3}{c^2} n_{sz}$$

For $y_\gamma \gg 1$ equilibrium is established.

T_e and T_γ converge to common value

The photon spectrum relaxes to equilibrium Bose-Einstein distribution

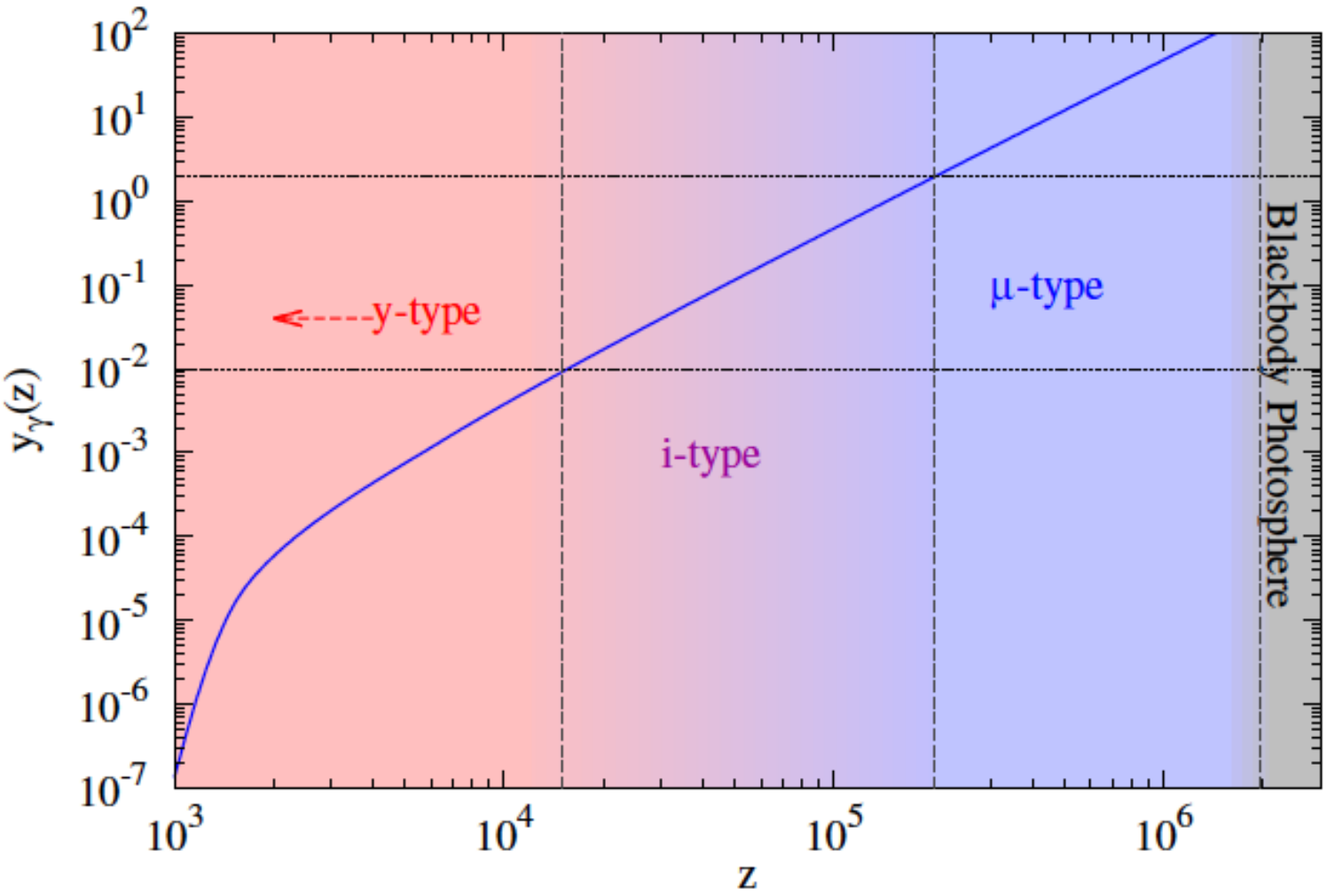

Bose-Einstein spectrum- Chemical potential (μ)

$$n(x) = \frac{1}{e^{x+\mu} - 1}$$

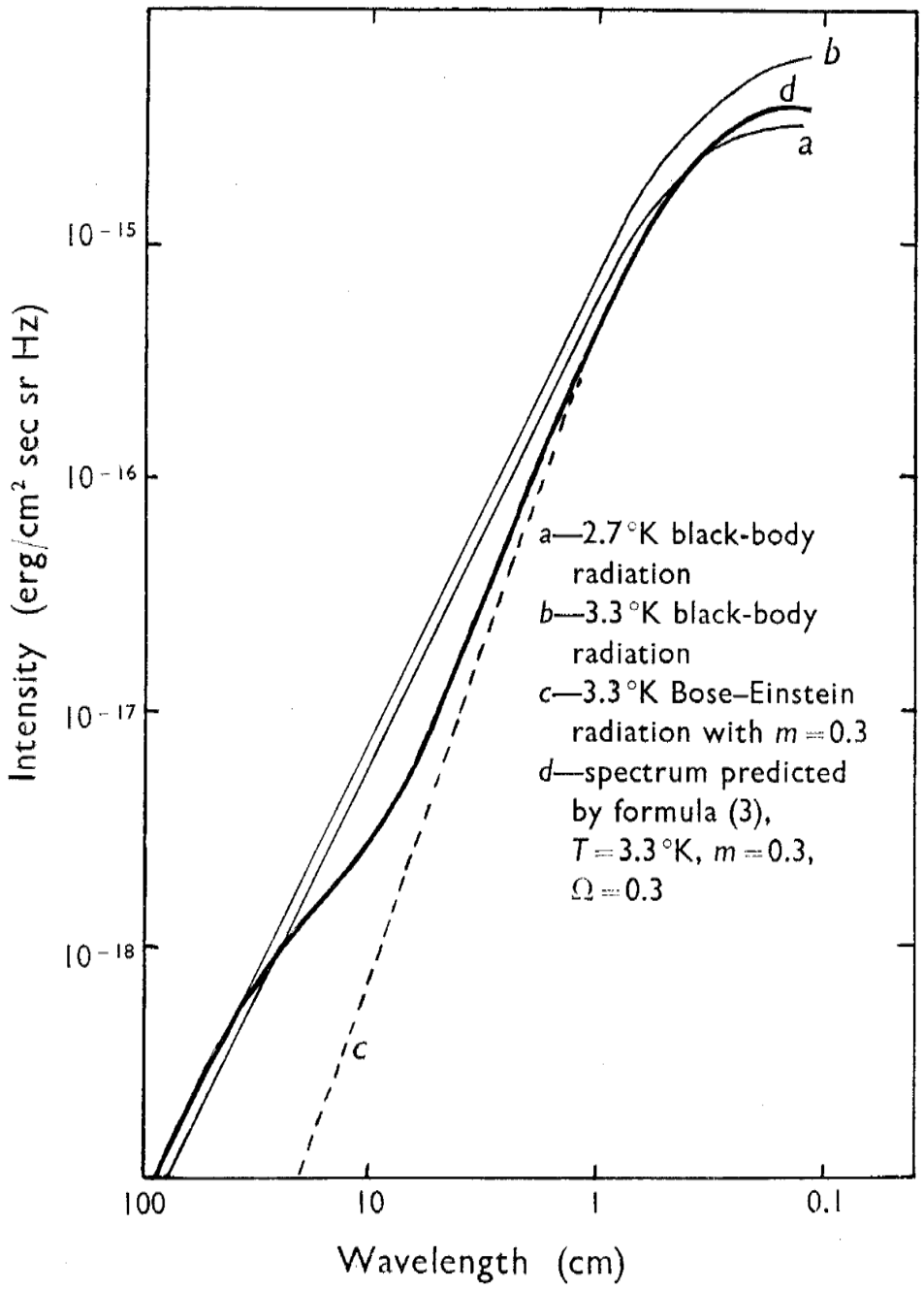

myu-type CMB distortions due to energy release in the early Universe 10^5 < z < 210^6

Sunyaev, Zeldovich, 1970

Bose-Einstein spectrum- Chemical potential (μ)

$$n(x) = \frac{1}{e^{x+\mu} - 1}$$

Given two constraints, energy density (E) and number density (N) of photons, T, μ uniquely determined.

Bose-Einstein spectrum

$$
\begin{aligned}
n_{\mathrm{BE}} &= \frac{1}{e^{\frac{h\nu}{k_{\mathrm{B}}T_{\mathrm{BE}}}+\mu}-1} \\
&= \frac{1}{e^{x-0.456\mu x+\mu}-1} \\
&\approx n_{\mathrm{pl}}(x) + \frac{\mu e^x}{(e^x-1)^2}\left(\frac{x}{2.19}-1\right),
\end{aligned}
$$

Bose-Einstein spectrum- Chemical potential (μ)

$$n(x) = \frac{1}{e^{x+\mu} - 1}$$

Given two constraints, energy density (E) and number density (N) of photons, T, μ uniquely determined.

Idea behind analytic solutions:

If we know rate of production of photons and energy injection rate, we can calculate the evolution/production of μ (and T)

μ-distortion: Bose-Einstein spectrum, $y_\gamma \gg 1$

COBE-FIRAS limit (95%): $\mu \lesssim 9 \times 10^{-5}$ *(Fixsen et al. 1996)*

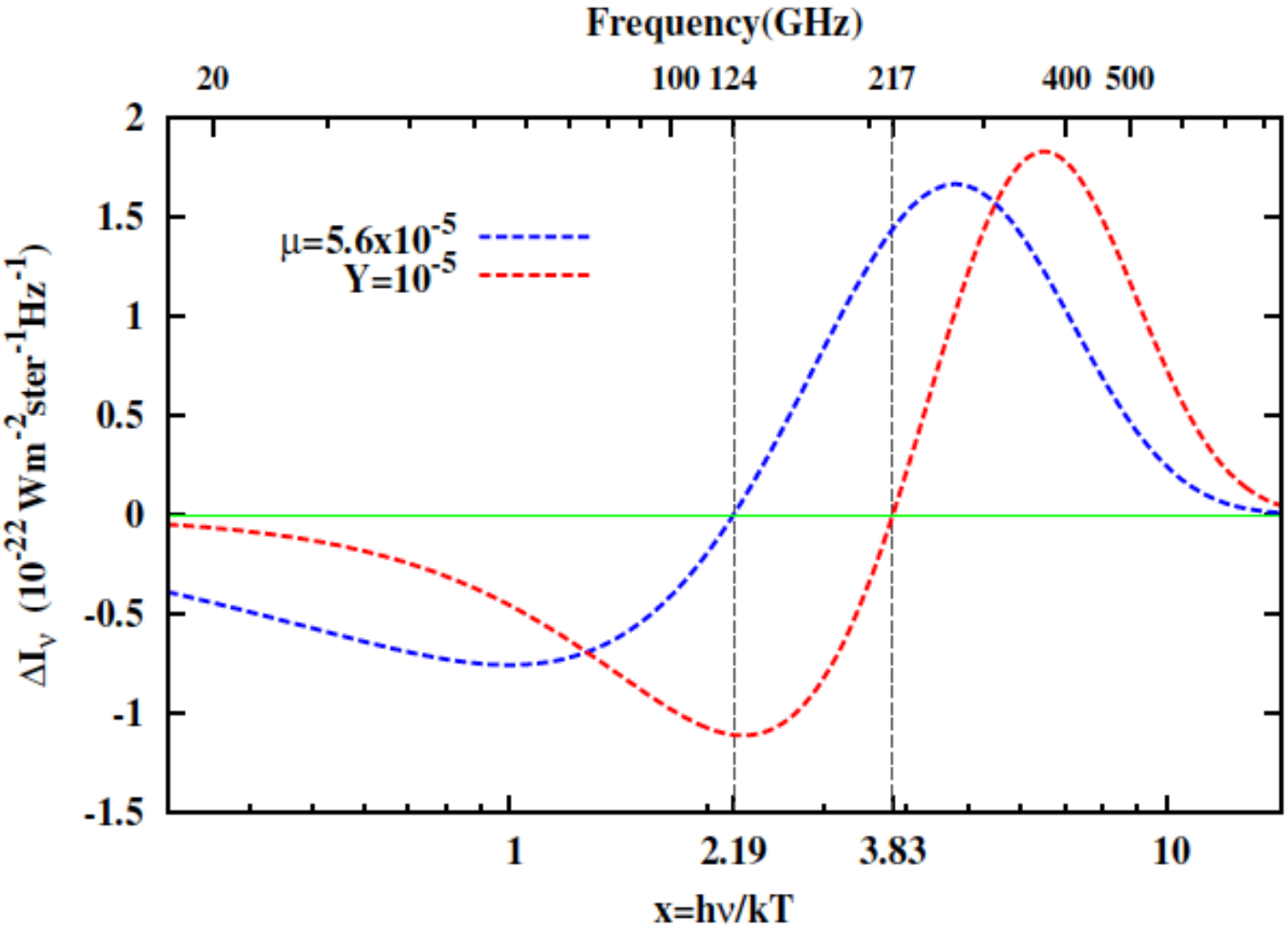

Intermediate-type distortions *(Khatri and Sunyaev 2012b)*

Solve Kompaneets equation with initial condition of $y-$type solution.

$$\frac{\partial n}{\partial y_\gamma} = \frac{1}{x^2}\frac{\partial}{\partial x}x^4\left(n+n^2+\frac{T_e}{T}\frac{\partial n}{\partial x}\right), \quad \frac{T_e}{T} = \frac{\int (n+n^2)x^4dx}{4\int nx^3dx}$$

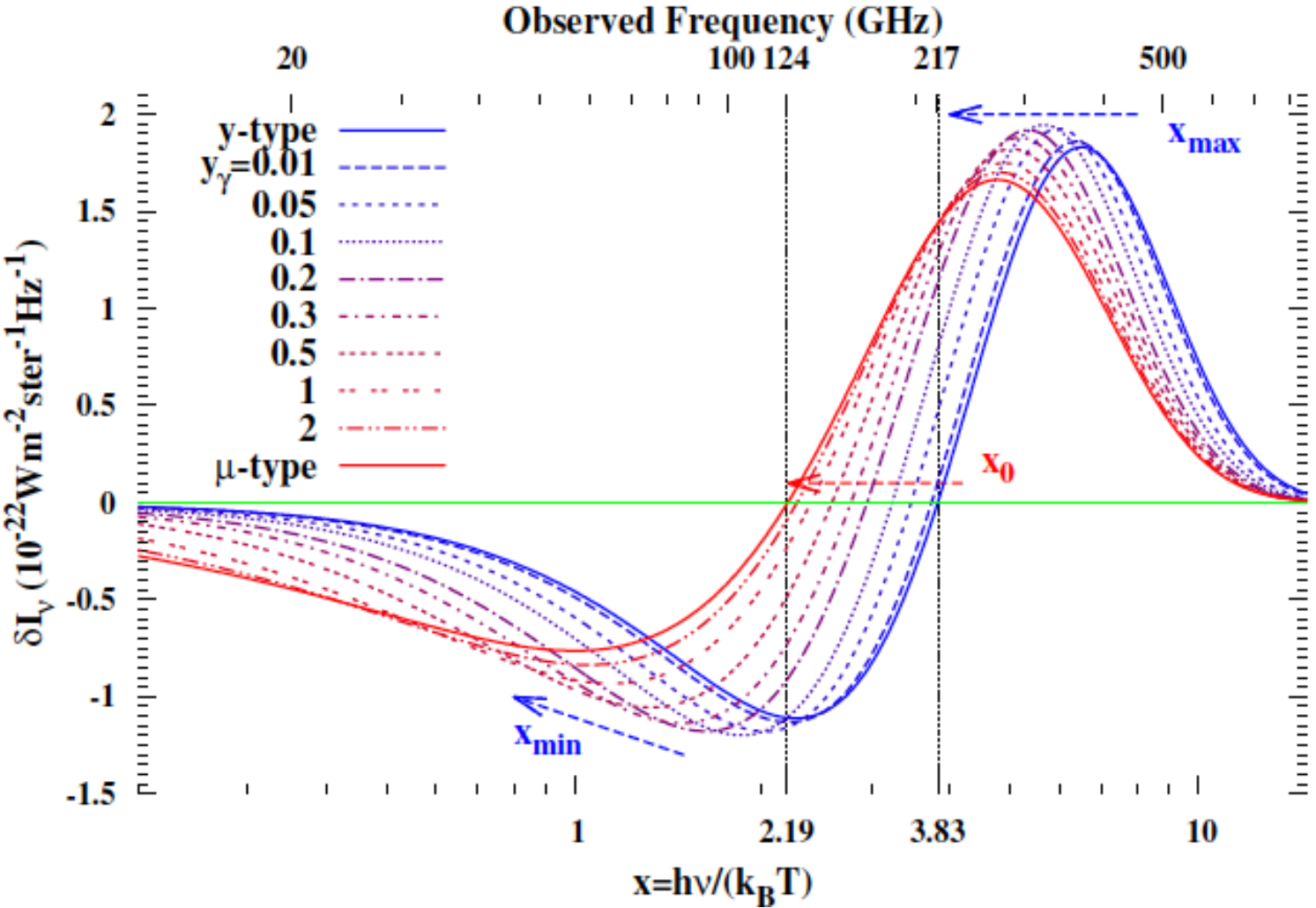

Processes responsible for creation of CMB spectrum

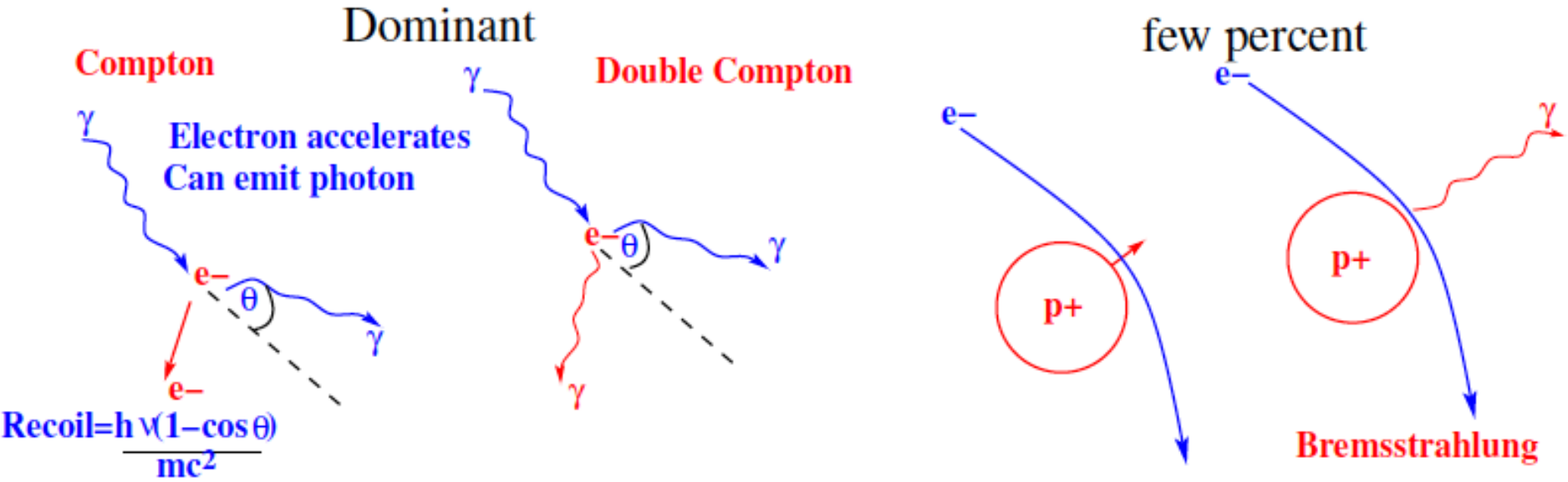

- Double Compton and bremsstrahlung create/absorb photons ($\propto 1/x^2$)
- Compton scattering distributes them over the whole spectrum

Creation of CMB Planck spectrum

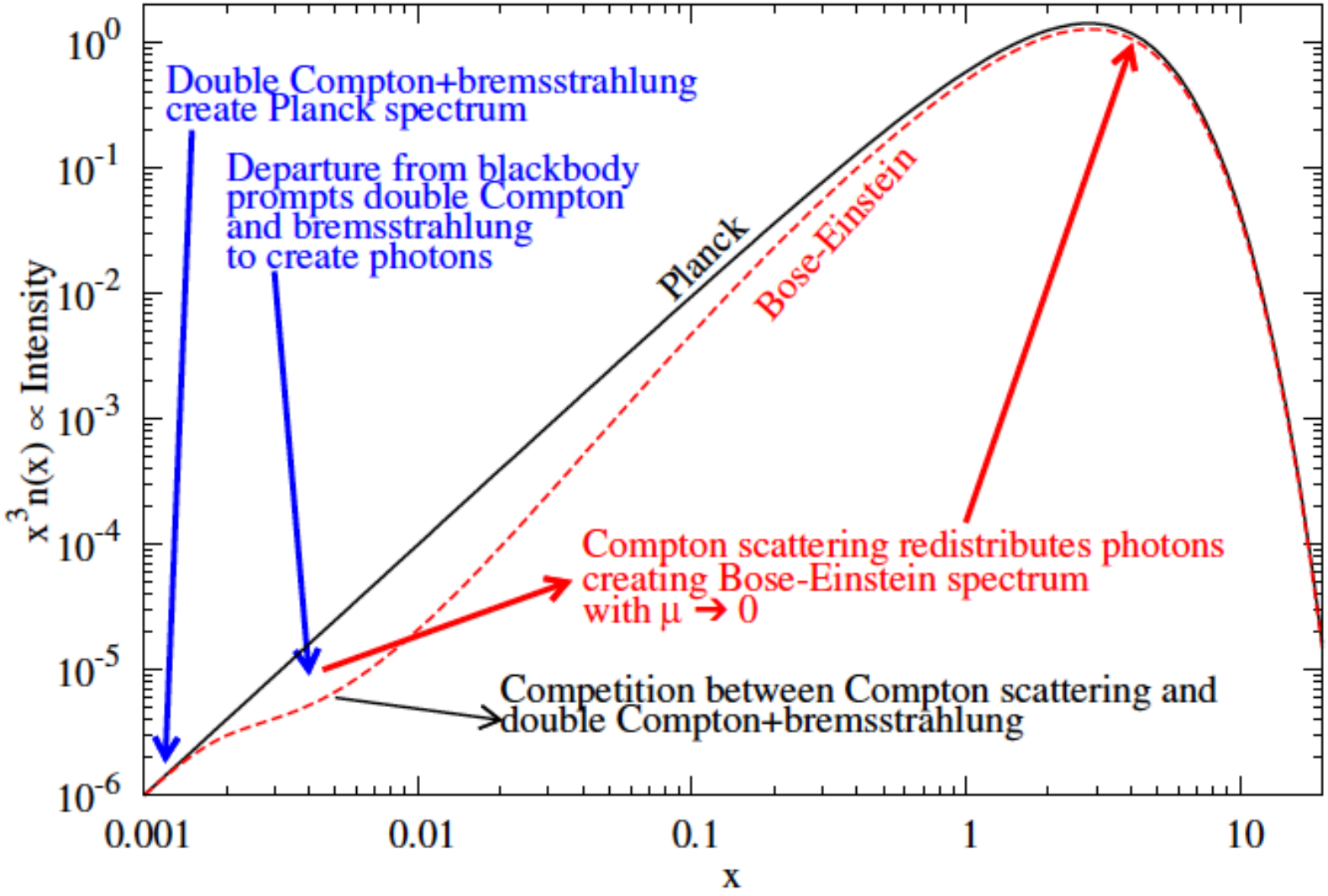

Analitical solution(Sunyaev, Zeldovich, 1970

$$\mu = \mu(t_0)\, e^{-2\sqrt{(ak)}\,(t-t_0)}$$

Where a and k are scattering (Comptonisation) and real absorption coefficients correspondently

In the case of Double Compton (emission of second photon during scattering) spectral deviations decrease with time

$$\frac{\mu^{\text{final}}}{\mu^{\text{initial}}} \approx e^{-(z_i/z_{dc})^{5/2}}$$

Danese, de Zotti, 1984

μ-type distortions

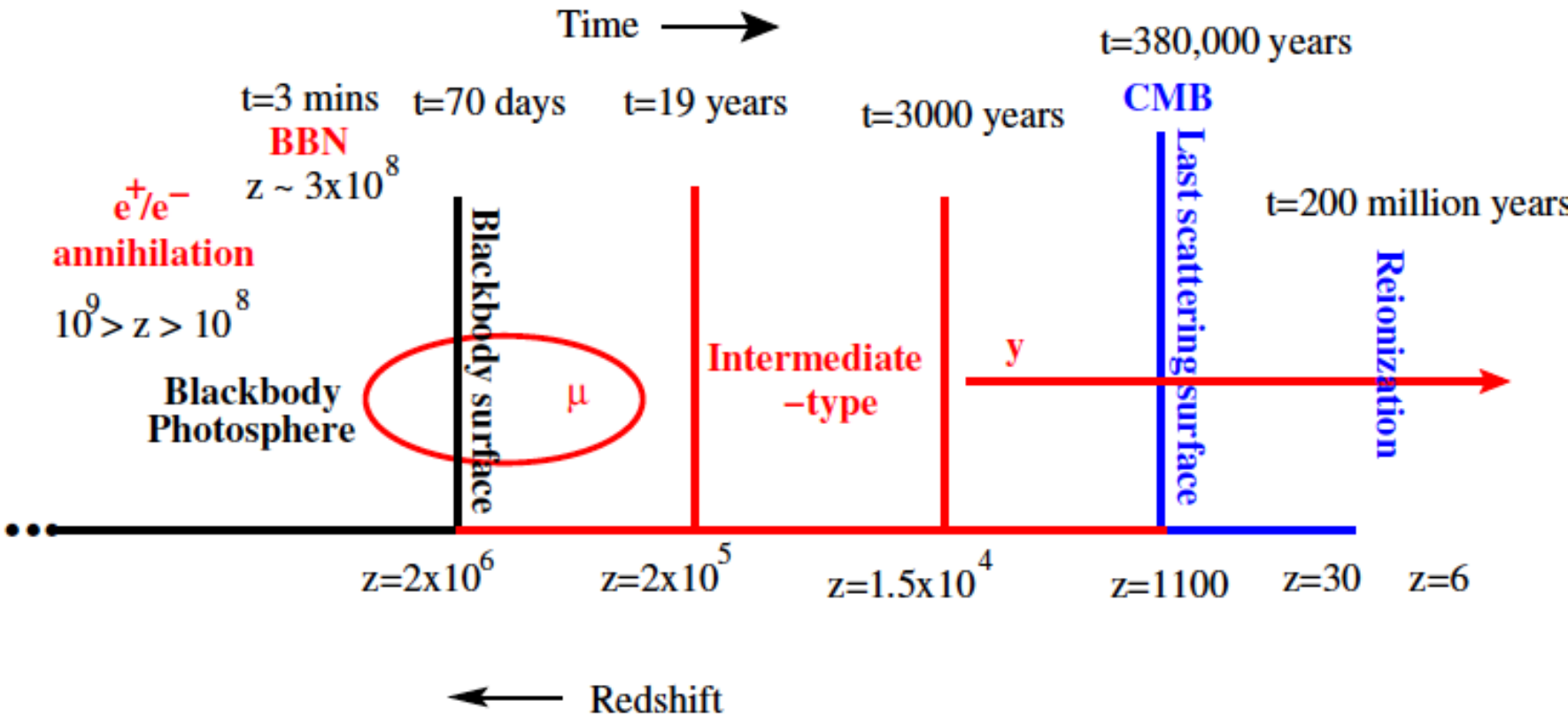

Compton + double Compton + bremsstrahlung

Analytic solution: $\mu = 1.4 \int \frac{dQ}{dz} e^{-\mathcal{J}(z)} dz$

(Sunyaev and Zeldovich 1970)

The general picture

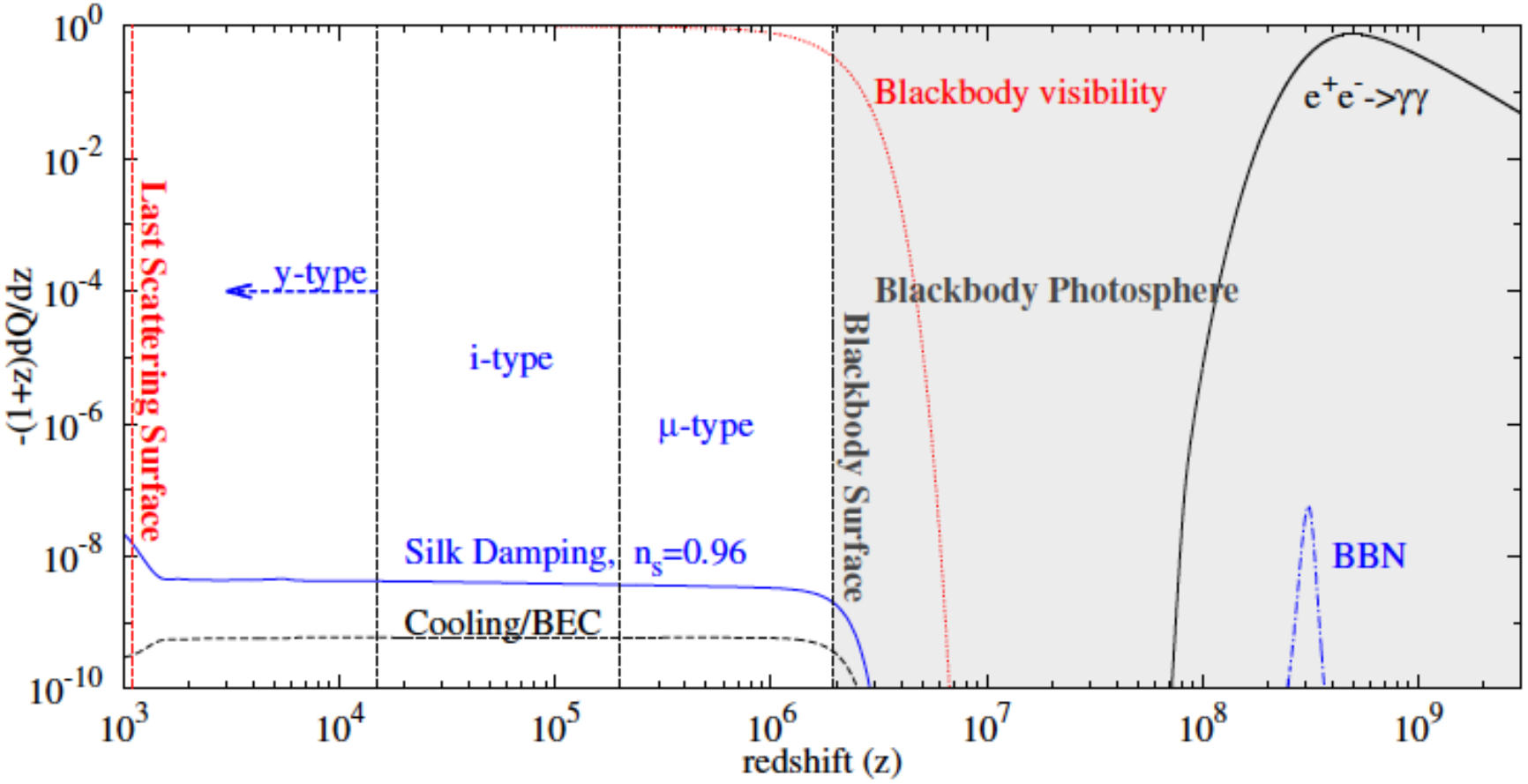

The Silk damping scale

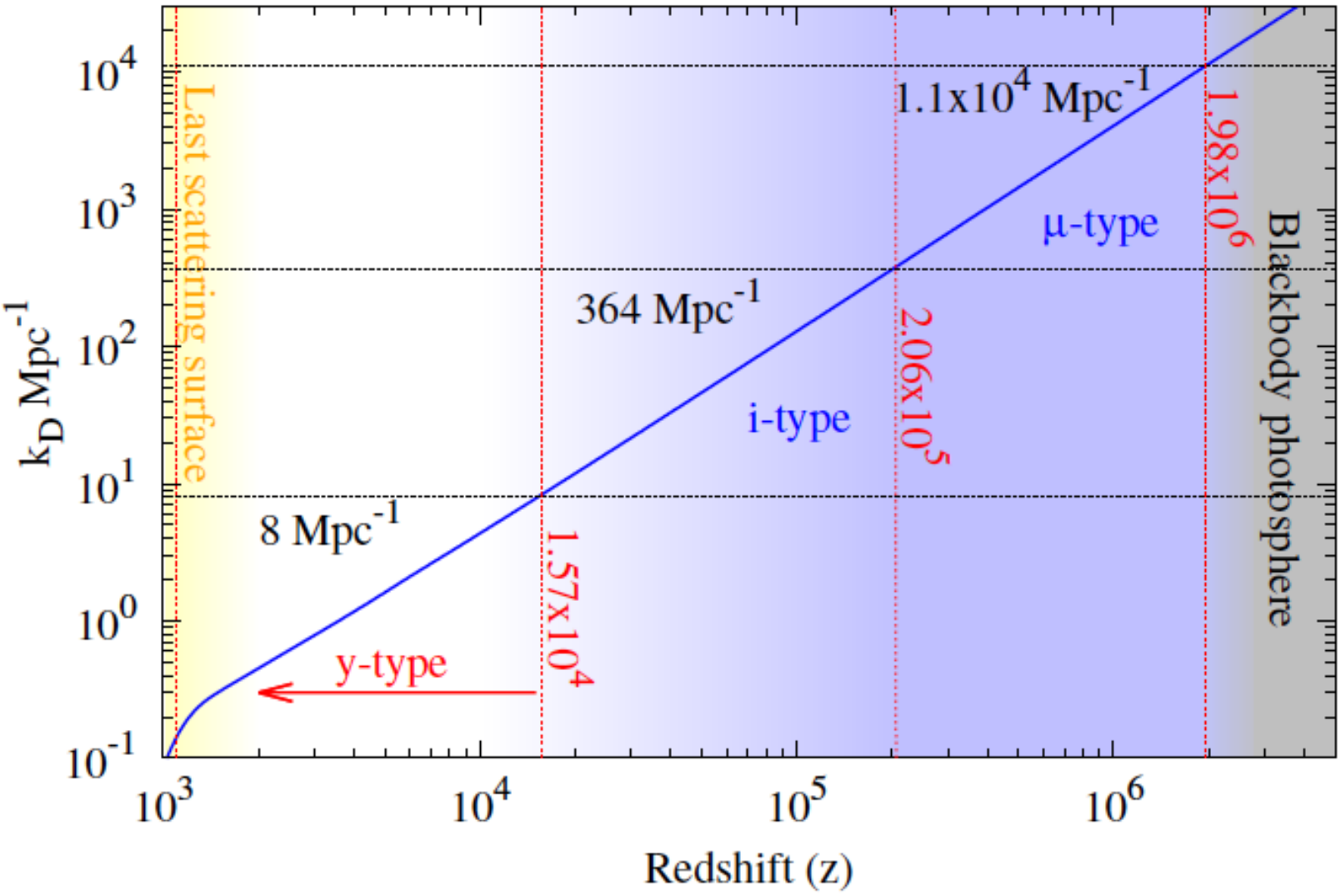

Pivot point $k_0 = 42\ \mathrm{Mpc}^{-1}$

$$P_\zeta = (A_\zeta 2\pi^2/k^3)(k/k_0)^{n_s-1+\frac{1}{2}\mathrm{d}n_s/\mathrm{d}\ln k(\ln k/k_0)}$$

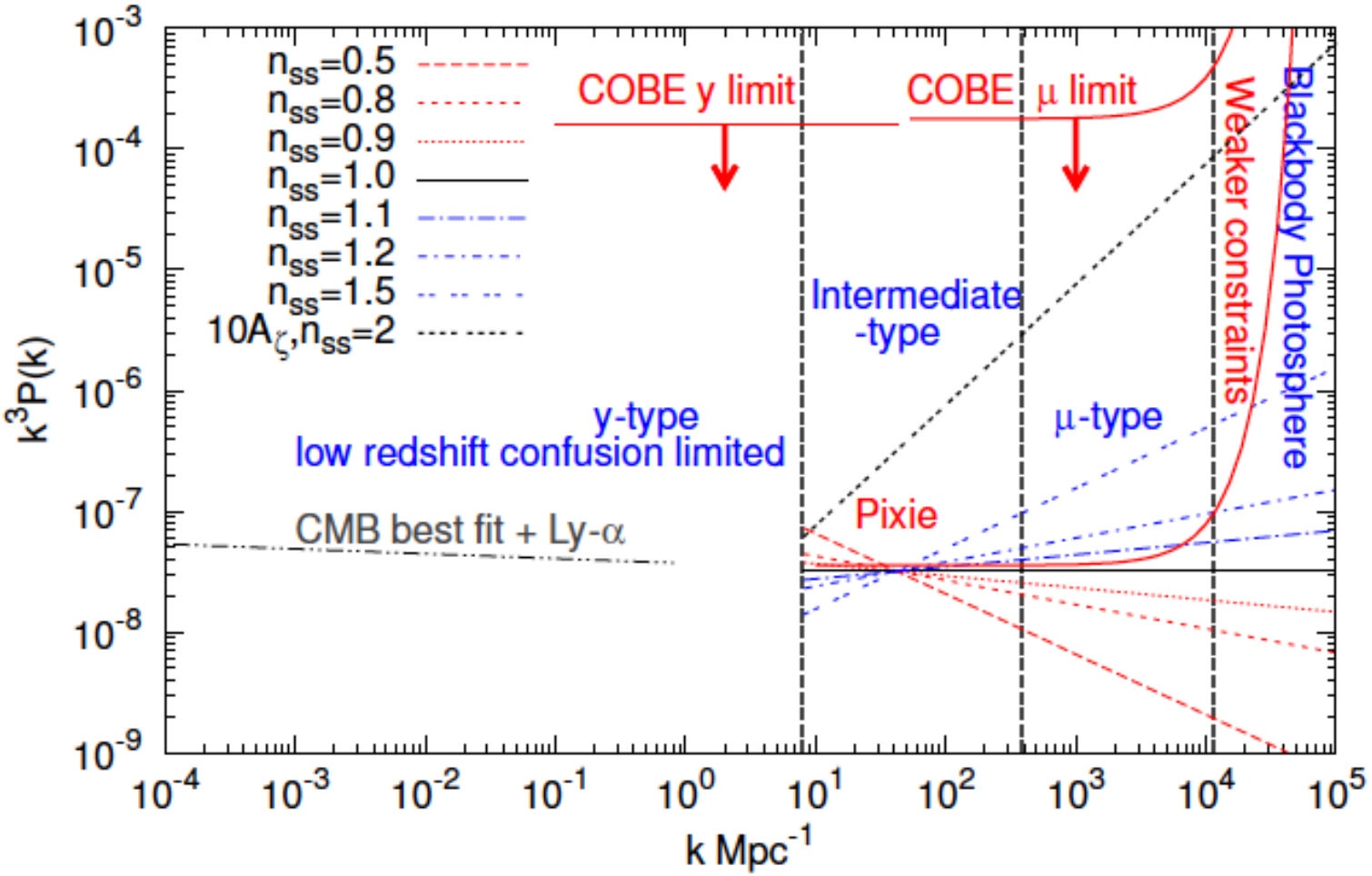

Summary

- The shape of the μ and intermediate type distortions is rich in information
- With spectral distortions we can extend our 'view' of inflation from 6-7 e-folds at present to 17 e-folds
- Spectral distortions take us a little nearer to the end of inflation
- μ-type and intermediate type distortions can be calculated very fast using analytic and pre-calculated cosmology-independent high precision numerical solutions (Green's functions). This allows us to explore the rich multidimensional parameter space
- i-type distortions are quite powerful in removing degeneracies between power spectrum parameters. The extra information comes from the shape of the i-type distortion

Summary continued

With intermediate-type distortions we can distinguish between different mechanisms of energy injection which have different redshift dependence

There is more....

- Cosmological recombination spectrum gives measurement of primordial helium

  Kurt,Zeldovich,Sunyaev,Peebles,Dubrovich,Chluba,Rubino-Martin

- Resonant scattering on C,N,O and other ions during and after reionization makes the optical depth to the last scattering surface frequency dependent

  Basu, Hernandez-Monteagudo, and Sunyaev 2004

- Sunyaev-Zeldovich effect from hot electrons during reionization/WHIM can give a measurement of average electron temperature, find missing baryons

  Zeldovich & Sunyaev 1969, Hu, Scott, Silk 1994, Cen and Ostriker 1999,2006,

- Primordial non-gaussianity on extremely small scales
  Pajer and Zaldarriaga 2012, Ganc and Komatsu 2012

Summary continued

- Silk damping: $\frac{dQ}{dz} \propto (1+z)^{(3n_s-5)/2}$
  (Chluba, Khatri and Sunyaev 2012, Khatri, Sunyaev and Chluba 2012)
- Adiabatic cooling: Opposite sign to Silk damping with $n_s = 1$
  (Chluba and Sunyaev 2012, Khatri, Sunyaev and Chluba 2012b)
- Particle decay: $\frac{dQ}{dz} \propto \frac{e^{-\left(\frac{1+z_{\rm decay}}{1+z}\right)^2}}{(1+z)^4}$
  (Hu and Silk 1993, Chluba and Sunyaev 2012, Khatri and Sunyaev 2012a, 2012b)
- Cosmic strings: $\frac{dQ}{dz} \propto$ constant
  Tashiro, Sabancilar, Vachaspati 2012
- Primordial magnetic fields : $\propto (1+z)^{(3n+7)/2}$, n is the spectral index of magnetic field power spectrum *(Jedamzik, Katalinic, and Olinto 2000)*
- Black holes: Depends on the mass function
  Tashiro and Sugiyama 2008, Carr et al. 2010
- Quantum wave function collapse: $\frac{dQ}{dz} \propto (1+z)^{-4}$
  Lochan, Das and Bassi 2012

There is still a long road ahead for CMB cosmology

CMB spectrum is very rich in information about the early Universe, late time Universe and fundamental physics

This information is accessible and within reach of experiments in not too far future: Pixie, PRISM

Thank you !!!

the blurring of primordial fluctuations. Thomson tau = 0.85 (WMAP)

full analogy with Gunn-Peterson effect, but Tr inhomogeneities on the sky are playing the role of quasars and submm lines are used instead Ly-alpha.

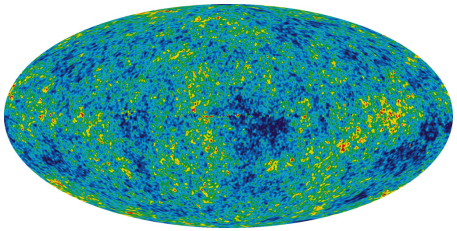

Hot and cold spots

zero effect for monopole, polarization from quadrupole

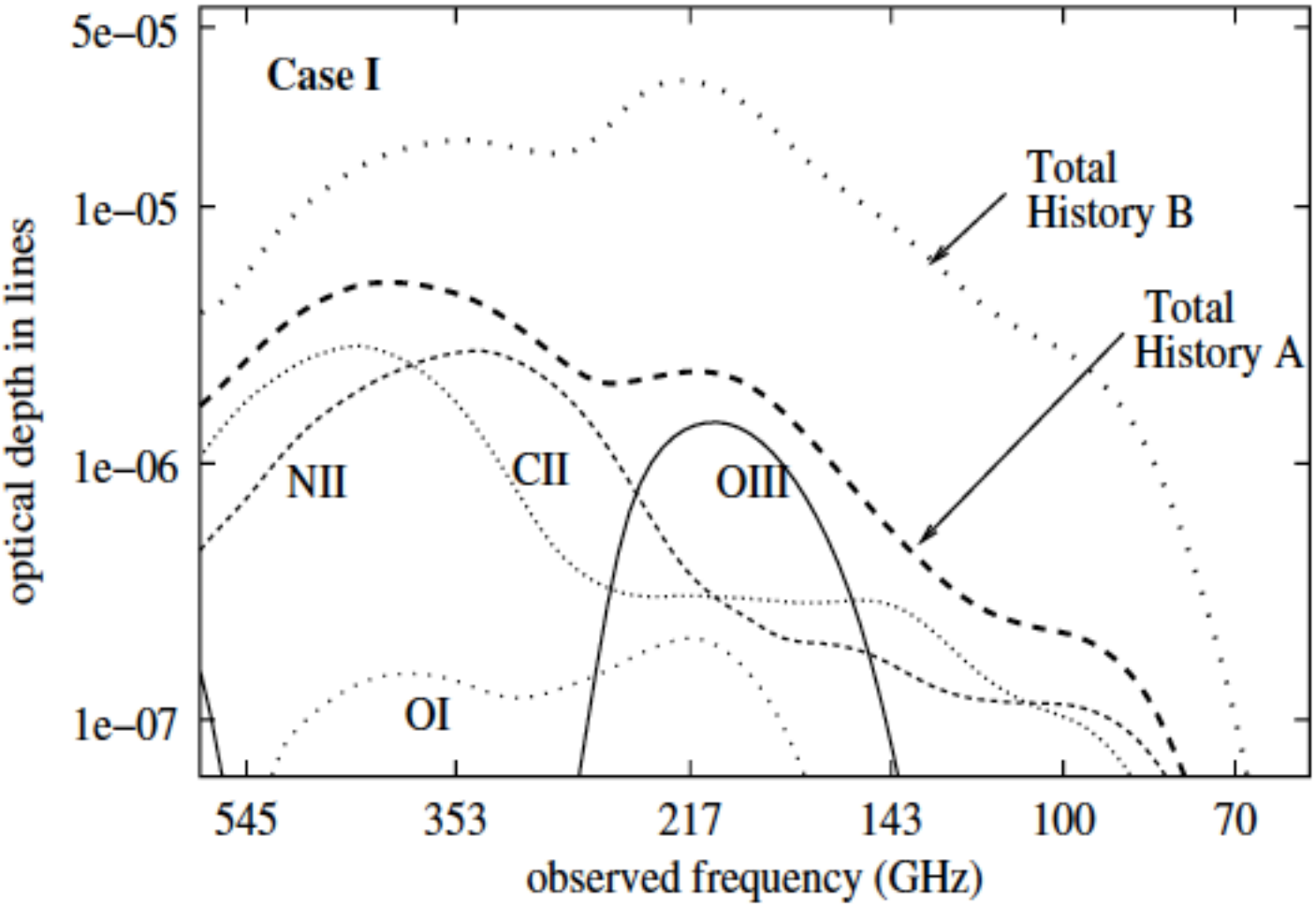

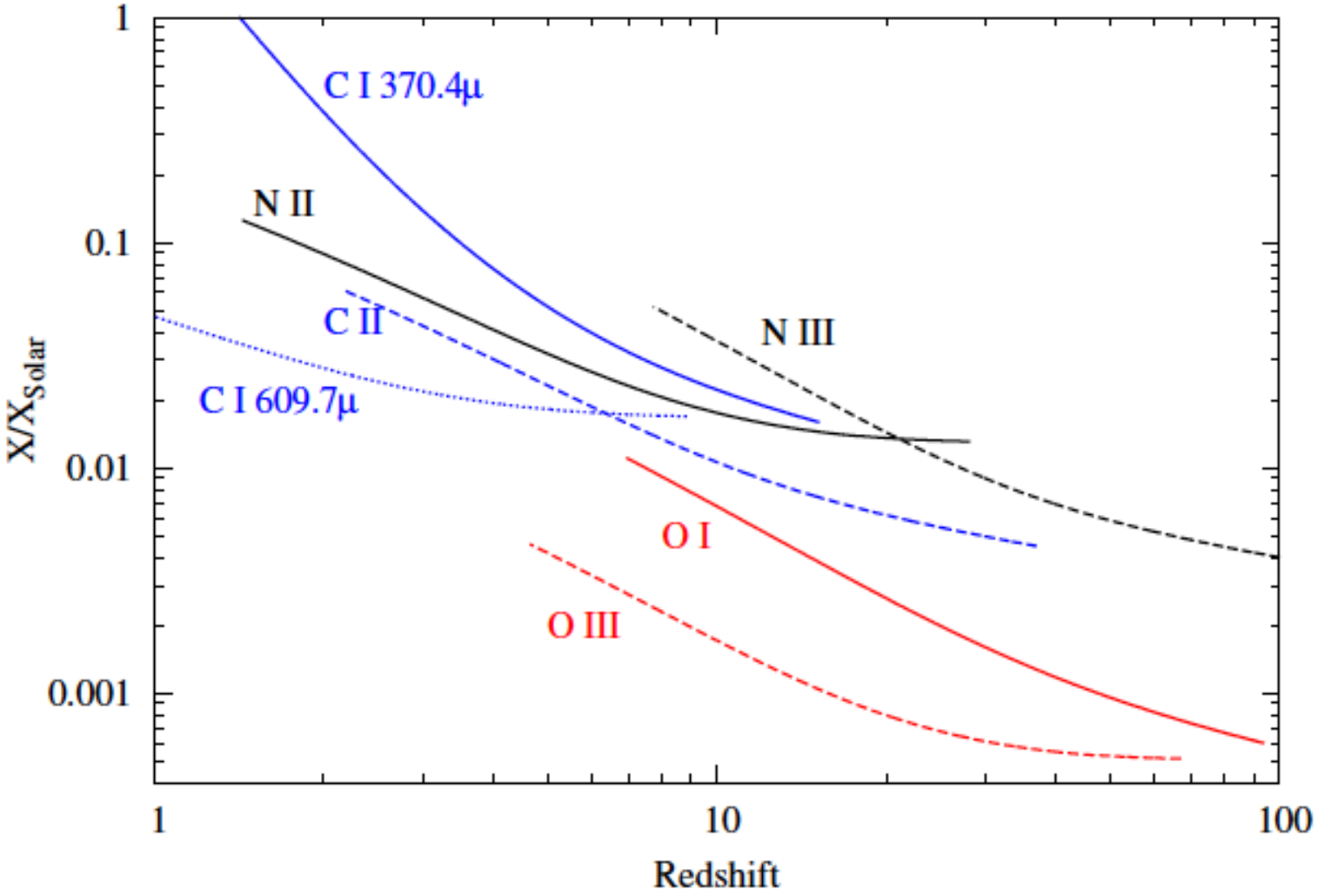

Figure 47. Projected constraints on abundance of C,N,O atoms and ions from 50-600 GHz channels of PRISM assuming it will have the inter-channel calibration accuracy of 0.001% to be able to measure the difference in the optical depth (to the last scattering surface) seen by different channels of $\tau_{LSS} = 10^{-5}$. The highest and lowest redshifts at the endpoints of the each curve correspond to 50 GHz and 600 GHz observed frequency respectively. The constraints as a fraction of solar abundance are plotted, with the reference solar abundances taken to be photosphere abundances in [399].

COrE mission with internal calibrator ? and angular resolution < 20’ will be able to provide C_l on the level of 10^-2 microK^2 and detect O III ions with 4 10^-5 of solar abundance of oxygen

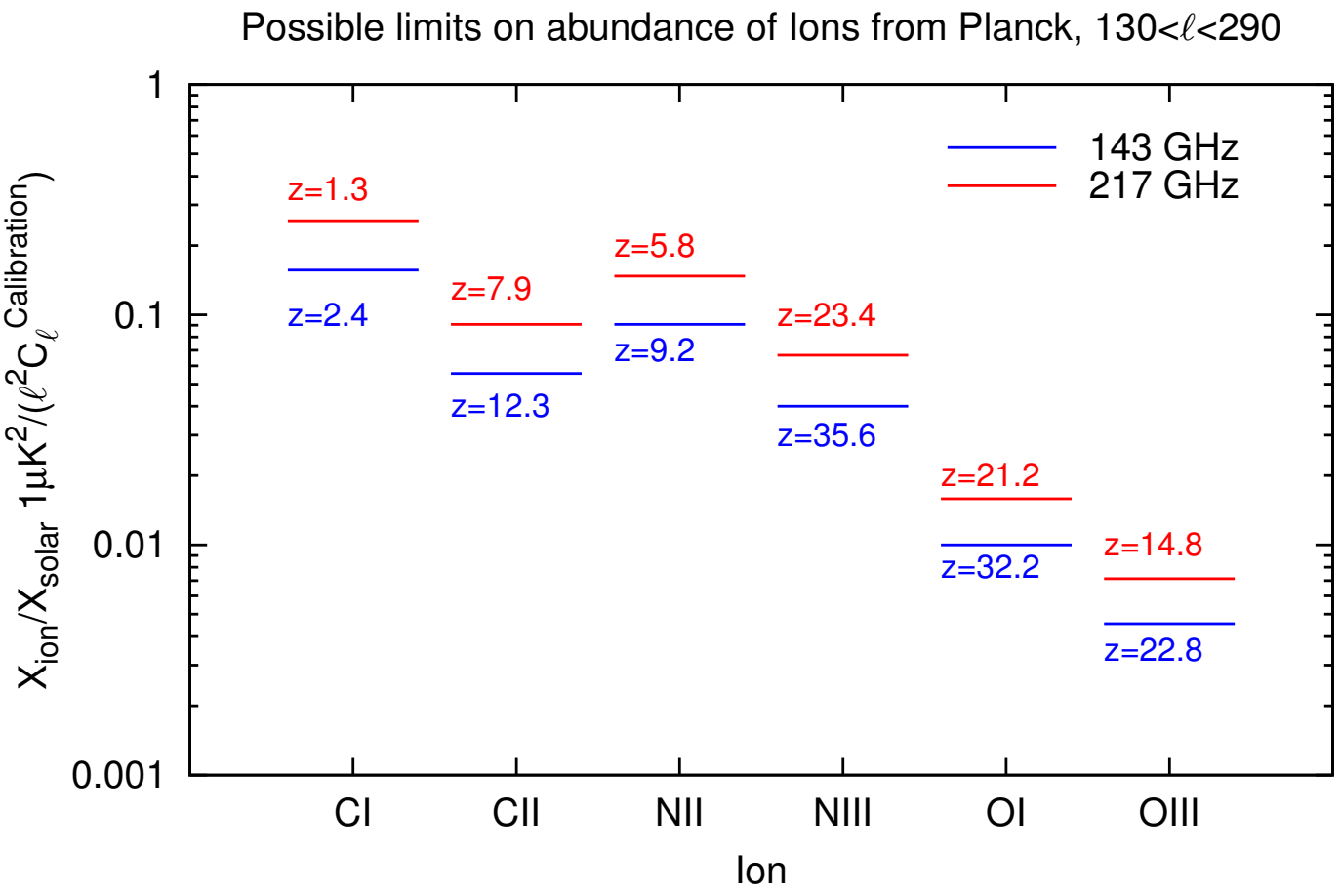

Khatri, Sunyaev, 2012

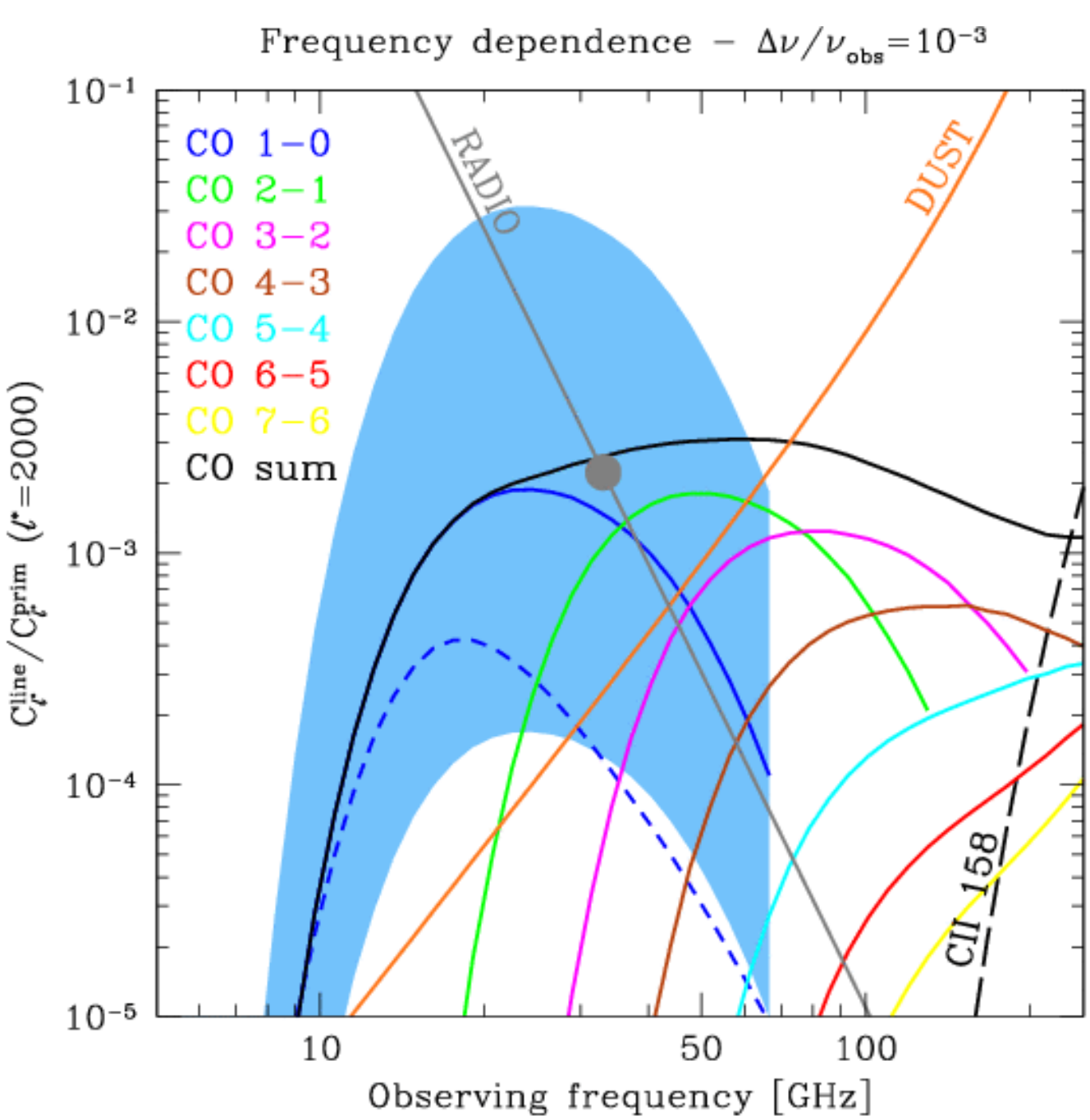
Frequency dependence – $\Delta\nu/\nu_{obs}=10^{-3}$
CO 1–0
CO 2–1
CO 3–2
CO 4–3
CO 5–4
CO 6–5
CO 7–6
CO sum
RADIO
DUST
CII 158
$C_\ell^{line}/C_\ell^{prim}$ ($\ell^*=2000$)
10^{-1}
10^{-2}
10^{-3}
10^{-4}
10^{-5}
10
50
100
Observing frequency [GHz]

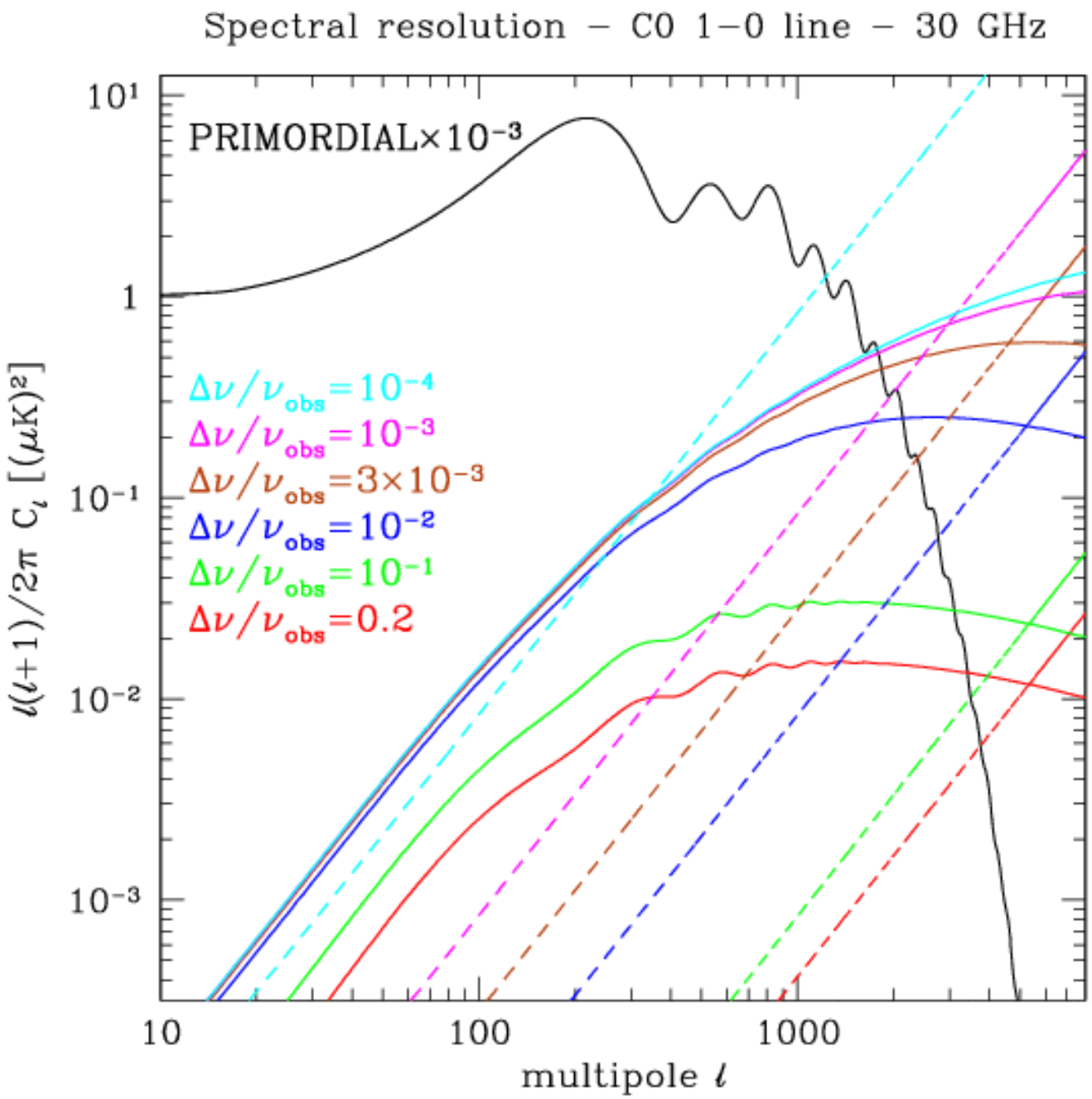

Correlated contribution (solid curves)

Poisson contribution (dashed lines) behaves differently

too high spectral resolution is useless for correlated contribution

SZ effect in electron rest frame: Mixing of blackbodies in the dipole seen by the electron

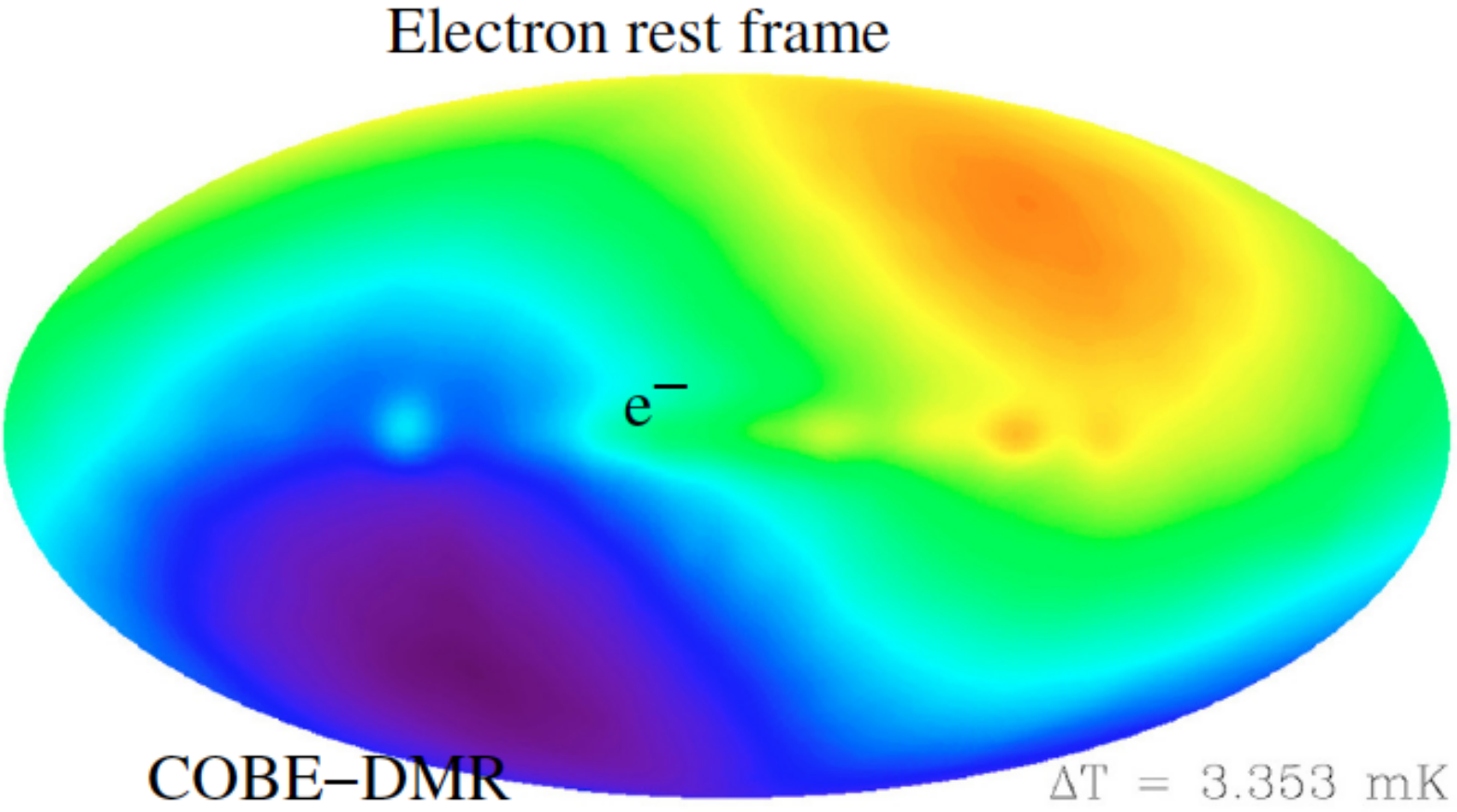

Solutions for $\mathscr{T}(Z)$

Old solutions

(*Sunyaev and Zeldovich 1970, Danese and de Zotti 1982*)
Extension of old solutions to include both double Compton and bremsstrahlung

$$\mathscr{T}(z) \approx \left[\left(\frac{1+z}{1+z_{\rm dC}}\right)^5 + \left(\frac{1+z}{1+z_{\rm br}}\right)^{5/2}\right]^{1/2} + \varepsilon \ln\left[\left(\frac{1+z}{1+z_\varepsilon}\right)^{5/4} + \sqrt{1+\left(\frac{1+z}{1+z_\varepsilon}\right)^{5/2}}\right]$$

This solution has accuracy of $\sim 10\%$, $z_{\rm dC} \approx 1.96 \times 10^6$

Numerical studies: Illarionov and Sunyaev 1975, Burigana, Danese, de Zotti 1991, Hu and Silk 1993, Chluba and Sunyaev 2012

New solution, accuracy $\sim 1\%$
(*Khatri and Sunyaev 2012a*)

$$\mathscr{T}(z) \approx 1.007\left[\left(\frac{1+z}{1+z_{\rm dC}}\right)^5 + \left(\frac{1+z}{1+z_{\rm br}}\right)^{5/2}\right]^{1/2} + 1.007\varepsilon \ln\left[\left(\frac{1+z}{1+z_\varepsilon}\right)^{5/4} + \sqrt{1+\left(\frac{1+z}{1+z_\varepsilon}\right)^{5/2}}\right]$$
$$+ \left[\left(\frac{1+z}{1+z_{\rm dC}'}\right)^3 + \left(\frac{1+z}{1+z_{\rm br}'}\right)^{1/2}\right],$$

Compton y parameter

$$y(z) = -\int_z^0 (n_e \sigma_T c)\, \frac{k_B T}{m_e c^2}\, \frac{dz}{H(1+z)}$$

describes the broadening and shift of the spectrum,
i.e. redistribution of photons along frequency axis

$$Y(z) = -\int_z^0 (n_e \sigma_T c)\quad k(Te - Tr)/mc^2 \;*\; dz/H(1+z)$$

describes the deviation of the conditions from equilibrium,
energy release leads to Te > Tr and spectral distortions

In the case of Te < Tr comptonization leads to Bose-Einstein condensation of photons – their flow toward low frequencies

Kompaneets equation (1956)

Compton scattering when energy exchange is small (Focker-Planck approximation)

$$\gamma + e^- \rightarrow \gamma + e^-$$

$$\frac{\partial n}{\partial y} = \frac{1}{x^2}\frac{\partial}{\partial x}x^4\left(n + n^2 + \frac{T_e}{T}\frac{\partial n}{\partial x}\right).$$

Recoil

Induced recoil

Doppler diffusion

Bose-Einstein spectrum- Chemical potential (μ)

$$n(x) = \frac{1}{e^{x+\mu} - 1}$$

Given two constraints, energy density (E) and number density (N) of photons, T, μ uniquely determined.

Idea behind analytic solutions:

If we know rate of production of photons and energy injection rate, we can calculate the evolution/production of μ (and T)

HYDROGEN LINES FROM COSMOLOGICAL RECOMBINATION ARE REDSHIFTED 1500 TIMES INTO RADIOBAND !!!

100-shell hydrogen atom and continuum

CMB spectral distortions

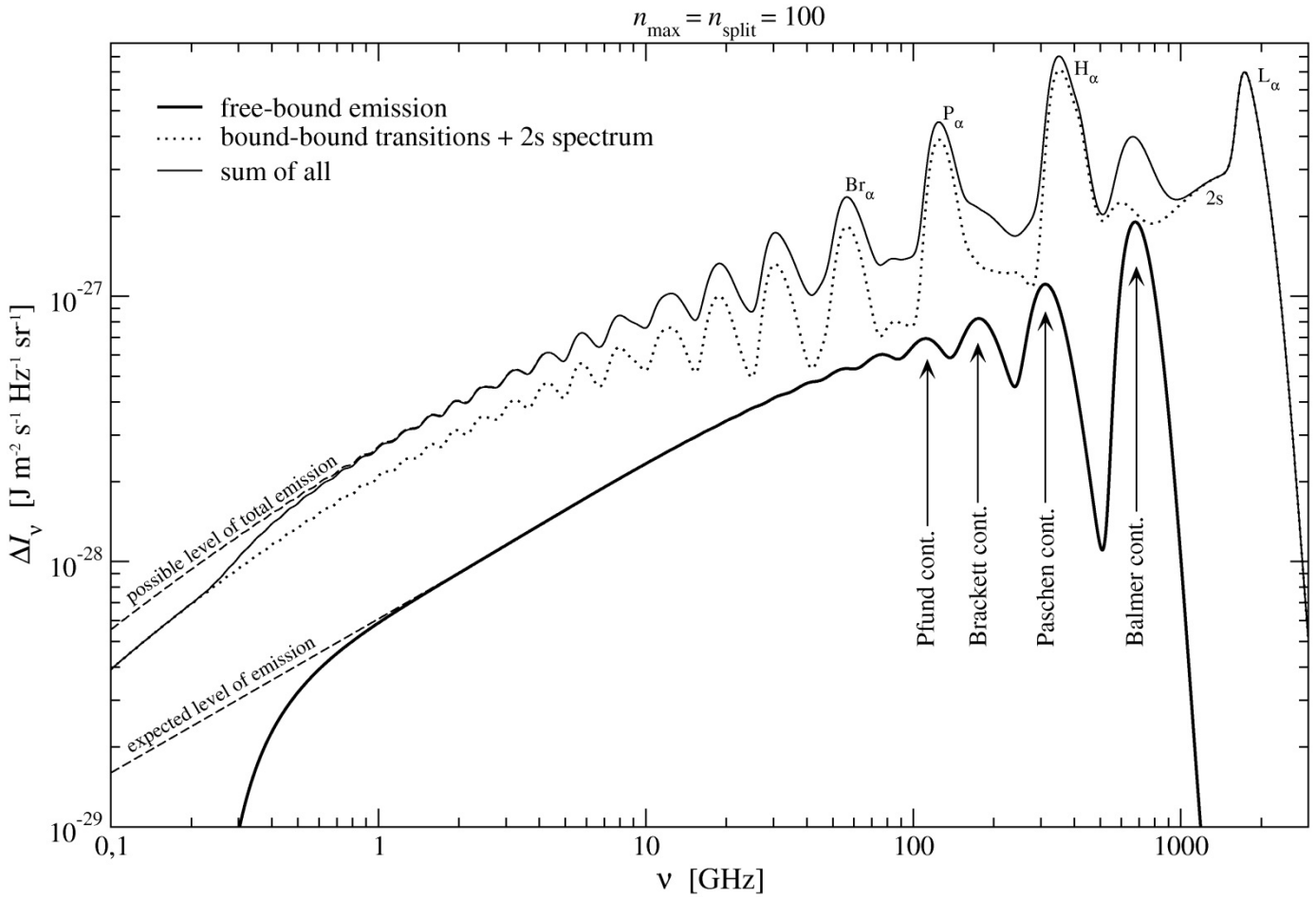

bound-bound & 2s:

- at ν>1GHz: distinct features
- slope ~ 0.46

free-bound:

- only a few features distinguishable
- slope ~ 0.6

Total:

- f-b contributes ~30% and more
- Balmer cont. ~90%
- Balmer: 1γ per HI
- **in total 5γ per HI**

Chluba & RS, 2006, A&A, 458, L29 (astro-ph/0608120)

PIXIE *SHOULD DETECT THESE LINES ON THE LEVEL OF 5-6 SIGMA*

A possibility of the Bose-Einstein condensation of CMB photons

Entropy is conserved in thermodynamic equilibrium

Entropy per baryon of radiation + baryons

$$\sigma = \frac{4a_R T^3}{3n_B} + Nk_B \ln\left(\frac{T^{3/2}}{n_B C}\right)$$

baryon density

$n_B \propto (1+z)^3$

Constant entropy

$T_{\text{radiation}} \propto 1+z$ $\quad$ $T_{\text{baryons}} \propto (1+z)^2$

Adiabatic indices of radiation (4/3) and baryons (5/3) are different.

- Baryons cool faster $\propto (1+z)^2$than radiation $\propto (1+z)$
- Radiation transfers energy to baryons to maintain equilibrium: Comptonization
- Cooling of radiation gives rise to spectral distortions

This fact was recognized long ago: Zeldovich, Kurt, Sunyaev, 1968 in the paper about recombination of hydrogen in the Universe showed that e-p collisions and Comptonization are able to keep Te = Tp = Tr up to z ~ 150. At z < 150, Te << Tr. This defines the behavior of the hydrogen hyperfine structure spin temperature.

Positive and negative μ-type distortions

(negative distortion far from singularity)

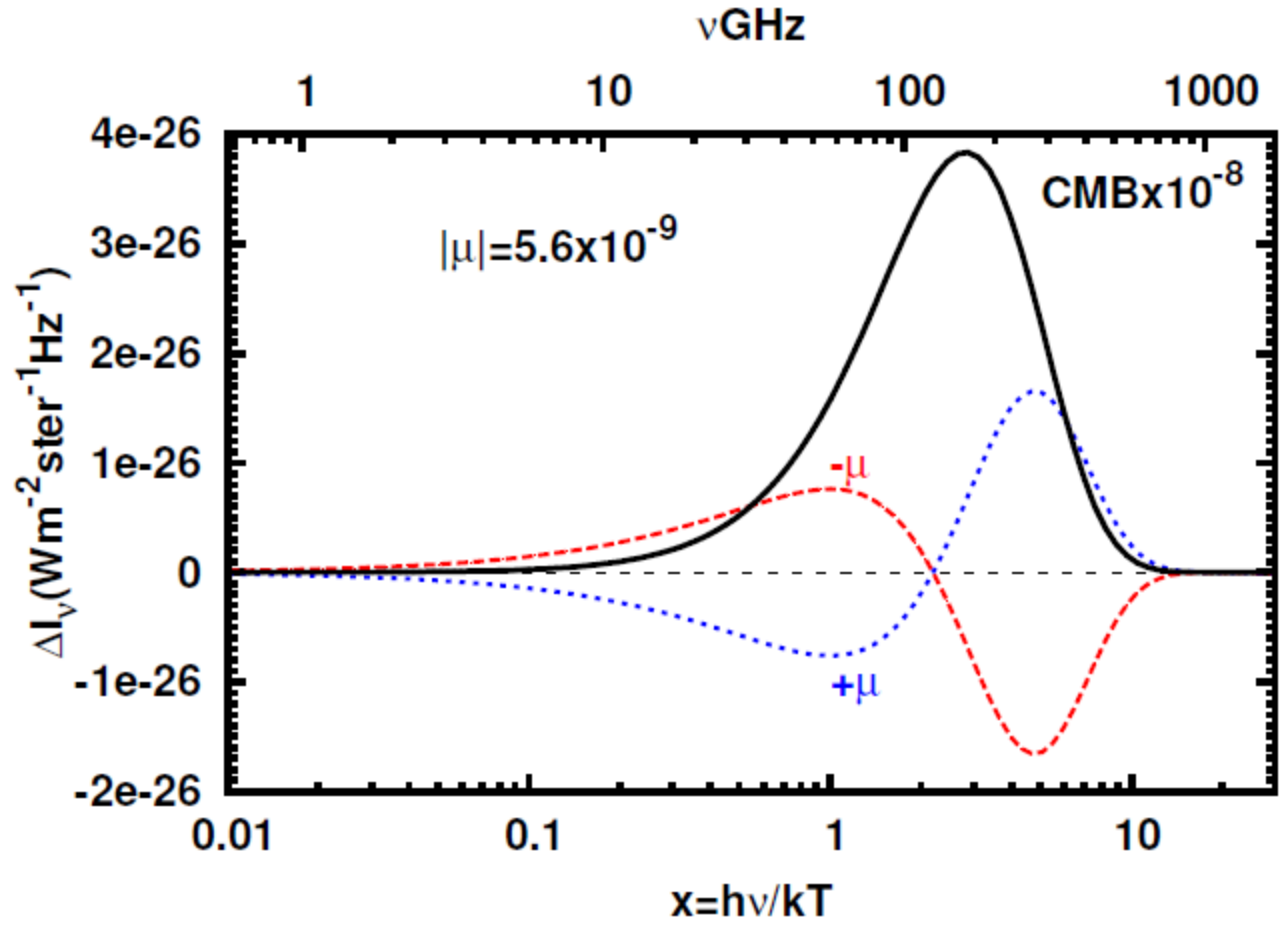

Atom/ Ion	Wavelength (in μ)	Oscillator strength	HFI freq. (GHz)	Scattering redshift	$\mathcal{B}$ factor	Opt. depth for 10^{-2} solar abundance	$[X]_{\rm min}$ for $l = 10$	$\langle [X]_{\rm min} \rangle$ in $l = 10$–20
C I	609.70	1.33×10^{-9}	143	2.4	0.76	6.4×10^{-6}	5.3×10^{-3}	2.6×10^{-3}
			217	1.3	0.92	3.9×10^{-6}	1.4×10^{-2}	6.8×10^{-3}
			353	0.4	0.99	1.6×10^{-6}	2.1×10^{-1}	1.2×10^{-1}
	370.37	9.08×10^{-10}	143	4.7	0.15	1.2×10^{-6}	2.8×10^{-2}	1.3×10^{-2}
			217	2.8	0.09	3.7×10^{-7}	1.6×10^{-1}	8.1×10^{-2}
C II	157.74	1.71×10^{-9}	143	12.3	0.79	1.8×10^{-5}	2.7×10^{-2}	6.2×10^{-3}
			217	7.9	0.94	1.1×10^{-5}	7.7×10^{-3}	3.0×10^{-3}
			353	4.4	0.99	5.6×10^{-6}	7.7×10^{-2}	3.6×10^{-2}
N II	205.30	3.92×10^{-9}	143	9.2	0.76	1.1×10^{-5}	7.6×10^{-3}	2.6×10^{-3}
			217	5.8	0.92	6.8×10^{-6}	8.6×10^{-3}	3.8×10^{-3}
			353	3.1	0.99	3.5×10^{-6}	1.3×10^{-1}	6.8×10^{-2}
	121.80	2.74×10^{-9}	143	16.2	0.16	2.1×10^{-6}	1.3×10^{-1}	3.8×10^{-2}
			217	10.5	0.09	6.4×10^{-7}	3.4×10^{-1}	1.1×10^{-1}
N III	57.32	4.72×10^{-9}	143	35.6	0.79	2.5×10^{-5}	2.3×10^{-3}	7.4×10^{-4}
			217	23.4	0.94	1.5×10^{-5}	6.1×10^{-3}	2.0×10^{-3}
O I	63.18	3.20×10^{-9}	143	32.2	0.88	1.0×10^{-4}	5.3×10^{-4}	1.7×10^{-4}
			217	21.2	0.96	6.3×10^{-5}	2.0×10^{-3}	6.4×10^{-4}
			353	12.5	1.00	3.1×10^{-5}	2.2×10^{-1}	4.9×10^{-2}
O III	88.36	9.16×10^{-9}	143	22.8	0.76	2.2×10^{-4}	3.5×10^{-4}	1.2×10^{-4}
			217	14.8	0.92	1.4×10^{-4}	8.4×10^{-3}	1.8×10^{-3}
			353	8.6	0.99	7.4×10^{-5}	1.2×10^{-2}	4.4×10^{-3}
	51.81	6.55×10^{-9}	143	39.5	0.17	4.5×10^{-5}	1.4×10^{-3}	4.7×10^{-4}
			217	26.0	0.10	1.4×10^{-5}	6.5×10^{-3}	2.2×10^{-3}

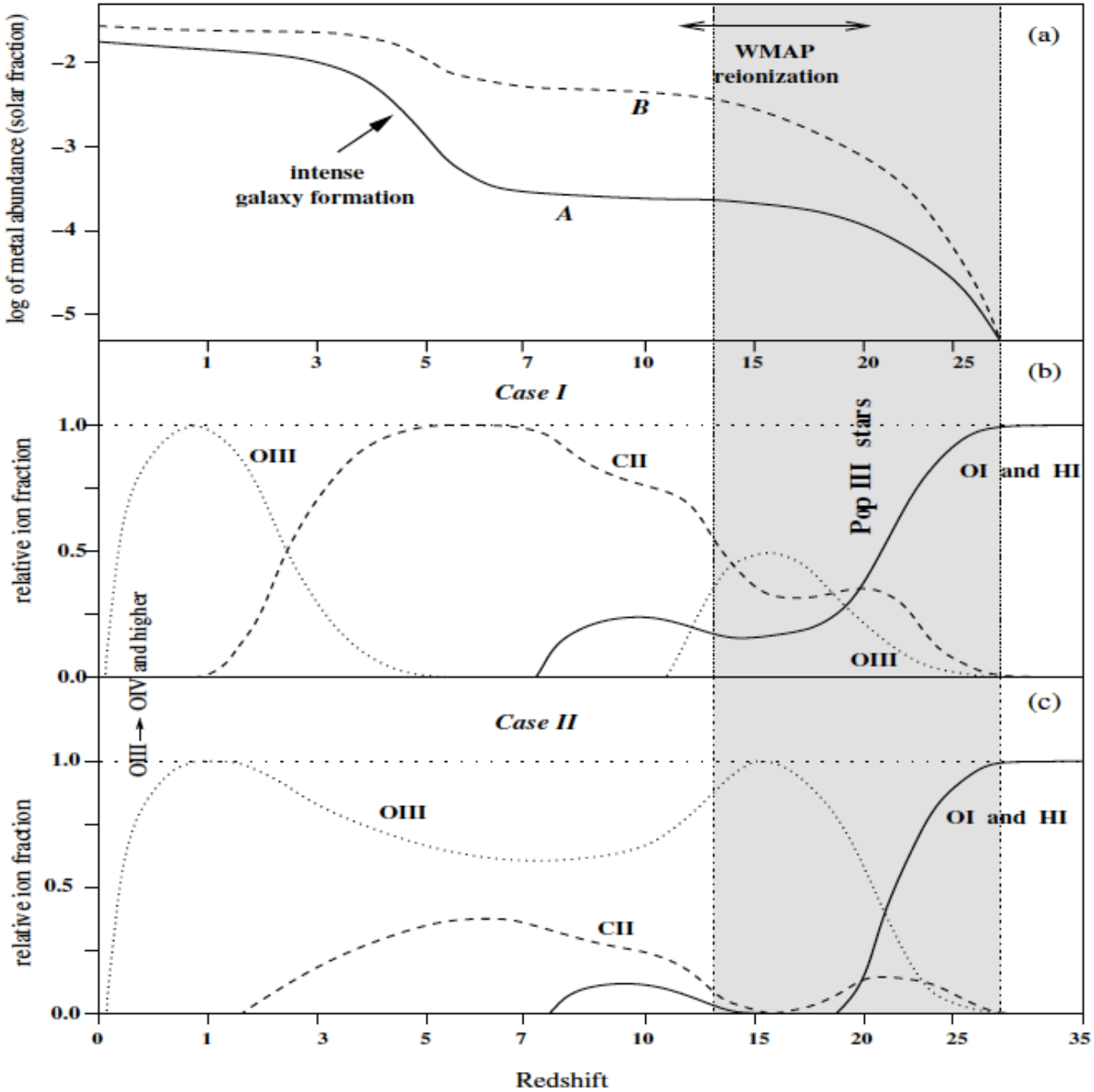
(a)
log of metal abundance (solar fraction)
WMAP
reionization
B
A
intense
galaxy formation
(b)
Case I
relative ion fraction
OIII
CII
Pop III stars
OI and HI
OIII
OIII → OIV and higher
(c)
Case II
relative ion fraction
OIII
CII
OI and HI
Redshift

COrE mission with internal calibrator ? and angular resolution < 20’ will be able to provide C_l on the level of 10^-2 microK^2 and detect O III ions with 4 10^-5 of solar abundance of oxygen

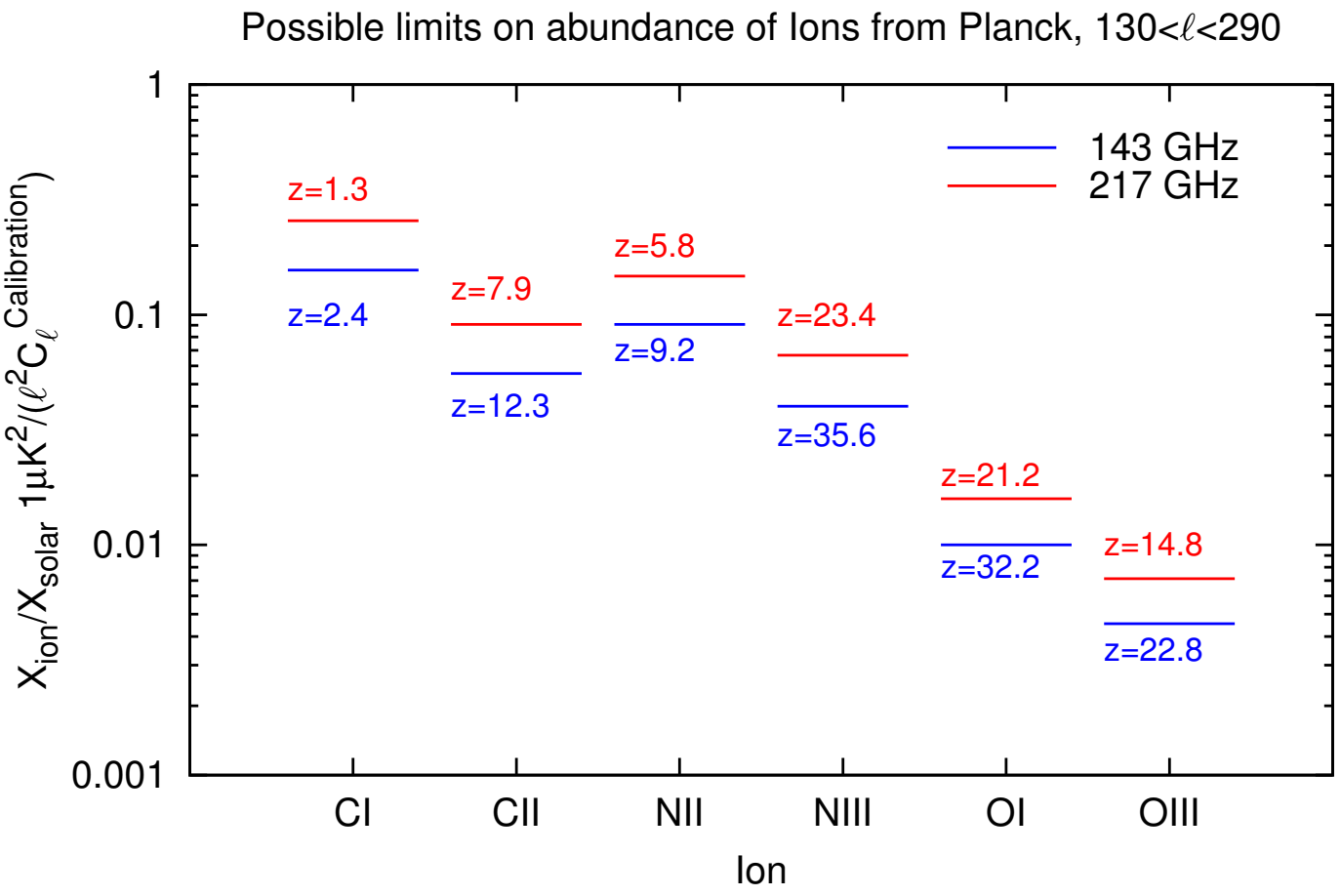

Khatri, Sunyaev, 2012

the blurring of primordial fluctuations. Thomson tau = 0.85 (WMAP)

full analogy with Gunn-Peterson effect, but Tr inhomogeneities on the sky are playing the role of quasars and submm lines are used instead Ly-alpha.

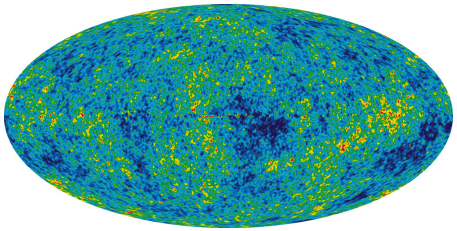

Hot and cold spots

zero effect for monopole, polarization from quadrupole

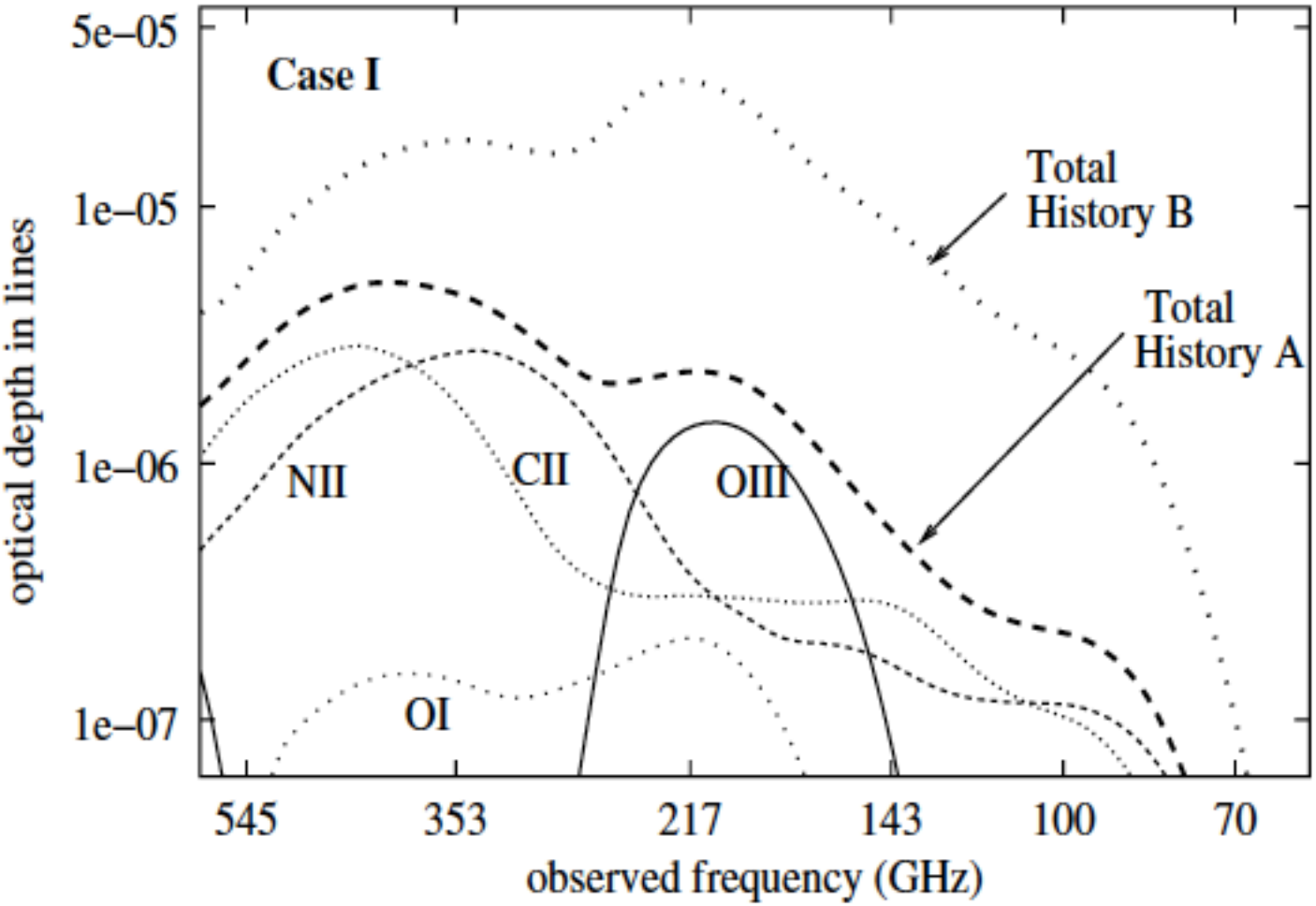

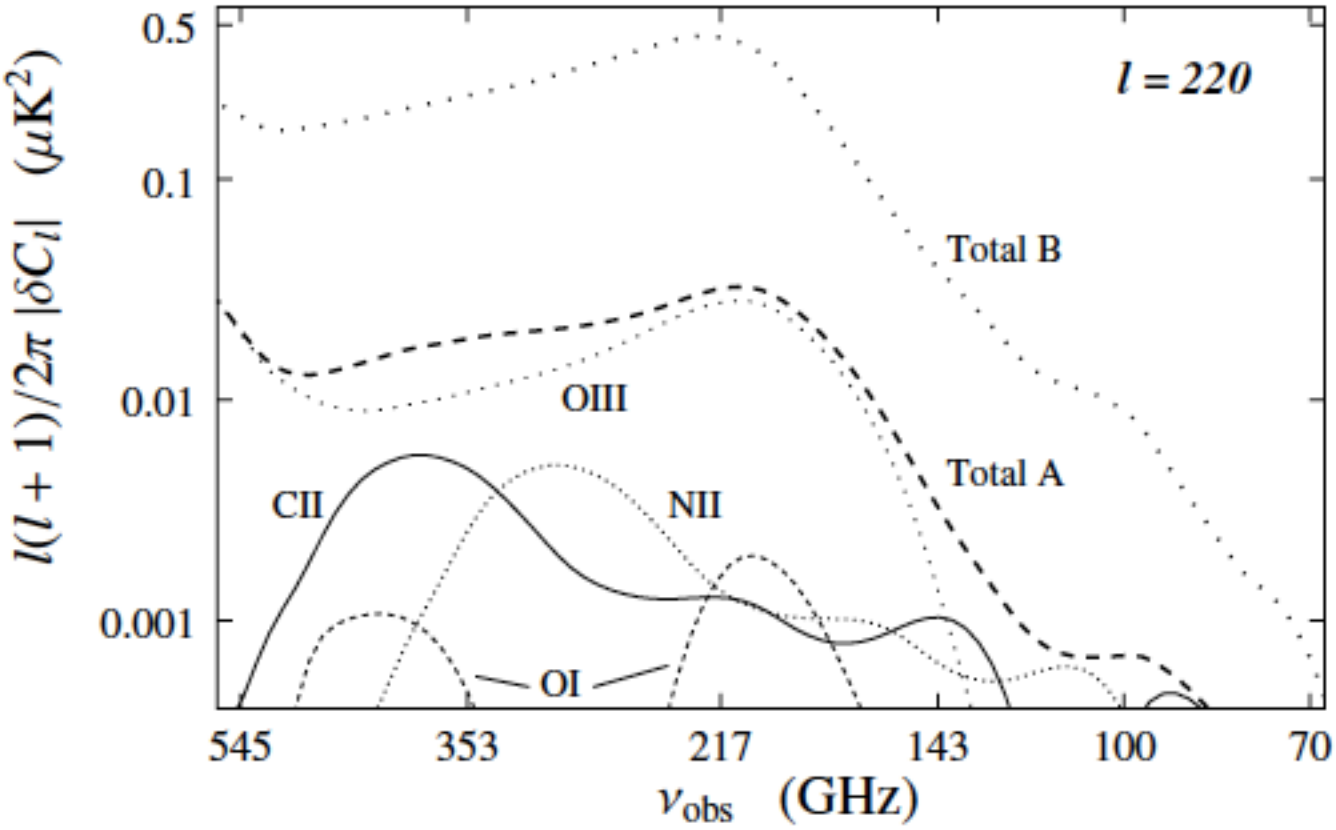

Basu, Hernandez-Monteagudo, Sunyaev, 2004

Adiabatic cooling due to Universe expansion - different indices

Radiation - Tr ~ (1+z)

Barions and electrons – Te ~ (1+z)^2

Electrons colder than radiation Te < Tr

Comptonization (the energy exchange between plasma and radiation due to Compton scatterings on thermal electrons, Doppler and recoil effects) is trying to establish new thermodynamic equilibrium with Te=Tr.

When Tr > Te, we have black body radiation with excess of photons. Due to recoil and induced recoil frequencies photons move toward lower frequencies

$$\frac{\partial n}{\partial y} = \frac{1}{x^2}\frac{\partial}{\partial x}x^4\left(n + n^2 + \frac{T_e}{T_{BB}}\frac{\partial n}{\partial x}\right)$$

$$\frac{\partial n}{\partial y} = (1 - \frac{T_e}{T_{BB}})\frac{1}{x^2}\frac{\partial}{\partial x}x^4\left(n + n^2\right)$$

Kompaneets equation, 1956

Statement of the problem

Inject small amount of energy at $\Delta E/E_\gamma$ at $z < 10^6$.

- **We get very rapidly :**

$$Y = 0.25\frac{\Delta E}{E_\gamma}$$

$$T_e = T(1 + 1.35\frac{\Delta E}{E_\gamma})$$

Zeldovich, Sunyaev, 1969

Statement of the problem

Inject small amount of energy at $\Delta E/E_\gamma$ at $z < 10^6$.

- **Equilibrium solution: Bose-Einstein**

$$\mu = 1.4\frac{\Delta E}{E_\gamma}$$

$$T_e = T(1 + 0.64\frac{\Delta E}{E_\gamma})$$

(Illarionov and Sunyaev 1975)

Statement of the problem

Inject small amount of energy at $\Delta E/E_\gamma$ at $z < 10^6$.

- **We want to study the evolution of the spectrum**

  from Y to BE while conserving energy and photon number

  - **$\Delta T_e/T$ is not constant (1.35 $\longrightarrow$ 0.64 $\Delta E/E_\gamma$)**

Statement of the problem

Solve for Kompaneets equation and electron temperature simultaneously.

$$\frac{\partial n}{\partial y} = \frac{1}{x^2}\frac{\partial}{\partial x}x^4\left(n + n^2 + \frac{T_e}{T}\frac{\partial n}{\partial x}\right)$$

$$T_e = T\frac{1}{4}\frac{\int n(n+1)x^4 dx}{\int n x^3 dx}$$

$x \equiv h\nu/kT$.

WIMP dark matter annihilation: Energy injection into CMB

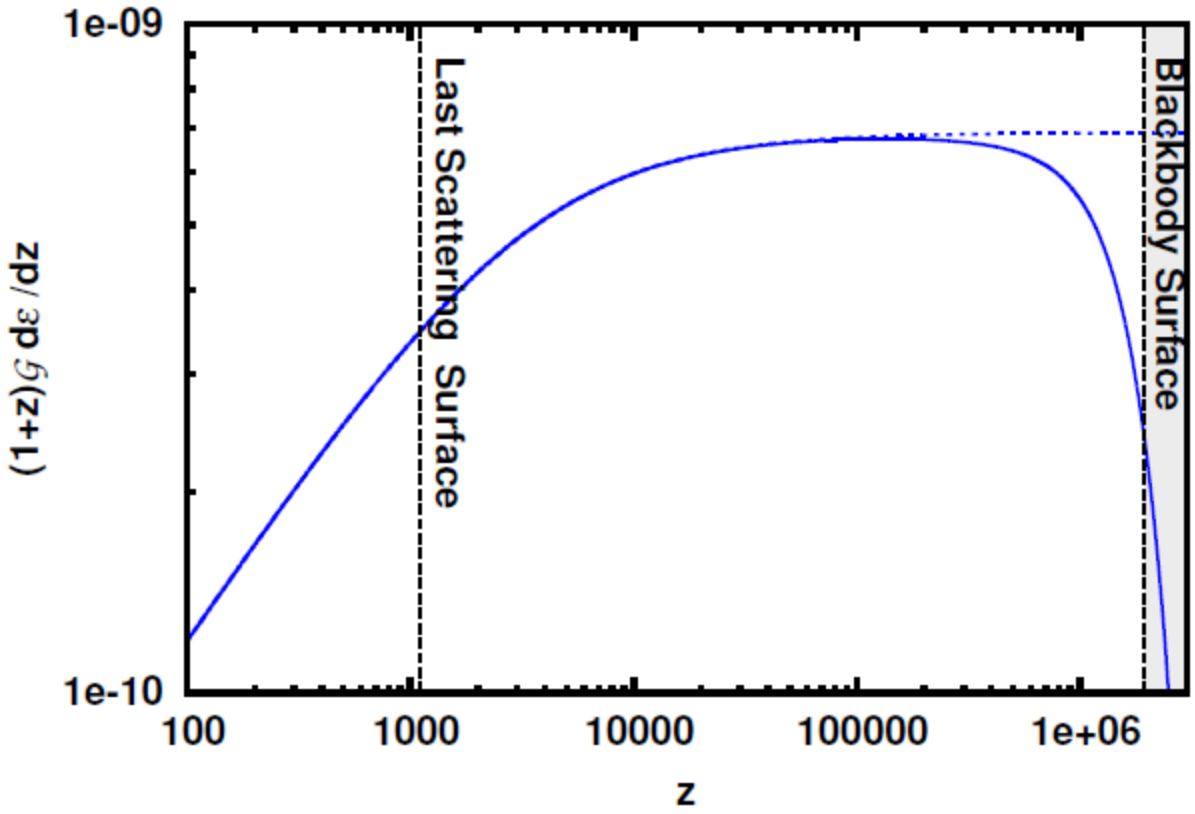

Annihilation cross-section corresponding to the recent Fermi spacecraft upper limits

Experimental prospects

2-3 orders of magnitude improvement over COBE is possible.
(*Fixsen and Mather 2002*)

Next proposed experiment: Pixie
(*Kogut et al. 2011*)

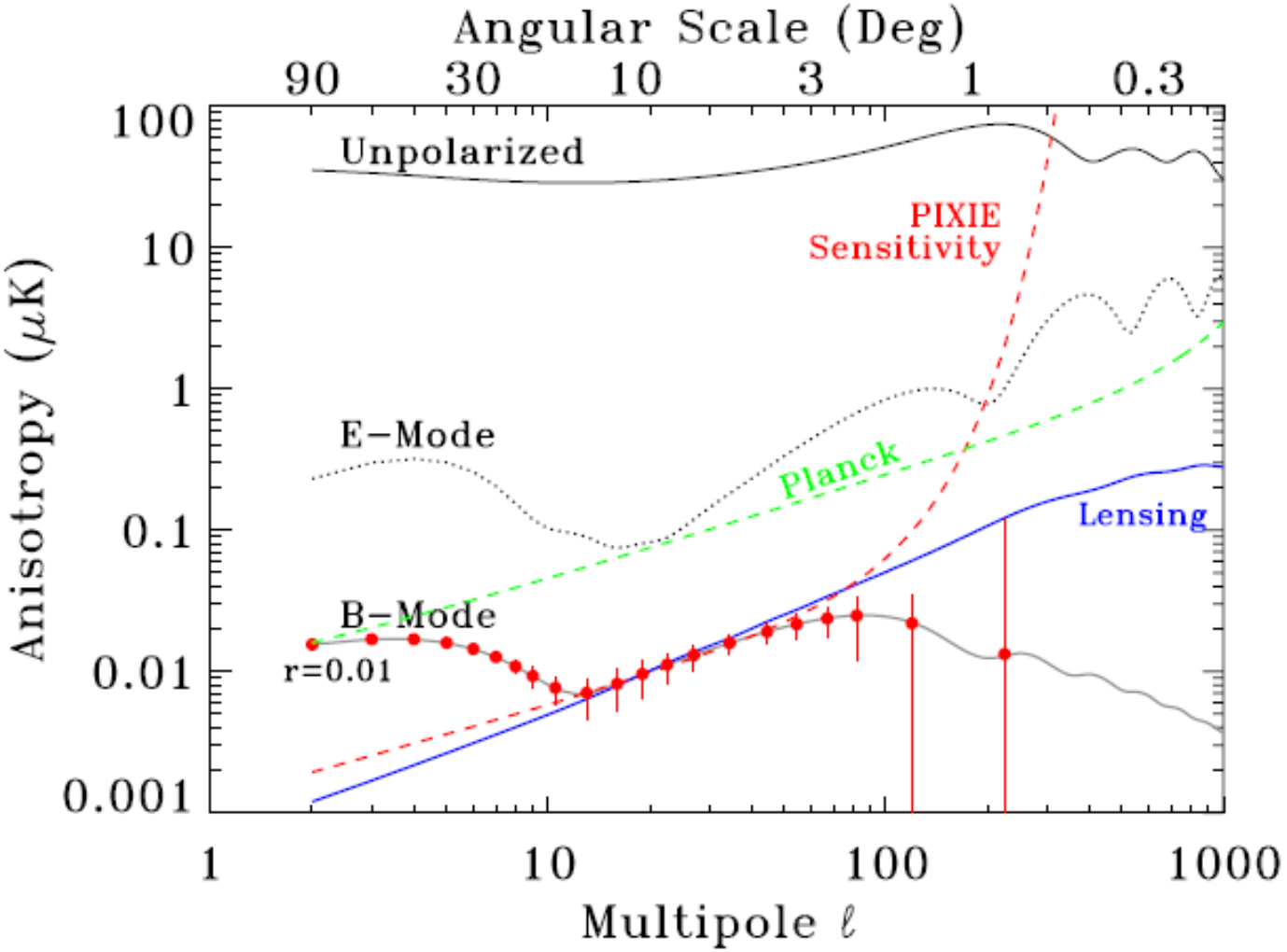

Figure 1. Angular power spectra for unpolarized, E-mode, and B-mode polarization in the cosmic microwave background. The dashed red line shows the PIXIE sensitivity to B-mode polarization at each multipole moment $\ell \sim 180^\circ/\theta$. The sensitivity estimate assumes a 4-year mission and includes the effects of foreground subtraction within the cleanest 75% of the sky combining PIXIE data at frequencies $\nu < 600$ GHz. Red points and error bars show the response within broader ℓ bins to a B-mode power spectrum with amplitude $r = 0.01$. PIXIE will reach the confusion noise (blue curve) from the gravitational lensing of the E-mode signal by cosmic shear along each line of sight, and has the sensitivity and angular response to measure even the minimum predicted B-mode power spectrum at high statistical confidence.

Sources of CMB spectral distortions in standard cosmology

Different shapes would make separation possible

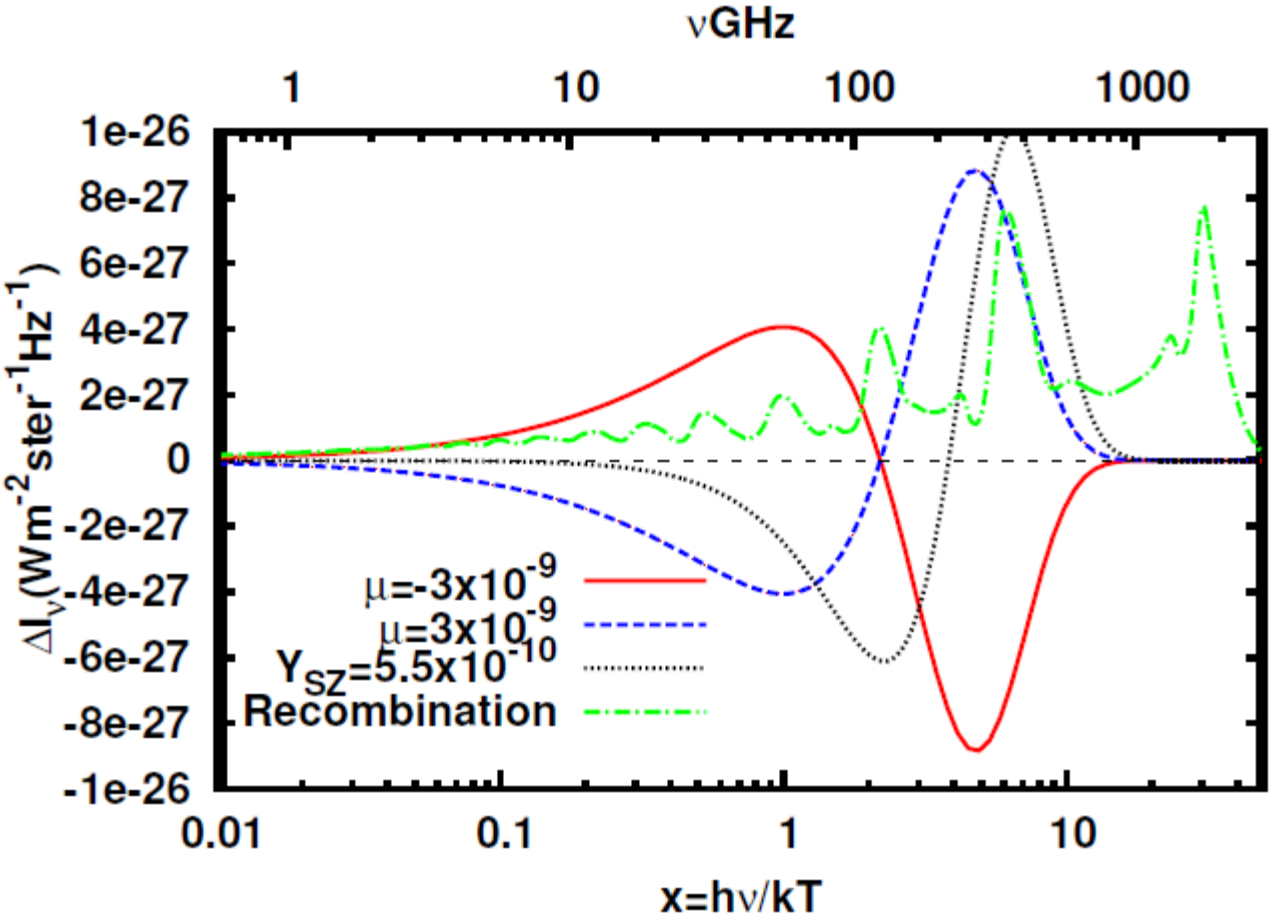

Energy losses by CMB until recombination

$$\frac{\Delta E}{E} = -5.9 \times 10^{-10} \ln\left(\frac{1+z_i}{1+z}\right)$$

$$z_i = 2 \times 10^6, z = 1000 \Rightarrow \frac{\Delta E}{E} = -4.5 \times 10^{-9}$$